

Dissertation zur Erlangung des Doktorgrades  
der Fakultät für Chemie und Pharmazie  
der Ludwigs-Maximilians Universität München

**Structural and Functional Characterization**  
**of the**  
**Yeast Ski2-Ski3-Ski8 Complex**

Felix Johannes Halbach

aus

Prien am Chiemsee in Deutschland

2013

## Erklärung

Diese Dissertation wurde im Sinne von §7 der Promotionsordnung vom 28. November 2011 von Frau Prof. Dr. Elena Conti betreut.

## Eidesstattliche Versicherung

Diese Dissertation wurde eigenständig und ohne unerlaubte Hilfe erarbeitet.

München, den 31. Januar 2013

.....  
(Unterschrift des Autors)

Dissertation eingereicht am 29. Januar 2013

Erstgutachter: Prof. Dr. Elena Conti

Zweitgutachter: Prof. Dr. Karl-Peter Hopfner

Mündliche Prüfung am 9. April 2013





# Contents

<b>Summary</b>	<b>xiii</b>
<b>1 Preface</b>	<b>1</b>
<b>2 Introduction</b>	<b>3</b>
2.1 mRNA degradation in eukaryotes . . . . .	3
2.1.1 Canonical mRNA decay is initiated by the deadenylation machinery and driven by exonucleases . . . . .	4
2.1.2 Alternative decay pathways . . . . .	6
2.1.3 Relative contributions of 5' and 3' decay routes . . . . .	6
2.2 The exosome is the major eukaryotic 3' to 5' ribonuclease complex . . . . .	7
2.2.1 Functions of the eukaryotic exosome: From maturation to degradation	7
2.2.2 The architecture of the core exosome and its conservation through all domains of life . . . . .	9
2.2.3 Rrp44 and Rrp6 confer activity to the eukaryotic exosome . . . . .	11
2.2.4 The inactive eukaryotic exosome core retains functionality . . . . .	12
2.3 Exosome cofactors . . . . .	14
2.3.1 General cofactors of the exosome . . . . .	14
2.3.2 Specific exosome cofactors . . . . .	17
2.4 The SKI complex is a general cofactor of the cytoplasmic exosome . . . . .	18
2.4.1 Functions of the Ski2-Ski3-Ski8 complex . . . . .	18
2.4.2 Towards the architecture of the <i>S. cerevisiae</i> Ski2-Ski3-Ski8 complex	20
2.4.3 Conservation of the Ski2-Ski3-Ski8 complex and Ski7 in higher eu- karyotes . . . . .	25
2.5 Scope of this work . . . . .	26

---

<b>3</b>	<b>Results</b>	<b>27</b>
3.1	Crystal Structure of the <i>S. cerevisiae</i> Ski2 helicase . . . . .	27
3.2	The Ski complex: Crystal structure and substrate channeling to the exosome	42
<b>4</b>	<b>Discussion</b>	<b>65</b>
4.1	Ski2 contains a conserved DExH box core and a variable insertion domain .	65
4.2	The structure of the SKI complex: a framework for Ski2 to function in concert with the exosome . . . . .	67
4.3	The Ski3 TPR scaffold organizes the SKI complex . . . . .	68
4.4	Ski8 is a versatile adapter protein with multiple roles . . . . .	71
4.5	The SKI complex regulates exosome function . . . . .	76
4.6	Major conclusions . . . . .	80
<b>5</b>	<b>Outlook</b>	<b>81</b>
<b>A</b>	<b>Appendix</b>	<b>83</b>
	<b>Bibliography</b>	<b>95</b>
	<b>Acknowledgements</b>	<b>110</b>

# Abbreviations

ADP	= adenosine diphosphate.
AMPPNP	= adenosine 5' -( $\beta,\gamma$ -imido)triphosphate.
ARE	= AU-rich elements.
ATP	= adenosine triphosphate.
ATPase	= ATP hydrolase.
CBC	= cap-binding complex.
CUT	= cryptic unstable transcript.
DNA	= deoxyribonucleic acid.
DSB	= double-strand break.
EMSA	= electrophoretic mobility shift assay.
GTPase	= GTP hydrolase.
HLH	= helix-loop-helix.
HRDC	= helicase RNase D C-terminal domain.
mRNA	= messenger RNA.
NGD	= no-go decay.
NMD	= nonsense-mediated decay.
NSD	= non-stop decay.
nt	= nucleotides.
Pab1	= poly(A)-binding protein.
PAP	= poly(A) polymerase.
PCR	= polymerase chain reaction.
PIN	= PiLT protein N-terminus.
PNPase	= polynucleotide phosphorylase.
poly(A)	= polyadenylate.
r.m.s.d.	= root mean square deviation.
RISC	= RNAi-induced silencing complex.

---

RNA	= ribonucleic acid.
RNAi	= RNA interference.
RNase	= ribonuclease.
RNP	= ribonucleoprotein.
rRNA	= ribosomal RNA.
SAD	= single wavelength anomalous diffraction.
SF2	= superfamily II.
SKI	= Superkiller.
snoRNA	= small nucleolar RNA.
snRNA	= small nuclear RNA.
topo VI-A	= subunit A from archaeal topoisomerase VI.
TPR	= tetratricopeptide repeat.
TRAMP	= Trf4/5-Air1/2-Mtr4 polyadenylation complex.
tRNA	= transfer RNA.
WD40	= Trp-Asp 40.
WH	= winged helix.

# List of Figures

## Introduction

2.1	General pathways of mRNA decay . . . . .	5
2.2	Functions of the RNA exosome . . . . .	8
2.3	The molecular architecture of exosome-like complexes . . . . .	10
2.4	RNA channeling by the exosome . . . . .	13
2.5	Domain structure of the Ski2, Ski3, Ski8 and Ski7 proteins . . . . .	21
2.6	Molecular architecture of DExH box helicases . . . . .	22
2.7	The crystal structure of yeast Ski8 . . . . .	23

## Results

3.2.1	The crystal structure of <i>S. cerevisiae</i> Ski2 $\Delta$ N . . . . .	30
3.2.2	A comparison of the Ski2 and Mtr4 insertion domains . . . . .	32
3.2.3	RNA-binding properties of the Ski2 insertion domain . . . . .	34
3.2.4	The Ski2 insertion is dispensable Ski2-Ski3-Ski8 complex formation . . .	35
3.2.S1	Structural features of the Ski2 insertion domain . . . . .	39
3.2.S2	A sequence alignment of Ski2 . . . . .	40
3.3.1	The biochemical properties of the Ski2-Ski3-Ski8 complex . . . . .	44
3.2.2	Structure of the <i>S. cerevisiae</i> Ski2 $\Delta^{\text{insert}}$ -Ski3-Ski8 complex . . . . .	46
3.2.3	Subunit interactions of the Ski3 TPR scaffold . . . . .	47
3.2.4	Ski8 and Spo11 share a Ski3-binding motif . . . . .	49
3.2.5	RNA-binding path and regulation in the Ski complex . . . . .	51
3.2.6	RNA channeling between Ski2-Ski3-Ski8 complex and the exosome . . .	52
3.2.S1	Structure determination of the Ski2 $\Delta^{\text{insert}}$ -Ski3-Ski8 complex . . . . .	59
3.2.S2	Structural properties of the Ski3 N-terminus . . . . .	60

---

3.2.S3	Conservation of the Ski2 binding sites in the Ski3 scaffold . . . . .	61
3.2.S4	A Q-R-x-x-F/Y motif in Ski8 and Spo11 mediates binding to Ski3 . . .	62
3.2.S5	Properties of the Ski2 RG-Loop segment and the Ski3 N-terminal arm .	63
3.2.S6	Interactions and activities of the Ski2-Ski3-Ski8 complex . . . . .	64
Discussion		
4.1	Overview of solved crystal structures . . . . .	74
4.2	Versatility in subunit binding modes of the Ski3 TPR scaffold . . . . .	76
4.3	A structural model of the Spo11-Ski8 complex . . . . .	80
4.4	A model for the exosome activation by the Ski2-Ski3-Ski8 complex . . .	84

# List of Tables

## Introduction

2.1 Cofactors of the yeast RNA exosome . . . . .	15
--	----

## Results

3.1.1 Data collection statistics of the Ski2 $\Delta$ N structure . . . . .	31
3.2.1 Data collection statistics of the Ski2 $\Delta^{insert}$ -Ski3-Ski8 structure . . . . .	45

## Appendix

A.1 List of constructs . . . . .	84
A.2 List of PCR primers . . . . .	90



# Summary

The Ski2-Ski3-Ski8 (SKI) complex is a conserved multi-protein assembly required for the cytoplasmic functions of the exosome, including messenger RNA (mRNA) turnover, surveillance and interference. The helicase Ski2, the tetratricopeptide repeat (TPR) protein Ski3 and the  $\beta$ -propeller Ski8 assemble in a heterotetramer with 1:1:2 stoichiometry. While the function of the Ski2-Ski3-Ski8 complex as a general cofactor of the cytoplasmic exosome has been well established, it remains largely unclear how it contributes to the regulation of the exosome. The PhD thesis at hand addresses this question by investigating the structural and biochemical properties of the Ski2-Ski3-Ski8 complex.

Solving the crystal structure of the 113 kDa helicase region of *S. cerevisiae* Ski2 by experimental phasing revealed the presence of a canonical DExH core and an atypical accessory domain that is inserted in the helicase core. This insertion domain binds ribonucleic acid (RNA) unspecifically and is located at the RNA entry site of the helicase core. The overall architecture of Ski2 including the presence of an accessory domain is similar to the structure of the related helicase Mtr4, but the structural and biochemical properties of the accessory domains from both proteins are different.

The Ski2 insertion domain is not required for formation of the Ski2-Ski3-Ski8 complex. Its removal allowed to crystallize a Ski2 <sup>$\Delta$ insert</sup>-Ski3-Ski8 complex from *S. cerevisiae*, and the crystal structure of this 370 kDa core complex was determined experimentally. It shows that Ski3 forms an array of 33 TPR motifs, creating a scaffold for the other subunits. Ski3 and the two Ski8 subunits bind the helicase core of Ski2 and position it centrally within the complex. This creates an extended internal RNA channel and modulates the enzymatic properties of the Ski2 helicase. Both Ski8 subunits are bound through a structurally conserved motif. A similar motif is present and functional in yeast Spo11, a protein that initiates deoxyribonucleic acid (DNA) double strand breaks during meiotic recombination. Association of Ski8 to either complex is mutually exclusive, rationalizing how Ski8 can perform its two distinct roles in mRNA metabolism and meiotic recombination.

Biochemical studies suggest that the SKI complex can thread RNAs directly to the exosome, coupling the helicase and the exoribonuclease through a continuous channel of 43-44 nucleotides length. Finally, an internal regulatory mechanism in the Ski2-Ski3-Ski8 complex was identified. Both the Ski2-insertion domain and the Ski3 N-terminus cooperate to inhibit ATPase and helicase activity of Ski2 when bound in the SKI complex. Thus, the SKI complex regulates exosome activity in two ways. First by a direct substrate channeling mechanism to the exosome that connects helicase and nuclease activities of both complexes which may activate the exosome towards certain substrates. Second, by an inhibitory mechanism that regulates substrate access to the helicase complex, which is a prerequisite for controlling the exosome's substrate specificity.

This doctoral thesis provides the first structural description of the entire yeast SKI complex and identifies two mechanisms that may contribute to regulation of the activity of the cytoplasmic exosome.

# 1 Preface

My doctoral work led to publication of two research articles<sup>1 2</sup>. Since both manuscripts are coherent and represent the main body of work undertaken in the course of my Ph.D. project, this thesis is written in cumulative style. The first chapter contains an introduction to the biological background and the current state of the research. The second chapter includes the classical “Results” and “Material and methods” sections in form of the original manuscripts. A third and last chapter features a comprehensive discussion that integrates the main aspects from both publications.

---

<sup>1</sup>The crystal structure of *S. cerevisiae* Ski2, a DExH helicase associated with the cytoplasmic functions of the exosome. F. Halbach, M. Rode and E. Conti *RNA*, 2012, 18(1), 124-34

<sup>2</sup>The yeast Ski complex: crystal structure and substrate channeling to the RNA exosome. F. Halbach, P. Reichelt, M. Rode, E. Conti *Cell*, 2013, 154, 814-26



## 2 Introduction

### 2.1 mRNA degradation in eukaryotes

The balance between constructive and destructive events is a crucial concept found in many biological systems at any level. In the metabolism of RNA, transcription and degradation are the competing key events that determine the cellular level of a given transcript. Thus, adjusting the turnover rate for a given transcript allows the cell to regulate the activity of its gene product. Other means exist to control gene expression, among these post-translational mechanisms. Nevertheless, degradation of mRNA provides the conceptually simplest and most direct way to regulate the expression level of a particular gene since it counteracts directly on transcription.

Degradation of mRNA is not only a means for the regulation of gene expression but also helps to ensure the fidelity of transcription. For instance, cellular quality control mechanisms identify improperly matured or otherwise erroneous transcripts and destine them for degradation. Finally, degradation is the last step in chemical recycling of RNA, a process that replenishes the cellular pools of nucleotides. Examples for this process include breakdown of splicing by-products or cleaved, inactive transcripts produced by RNA interference (RNAi) or other regulatory RNA mechanisms.

Most enzymes involved in the processes of RNA catabolism (e.g. nucleases, helicases or RNA-binding proteins) are found in all domains of life. However, the specific pathways of degradation and particularly their regulation can vary substantially. Nevertheless, in eukaryotes two conserved canonical mRNA decay routes have evolved through which the vast majority of all transcripts are degraded.

### 2.1.1 Canonical mRNA decay is initiated by the deadenylation machinery and driven by exonucleases

As soon as a given gene is transcribed in the nucleus, its mRNA is being processed and spliced. During these processes, various protein factors are deposited on the nucleic acid and the resulting protein-RNA complex is termed ribonucleoprotein (RNP). While these factors can be part of the processing machinery, they also facilitate the export of the RNP from the nucleus as well as cytoplasmic quality control mechanisms. Once the transcript arrives in the cytoplasm, it faces two fundamental fates: translation or decay. From the body of research conducted during the past decades it has now become clear that the ends of an RNA molecule hold the two key determinants that govern the translation-vs-decay decision: the 7-methylguanosine cap on the 5' end and the polyadenylate (poly(A)) tail on the 3' end (Fig. 2.1).

Both molecular features have their cognate receptors. In the nucleus, the cap structure of pre-mRNAs is bound by the cap-binding complex (CBC) that is formed by Cbp80 and Cbp20 (Izaurre et al., 1994). After export to the cytoplasm, the cytoplasmic eIF4F complex binds to the cap of error-proofed mRNAs and thus replaces the CBC. eIF4F consists of the cap-binding protein eIF4E, the scaffold protein eIF4G and the RNA helicase eIF4A (reviewed in Richter and Sonenberg, 2005). Formation of the eIF4F complex enhances the affinity of eIF4E for the 7-methylguanosine cap and forms a scaffold for other translational factors (see below).

In yeast<sup>1</sup>, the poly(A) tail comprises about 70 nucleotides (nt) (Manley and Takagaki, 1996; Keller and Minvielle-Sebastia, 1997) that are decorated by the poly(A)-binding protein (Pab1) (Kühn and Wahle, 2004). The 5' cap and the 3' poly(A) tail act as protective features and control translation and decay differentially. They promote translation, mainly by recruitment of the eIF4E to the 40S pre-initiation complex (Kessler and Sachs, 1998; Tarun and Sachs, 1995; Wells et al., 1998; Tarun and Sachs, 1996; Tarun et al., 1997). Conversely, they inhibit degradation by blocking access of exonucleases to the 5' and 3' ends (Hsu and Stevens, 1993; Mühlrad et al., 1994, 1995; Anderson and Parker, 1998), and this effect is apparently potentiated by circularization of the transcript through interaction of Pab1 and eIF4G (Kessler and Sachs, 1998; Tarun and Sachs, 1995, 1996; Wells et al., 1998).

---

<sup>1</sup>The yeast *S. cerevisiae* is the to-date best studied model system for mRNA degradation. This PhD project has thus focused on the *S. cerevisiae* proteins, and the introduction at hand is limited to the yeast system.

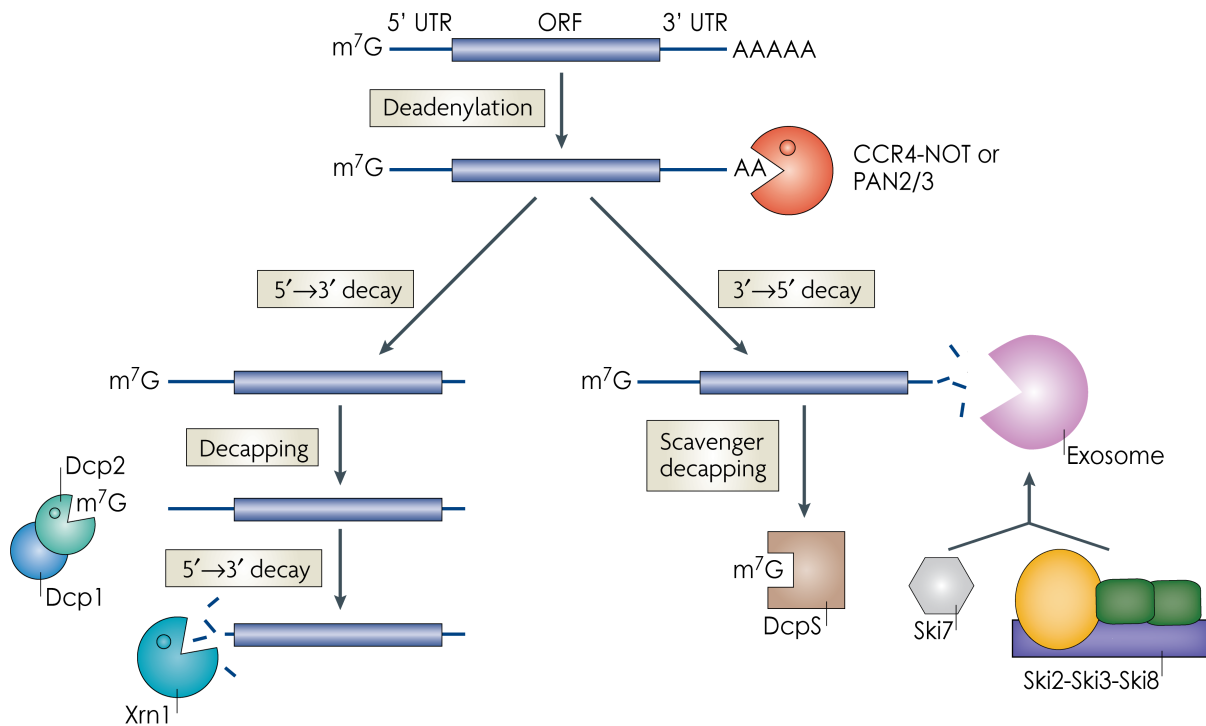


**Figure 2.1** | The two canonical pathways of mRNA degradation in eukaryotes. After nuclear export, the 5' cap of error-proofed mRNAs is bound to eIF4F complex while the poly(A) tail is decorated with Pab1. Bulk mRNA decay requires prior deadenylation by the Pan2/3 and the CCR4-Not complexes. RNA is then degraded either via the 5' to 3' path (Xrn1, requires prior decapping) or via the 3' to 5' pathway (exosome, Ski7 and Ski2-Ski3-Ski8, independent of decapping). Figure adapted from Garneau et al., 2007.

As a consequence, mRNA decay is initiated by removal of the protective features (for review see Wiederhold and Passmore, 2010; Garneau et al., 2007; Parker, 2012; Houseley and Tollervy, 2009). There are two canonical RNA decay routes: the 5' to 3' and 3' to 5' decay (see Fig. 2.1). Both pathways require prior deadenylation of the transcript.

In yeast, deadenylation is a two-step process that is initiated by the Pan2-Pan3 deadenylase complex. Pan2-Pan3 trims the poly(A) tail to about 65 nt (Brown and Sachs, 1998) and this process is stimulated by Pab1. Deadenylation is then continued by the Ccr4/Not complex until the poly(A) tail reaches approximately 10 nt (Fig. 2.1) (Daugeron et al., 2001; Tucker et al., 2001). At this point, the interaction of Pab1 with the 3' end is presumably lost, opening the way for 3' to 5' decay. In eukaryotes, the exosome is the major 3' to 5' exonuclease complex. The exosome, together with its cytoplasmic cofactors Ski7 and the Ski2-Ski3-Ski8 complex, processively degrades the free 3' end of the mRNA.

The remaining 5' cap structure is then degraded by the scavenger decapping enzyme DcpS (Liu et al., 2002). The second decay pathway operates from the 5' end of the transcript and thus requires prior decapping in addition to deadenylation (Fig. 2.1). Decapping is effected by the Dcp1-Dcp2 complex which is regulated by a host of factors including the activators Lsm1-7 complex and Edc3 (reviewed in Franks and Lykke-Andersen, 2008; Simon et al., 2006). Removal of the 7-methylguanosine cap leaves the mRNA with a 5' phosphate which is the preferred substrate of Xrn1, the major cytoplasmic 5' to 3' exonuclease (Larimer and Stevens, 1990).

### 2.1.2 Alternative decay pathways

Specialized pathways exist that lead to degradation but bypass prior deadenylation and/or decapping of the transcript. For instance, certain classes of transcripts recruit decapping enhancers (e.g. the Rpb28/Dcp3 system, (Kshirsagar and Parker, 2004; Badis et al., 2004)). These proteins promote decapping even though the poly(A) tail has not been shortened. This enables the Xrn1 pathway to degrade the transcript via the free 5' end. Other examples include the endonucleolytic cleavage of capped and polyadenylated mRNAs, for instance through the RNAi machinery. The 5' and 3' ends of the resulting 3' and 5' fragments, respectively, are not protected and thus accessible to the Xrn1 or exosome/Ski7/Ski2-Ski3-Ski8 pathways. Such bypass-mechanisms are also employed by certain mRNA quality control pathways like no-go decay and nonstop decay (see section 2.4.1).

### 2.1.3 Relative contributions of 5' and 3' decay routes

The Xrn1 (5' to 3') and exosome/Ski7/Ski2-Ski3-Ski8 (3' to 5') decay routes are not essential in yeast. Synthetic lethality only results when components of both pathways are deleted (Johnson and Kolodner, 1995; Anderson and Parker, 1998; van Hoof et al., 2000b), indicating that the two pathways operate redundantly. Currently it is still a matter of debate which pathway constitutes the major route for mRNA decay. Yeast strains deleted for either of the two pathways show a slow-growing phenotype only when the decapping/Xrn1 route is targeted (Beelman et al., 1996; Dunkley and Parker, 1999; Giaever et al., 2002; Anderson and Parker, 1998), suggesting that the 5' to 3' route prevails. On the other hand, more recent transcriptome-wide RNA profiling studies suggest that the impact of these deletions is less pronounced as thought in the first place (Houalla et al., 2006; He

et al., 2003). Ultimately, the decay route for a given transcript may depend on many factors like growth phase, nature of the studied transcripts etc., making it difficult (and possibly unnecessary) to discriminate major and minor pathways in a general fashion.

While both pathways may be similar in terms of quantitative contribution to overall decay, from a conceptual point of view the exosome-mediated 3' to 5' decay is set apart: the exosome is not only involved in degradation but also functions in processing and maturation of certain RNA precursors. This means that, depending on the given substrate, the exosome can either totally degrade an RNA substrate or partially trim it in an apparently very controlled fashion (see also section 2.2.1).

## **2.2 The exosome is the major eukaryotic 3' to 5' ribonuclease complex**

The exosome is a multi-subunit ribonuclease complex that was first identified from tandem affinity-purification experiments in budding yeast (Mitchell et al., 1997). It is a processive 3' exonuclease, i.e. it removes nucleotides one after the other from the 3' end of the RNA without dissociating from the substrate (Dziembowski et al., 2007; Liu et al., 2006). Subsequent work identified homologous complexes in other eukaryotes (including plants) and in archaea, highlighting its universally conserved role in RNA catabolism. Since then, biochemical and structural work has shaped our understanding of the molecular architecture of exosome complexes and their enzymatic function. Genetic experiments delineated many of the pathways and protein factors that deliver substrates to the exosome. In parallel, an ever-growing number of substrates for the exosome is being identified, particularly by systems-wide approaches.

### **2.2.1 Functions of the eukaryotic exosome: From maturation to degradation**

The exosome operates both in the cytoplasm and the nucleus of eukaryotic cells. It processes a set of substrates that is remarkably broad, including RNAs produced by each of the three major RNA polymerases. Nonetheless, the exosome displays differential activity towards these substrates: first, it can fully degrade a given substrate to remove it completely from the cellular pool. Second, it can partially trim the 3' end, a process important for maturation of certain RNA precursors.

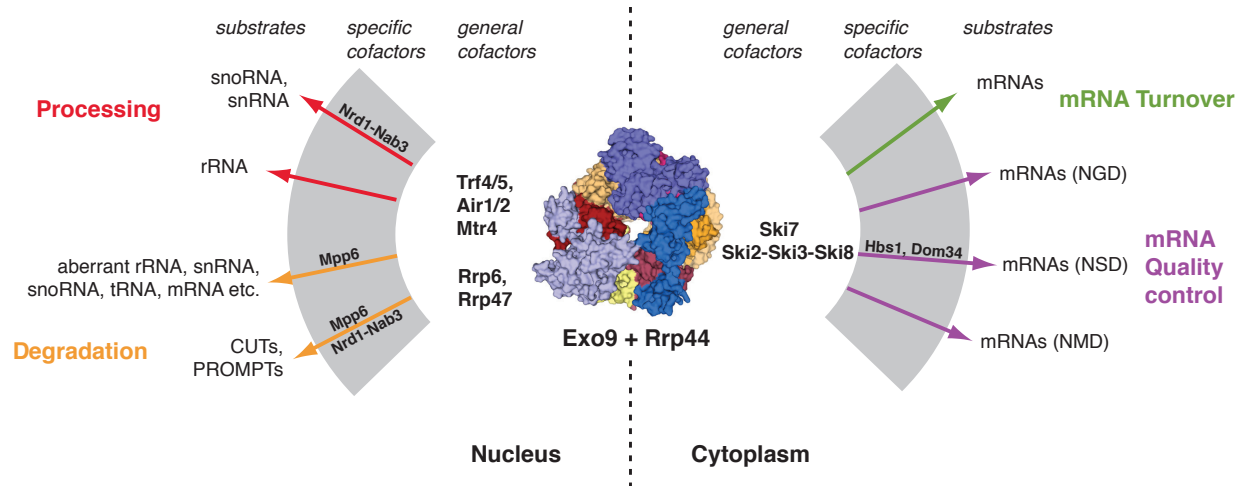


**Figure 2.2** | The many functions of the RNA exosome in the eukaryotic cell. Pathways that feed into the exosome in the nucleus (left panel) and in the cytoplasm (right panel) are indicated along with the required general and specific cofactors and reported substrates. Functions are grouped in the four categories Processing, Degradation, mRNA Turnover and mRNA Quality control (adapted from Lykke-Andersen et al., 2009).

The exosome's role as a maturation factor seems to be limited to the nucleus (Fig. 2.2). Here, it participates in 3' end processing of small nuclear RNAs (snRNAs) and small nucleolar RNAs (snoRNAs) (Allmang et al., 1999; Mitchell and Tollervy, 2003; van Hoof et al., 2000a; Egecioglu et al., 2006; Kim et al., 2006) as well as ribosomal RNAs (rRNAs) (Dez et al., 2006; Allmang et al., 1999; Kadaba et al., 2006). Moreover, the nuclear exosome has been involved in quality control and surveillance of snoRNAs, snRNAs, transfer RNAs (tRNAs) and pre-mRNAs, where it targets erroneous transcripts for degradation (Allmang et al., 1999; Torchet et al., 2002; Bousquet-Antonelli et al., 2000; Dez et al., 2006; Hilleren et al., 2001). More recently, evidence accumulated that the exosome clears promoter-associated transcriptional byproducts that are non-coding but may have regulatory functions, for instance cryptic unstable transcripts (CUTs) (Wyers et al., 2005; Davis and Ares, 2006).

To date, the cytoplasmic exosome has not been linked to processing but rather appears confined to total degradation of substrate RNAs (Fig. 2.2). In the cytoplasm, the exosome functions in general mRNA turnover, where it operates redundantly with the 5' to 3' degradation machinery (Anderson and Parker, 1998). It was also shown to elimi-

nate 5' fragments generated by the RNAi-induced silencing complex (RISC) during RNAi (Orban and Izaurralde, 2005). In mammalian cells, mRNAs containing AU-rich elements (ARE) are recruited to the exosome via dedicated ARE-binding proteins, resulting in rapid decay of substrates (Chen et al., 2001).

Besides its role in mRNA turnover, the exosome serves as endpoint for several cytoplasmic quality control pathways. Transcripts containing a premature termination codon are cotranslationally targeted by the nonsense-mediated decay (NMD) pathway and subsequently degraded by the cytoplasmic exosome (Mitchell and Tollervey, 2003). Transcripts that lack a stop codon altogether were shown to be eliminated in an exosome-dependent fashion (van Hoof et al., 2002). This pathway is referred to as non-stop decay (NSD). Another quality control pathway termed no-go decay (NGD) has been described that targets mRNAs that are stalled on the translating ribosome. Stalled transcripts are cleaved endonucleolytically which presumably releases them from the ribosome and generates free 5' fragments that are cleared by the cytoplasmic exosome (Doma and Parker, 2006).

## 2.2.2 The architecture of the core exosome and its conservation through all domains of life

### Structure and activity of the archaeal exosome

The first insights into the molecular architecture of the exosome came from crystal structures of the archaeal complexes (Büttner et al., 2005; Lorentzen and Conti, 2005; Lorentzen et al., 2007). The archaeal exosome is built from the three subunits Rrp41, Rrp42 and Rrp4 (or Csl4) (Fig. 2.3B, central panel). Rrp41 and Rrp42 are homologous to bacterial ribonuclease (RNase) PH, a phosphorolytic ribonuclease. Three Rrp41-Rrp42 hetero-dimers assemble into a six-membered ring (termed the RNase PH ring). Rrp4 contains an N-terminal S1-homology domain and a C-terminal K-homology (KH) domain. A trimeric ring of Rrp4 (termed the S1/KH cap) assembles on top of the RNase PH ring, creating the 9-subunit archaeal exosome (Fig. 2.3A, central panel). Rrp4 can be substituted by Csl4 which contains an S1 domain and a zinc-knuckle domain. *In vivo*, the S1/KH cap is homomeric for Rrp4 or Csl or contains a combination of both (Evgenieva-Hackenberg et al., 2003), and *in vitro* Rrp4 and Csl4 confer different substrate specificities to the archaeal exosome (Roppelt et al., 2010).

Biochemical studies showed that Rrp41 is the active subunit. It displays processive, phosphorolytic ribonuclease activity towards single stranded RNA (Büttner et al., 2005;

Lorentzen et al., 2005) but is unable to degrade through secondary structure elements like hairpins (Lorentzen and Conti, 2005). Rrp42 contributes to RNA-binding and to formation of the active site and it is required for nuclease activity of the complex (Lorentzen et al., 2005; Büttner et al., 2005). The S1/KH cap has been shown provide additional RNA binding sites to the complex that may help to regulate substrate access to the active sites.

The structures of the archaeal exosome revealed a surprisingly high similarity with bacterial polynucleotide phosphorylase (PNPase), an phosphorolytic RNase complex that forms part of the degradosome (Symmons et al., 2000). PNPase contains two RNase PH cassettes and C-terminal S1/KH domain, and this polypeptide assembles into a ho-

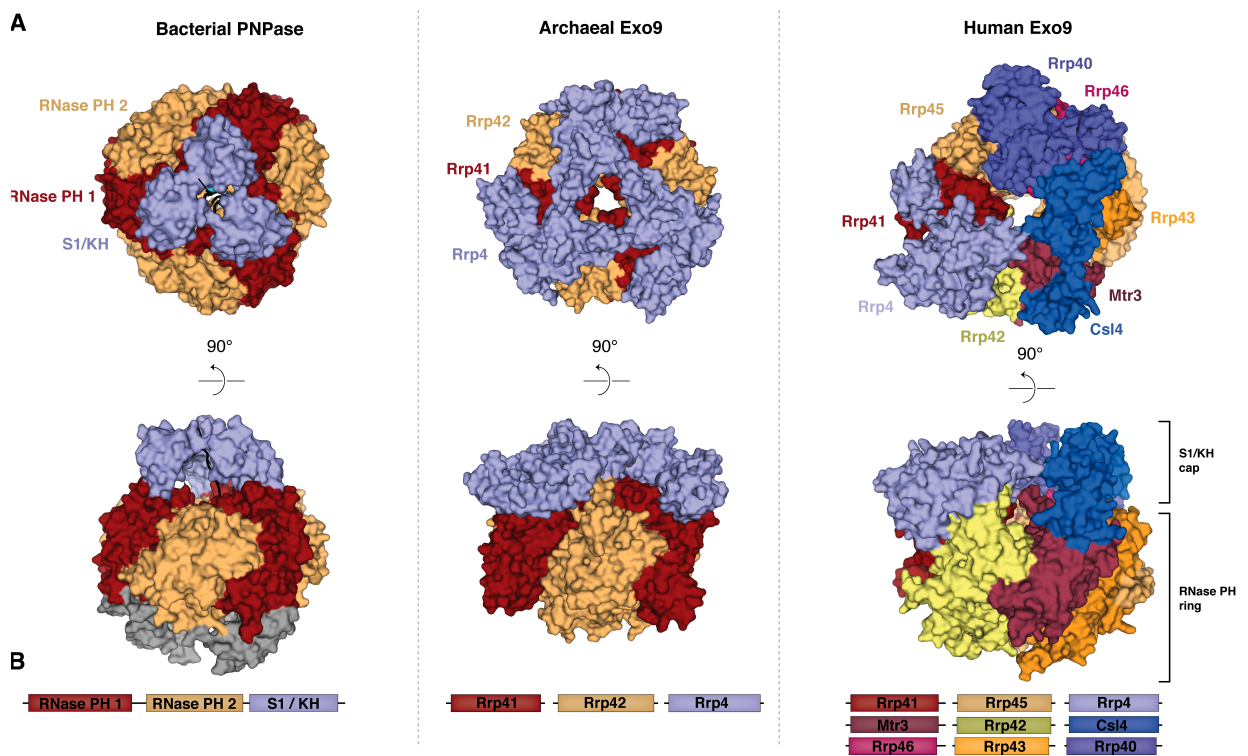


**Figure 2.3** | The molecular architecture of exosome-like complexes is conserved throughout evolution. (A) Structures of bacterial PNPase (Symmons et al., 2000), archaeal 9-subunit exosome (Lorentzen et al., 2007) and human 9-subunit exosome (Liu et al., 2006) are shown in the left, middle and right panels, respectively. RNase PH (domain 1), Rrp41 and Rrp41-like proteins are colored in red or shades thereof. RNase PH (domain 2), Rrp42 and Rrp42-like proteins in yellow or shades of yellow. S1/ KH domains or S1/ KH containing proteins in shades of blue. (B) The domain structures of the proteins corresponding to the structure in each panel are shown color-coded as above.

motrimeric complex (Fig. 2.3, left panel). Similar to the archaeal 9-subunit exosome, six RNase PH domains form a barrel-like structure that is topped by a ring containing three S1/KH domains (Fig. 2.3A, compare left and central panels). Thus, during evolution from of the archaeal complex, the RNase PH and S1/KH domains have become singled out into individual polypeptides.

### Structure of the human exosome

Subsequently, the crystal structure of the human exosome (Liu et al., 2006) showed that the 9-membered ring architecture of bacterial PNPase and archaeal exosome has been conserved during evolution of higher eukaryotes, too. In humans, the RNase PH ring of the exosome is now formed by a set of six different proteins, and the S1/KH ring by a group of three distinct polypeptides. All six RNase PH subunits are homologous to bacterial RNase PH. However two subsets can be distinguished according to sequence similarity with the two archaeal RNase PH subunits: human Rrp41, Mtr3 and Rrp46 are more similar to archaeal Rrp41 while human Rrp45, Rrp42 and Rrp43 are related more closely to archaeal Rrp42 (Fig. 2.3B). Again, three heterodimers of an Rrp41-like subunit and a Rrp42-like subunit (Rrp41-Rrp45, Rrp43-Rrp42 and Rrp46-Mtr3) assemble into the six-membered RNase PH ring of the human exosome (Fig. 2.3A, right panel). Finally, the proteins Csl4, Rrp40 and Rrp4 form the S1/KH cap of the eukaryotic exosome, completing the 9-subunit core exosome (designated Exo9). The eukaryotic S1/KH ring is structurally similar to the archaeal Rrp4/Csl4 ring, and its three subunits contain an N-terminal S1 and a C-terminal KH homology domain and are homologs of the archaeal S1/KH proteins. In the 9-subunit exosome, the S1/KH ring extend the axial cavity in the RNase PH ring, creating a central channel that reaches from the top to the bottom of the complex.

### 2.2.3 Rrp44 and Rrp6 confer activity to the eukaryotic exosome

While bacterial PNPase and the archaeal and eukaryotic exosomes share a similar architecture, their activities are markedly different. In the eukaryotic exosome, key residues of the three Rrp41-like subunits lack important catalytic residues (Liu et al., 2006). Consistently, the human and yeast 9-subunit core exosomes were found to be catalytically inactive as opposed to the phosphorolytic activity of their archaeal relative (Liu et al., 2006; Dziembowski et al., 2007). In yeast, two additional subunits impart activity to the 9-subunit exosome core: Rrp44, which localizes to nucleus and cytoplasm, and Rrp6, which

is exclusively found in the nucleus.

Rrp44 associates with the core exosome, resulting in the 10-subunit exosome (designated Exo10) that is identical in nucleus and cytoplasm. Rrp44 contains two distinct hydrolytic RNase activities. In the N-terminus, a PiLT protein N-terminus (PIN) domain confers endonuclease activity (Schneider et al., 2009; Schaeffer et al., 2009; Lebreton et al., 2008). In the C-terminus, an RNase II domain confers processive 3' to 5' exonuclease activity (Dziembowski et al., 2007; Liu et al., 2006). Structural studies have shown that Rrp44 associates via its PIN domain to the Rrp41-Rrp45 dimer (Bonneau et al., 2009), resulting in a location at the base of the RNase PH ring. In this conformation, both the PIN domain and RNase II active sites are accessible from the central channel of the core exosome.

In the yeast nucleus, Exo10 associates with another RNase, Rrp6, to create the 11-subunit exosome (Exo11). Rrp6 belongs to the RNase D family and degrades ribonucleic acids in a distributive, hydrolytic fashion from the 3' to the 5' end (Midtgaard et al., 2006; Zuo and Deutscher, 2001; Phillips and Butler, 2003). Rrp6 contains an N-terminal PMC2NT domain that mediates binding to Rrp47, followed by the RNase D catalytic core and two helicase RNase D C-terminal domains (HRDCs) (Midtgaard et al., 2006). The last HRDC domain mediates binding to Exo10 *in vivo* (Callahan and Butler, 2008). While Rrp6 remains attached to Exo10, recent experiments suggest that it can also operate independently of the Exo10 core (Callahan and Butler, 2008).

#### **2.2.4 The inactive eukaryotic exosome core retains functionality**

Even though the eukaryotic core exosome lost its activity during evolution, it retained an architecture remarkably similar to the archaeal exosome and bacterial PNPase. Moreover, in yeast all nine subunits of the exosome core are essential (Mitchell et al., 1997). This suggests that the exosome core kept certain functions distinct from nuclease activity. These functions must be closely linked to structural features that were conserved during evolution. The most striking of these features is the central pore that leads from the 3-membered S1/KH ring to the 6-membered RNase PH ring (Fig. 2.4B). The diameter of this channel is about 7 Å at its narrowest constriction and thus would allow accommodation of single stranded RNA. In case of the archaeal exosome, structural studies provide direct evidence that RNA is indeed conducted through the central pore to reach the active site of the Rrp41 subunits (Lorentzen et al., 2007; Hartung et al., 2010; Navarro et al., 2008; Lorentzen and Conti, 2005).

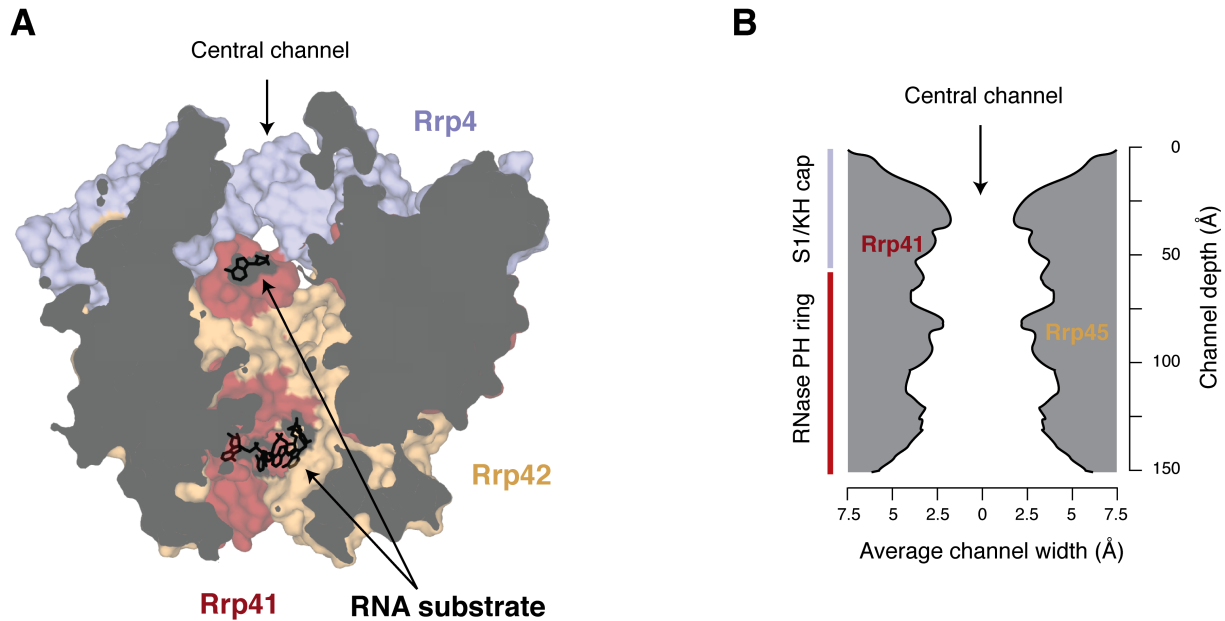


**Figure 2.4** | RNA channeling by the exosome. (A) Cut-open representation of the archaeal 9-subunit exosome bound to RNA (Lorentzen et al., 2007). Subunits are colored as in Fig. 2.3, RNA is shown in black. A central channel leads from the S1/KH ring down to the Rrp41 active sites. Electron density was observed at the entrance (top) and the active site (bottom). (B) Topology of the central channel found in the human Exo9 complex (Liu et al., 2006). The average diameter and depth (in Å) of the channel are plotted on an axial slice through the structure.

Similar results have been obtained for the yeast exosome. Electron microscopy data of Exo10 complexes bound to RNA reveal density for the nucleic acid at the S1/KH entry site and within the RNase PH ring (Malet et al., 2010). RNase protection assays demonstrated that the central pore accommodates about 31-33 nt of single stranded RNA, spanning from the S1/KH cap to the exoribonuclease site in Rrp44 (Bonneau et al., 2009). Moreover, reverse charge point mutations in conserved basic residues lining the channel decreased the activity of Rrp44 *in vitro* (Bonneau et al., 2009). Consistent with these observations, degradation of certain RNAs that contain structured regions is inhibited when Rrp44 is bound to Exo9 (Bonneau et al., 2009; Liu et al., 2006). More recently, degradation of many substrates by Exo10 *in vivo* was observed to depend on the central channel, too (Wasmuth and Lima, 2012). Taken together, these data suggest that the central cavity of the core exosome provides a transfer route for substrates to the Rrp44 active sites. Such a channeling mechanism also provides a tool to regulate access of RNA to the active sites, and this is a pre-requisite for the highly regulated functioning of the exosome in eukaryotes.

Another role for the exosome core has been proposed according to which it forms a platform for cofactor recruitment (see also section 2.1). Due to its location at the top of the RNA entry site, the S1/KH ring appears particularly suited to recruit upstream factors. Consistently, mutations in Csl4 have been shown to stabilize reporter mRNAs *in vivo* in a similar fashion as deletion of Ski7 does (Schaeffer et al., 2009). This suggests that Csl4 plays a pivotal role in cytoplasmic mRNA decay, possibly by providing a binding platform for Ski7 and the Ski2-Ski3-Ski8 complex.

The diverse substrate landscape of the exosome and its capability of differential processing (decay vs. maturation) raises the question of how exosome activity is regulated to ensure that each class of substrate is processed or degraded properly. For example, what factors discriminate an mRNA molecule that has exceeded its lifespan and is doomed to total degradation from an mRNA precursor that needs to be trimmed at the 3' end to fully mature? Since both the nuclear and the cytoplasmic exosome cores share an identical subunit composition, such factors are likely to reside outside of the core exosome complex.

## 2.3 Exosome cofactors

In fact, most functions of the exosome require a subset of helper proteins in addition to the Exo10 core complex. These proteins can be grouped into general and specific cofactors (See Fig. 2.2 and Tab. 2.1). General cofactors interact directly or indirectly with the core exosome and are required for several (sometimes unrelated) functions of the exosome. They appear to form an inner shell of regulation on the exosome.

Specific cofactors are more numerous and are only required for a small subset of substrates. Their function frequently depends on the presence of a general cofactor. Specific cofactors form an outer shell for the regulation of exosome functions.

### 2.3.1 General cofactors of the exosome

The two general cofactors of the yeast exosome are the Trf4/5-Air1/2-Mtr4 polyadenylation complex (TRAMP) and the Ski2-Ski3-Ski8 superkiller (SKI) complex which are conserved in higher eukaryotes. TRAMP and SKI localize to different cellular compartments and are required for different subsets of exosome functions (Fig. 2.2, Tab. 2.1). These differences are also reflected by differences in the subunit composition of both cofactors. While both complexes contain a homologous DExH box RNA helicase (Mtr4 in the TRAMP complex, Ski2 in the SKI complex), the remaining subunits are unrelated.

	Protein	Activity	Localization	Function
Exosome-associated	Ski7	Similar to translational GTPases like eRF3.	Cytoplasm	Binds the Ski2-Ski3-Ski8 and exosome complexes. Required for all functions of the cytoplasmic exosome, e.g. mRNA turnover and quality control.
	Rrp6	Belongs to RNase D family and has distributive 3' to 5' exonuclease activity.	Nucleus	Binds to the exosome and to Rrp47. Required for exosome-mediated processing of snRNAs, snoRNAs and rRNAs. Involved in pre-mRNA surveillance. Exosome-independent roles have been described.
General cofactors	Ski2-Ski3-Ski8 (SKI)	Contains the Ski2 DExH box helicase.	Cytoplasm	Required for all known functions of the cytoplasmic exosome. Interacts with the exosome via Ski7 N-terminus.
	Trf4/5-Air1/2-Mtr4 (TRAMP)	Contains polyadenylation (Trf4/5) and helicase activities (Mtr4).	Nucleus	Required for most functions of the nuclear exosome. Mtr4 can also operate independently. Physical interaction with the exosome unclear.
Specific cofactors	Rrp47	RNA-binding protein	Nucleus	Interacts genetically and physically with Rrp6. Preferably binds structured RNAs and is required for degradation of certain stable RNAs by Rrp6.
	Mpp6	RNA-binding protein	Nucleus	Involved in rRNA maturation. Knockout is synthetic lethal in $\Delta$ Rrp47, $\Delta$ Rrp6 strains. Binds pyrimidine-rich sequences.
	Nrd1-Nab3-Sen1	RNA-binding proteins (Nrd1, Nab3), RNA helicase (Sen1)	Nucleus	Promotes termination of noncoding genes and CUTs. Required with TRAMP and the exosome for degradation of CUTs.

**Table 2.1** | Cofactors of the *S. cerevisiae* exosome. The proteins are grouped into exosome-associated, general or specific cofactors.

## RNA helicases as cofactors for exosome-like complexes

Ski2 and Mtr4 are paralogs and share 29 % sequence identity and 45 % similarity. Both enzymes belong to the superfamily II (SF2) of helicases and utilize energy from adenosine triphosphate (ATP)-hydrolysis to unwind RNA duplexes (for review see Pyle, 2008; Singleton et al., 2007; Jankowsky and Fairman, 2007; Lohman et al., 2008). While to date no helicase has been associated with the function of the archaeal exosome, such a link has been found for the bacterial degradosome. The degradosome is a major prokaryotic RNase complex that is formed by PNPase, the archetype of the exosome, as well as RNase E and enolase (Carpousis, 2007). A fourth subunit was found to be RhlB, an ATP-dependent SF2 RNA helicase (Py et al., 1996). Degradation of certain structured RNA substrates requires ATP *in vitro* (Py et al., 1996), and several studies showed that degradosome-mediated RNA decay depends on RhlB *in vivo* (Bernstein et al., 2002, 2004; Khemici et al., 2005; Khemici and Carpousis, 2004).

These observations suggest that RhlB locally unwinds secondary structure elements in substrate RNAs to facilitate their degradation by the bacterial degradosome. The presence of an ATP-dependent RNA helicase in each of the general cofactor complexes of the eukaryotic exosome led to the extrapolation of this working hypothesis to the function of the TRAMP and SKI complexes in concert with the eukaryotic exosome. It is thought that both general cofactors harness the helicase activity (Ski2 or Mtr4) to assist degradation of challenging substrates.

## The Trf4/5-Air1/2-Mtr4 polyadenylation complex (TRAMP)

The yeast TRAMP complex is formed by a poly(A)-polymerase (Trf4 or Trf5), a DExH box RNA helicase (Mtr4) and a zinc knuckle-containing RNA-binding protein (Air1 or Air2) (LaCava et al., 2005). TRAMP was shown to stimulate the nuclear exosome *in vitro* and *in vivo* (Vanacova et al., 2005; LaCava et al., 2005). Remarkably, this stimulation depends on the poly(A) polymerase (PAP)-activity of TRAMP (Vanacova et al., 2005; Kadaba et al., 2006). Similarly, the Mtr4 helicase activity is essential *in vivo* to degrade structured substrates like initiator tRNA ( $tRNA_i^{Met}$ ) (Wang et al., 2008). Based on these observations, a model emerged according to which Trf4/5 adds poly(A) tails to the 3' end of a given substrate. This creates a "landing platform" that allows the helicase Mtr4 to efficiently bind and unwind secondary structure elements of a given substrate (e.g. tRNA). Unwinding of otherwise structured RNAs renders them accessible for degradation by the exosome.

Efforts to pin down the mechanism of TRAMP-mediated exosome activation on the molecular level are still ongoing. Recent advances include the crystal structure of the Trf5 catalytic domain bound to Air2, which suggests that the C-terminal zinc knuckles of Air2p mediate binding to the polymerase rather than being RNA-binding motifs (Hamill et al., 2010). Structural and biochemical studies on Mtr4 have confirmed its identity and activity as a DExH box helicase (Bernstein et al., 2008; Weir et al., 2010). Mtr4 was also found to contain an usual accessory domain that emerges from the helicase core. It has structural similarity to ribosomal KOW domains that are known to bind structured RNAs. Consistently, the Mtr4 KOW domain exhibits affinity towards structured RNAs (Weir et al., 2010) and is required for rRNA processing *in vivo* (Jackson et al., 2010).

### The Ski2-Ski3-Ski8 complex (SKI)

In the yeast cytoplasm, the proteins Ski2, Ski3, Ski8 as well as Ski7 have been found to be general cofactors for the exosome. Ski2 is a putative DExH box type RNA helicase that was shown to form a complex with Ski3 and Ski8 *in vivo* (Brown et al., 2000). This Ski2-Ski3-Ski8 was further shown to interact with the exosome via the eRF3-homolog Ski7 (Araki et al., 2001; Wang et al., 2005). The Ski2-Ski3-Ski8 complex is required for all cytoplasmic functions of the exosome. Because Ski2 is closely related to Mtr4, its helicase activity is assumed to contribute to exosome activation similarly to Mtr4 within the TRAMP complex. However, experimental evidence for such a mechanism is still lacking. A detailed introduction to the Ski2-Ski3-Ski8 complex is given in the section 2.4.

### 2.3.2 Specific exosome cofactors

Several specific exosome cofactors have been described (Tab. 2.1). Frequently, these factors are nuclear-specific RNA-binding proteins that operate in concert with other cofactors. For instance, the nuclear Rrp47 is a partner protein of Rrp6 with apparent specificity for structured RNAs (Stead et al., 2007; Mitchell et al., 2003). It is indispensable for certain aspects of Rrp6/exosome-mediated processing of stable RNAs like snRNAs and snoRNAs (Mitchell et al., 2003; Costello et al., 2011). Rrp47 has been proposed to act as a chaperone that stabilizes interactions of Rrp6 with its cognate substrates, thus enhancing substrate specificity and efficacy of degradation (Stead et al., 2007).

Another nuclear exosome cofactor, Mpp6, appears somewhat similar to Rrp47 in that it is an RNA-binding protein that is synthetic lethal in an Rrp6 deletion background

(Milligan et al., 2008). In contrast to Rrp47, Mpp6 preferentially binds pyrimidine-rich sequences (Milligan et al., 2008). Mpp6 co-purifies with exosome-containing complexes (Krogan et al., 2006) and plays a role in exosome-mediated decay of noncoding RNAs (Milligan et al., 2008), but additional data are needed to define its role more precisely.

Yet another annotated exosome cofactor is the nuclear Nrd1-Nab3-Sen1 complex, which is recruited by RNA polymerase II C-terminal domain to terminate CUTs (Carroll et al., 2007; Vasiljeva et al., 2008). CUTs are then degraded by the nuclear exosome in a TRAMP-dependent fashion that also requires Nrd1-Nab3-Sen1 (Arigo et al., 2006; Thiebaut et al., 2006), suggesting that this cofactor complex orchestrates transcription termination and degradation for certain transcript classes.

## 2.4 The SKI complex is a general cofactor of the cytoplasmic exosome

The SKI genes were originally identified from mutations in *S. cerevisiae* strains that were infected by the double-stranded Killer virus. These mutations raised the levels of viral RNA species which exacerbated the killer phenotype of infected cells (hence the name Superkiller) (Toh et al., 1978; Ridley et al., 1984). The phenotypes could later be mapped to a set of seven genes which were identified as Ski2, Ski3 and Ski8 (Widner and Wickner, 1993; Rhee et al., 1989; Matsumoto et al., 1993) as well as Ski7 (Benard et al., 1999), Ski1/Xrn1 (Larimer and Stevens, 1990), Ski4/Csl4 (van Hoof et al., 2000b) and Ski6/Rrp41 (Benard et al., 1998). Subsequent studies suggested that those proteins acted by repressing expression of viral poly(A) RNA (Widner and Wickner, 1993). Eventually, translational repression was found to be independent of the presence of viral RNA (Johnson and Kolodner, 1995), indicating a general role of the Ski proteins in mRNA catabolism.

### 2.4.1 Functions of the Ski2-Ski3-Ski8 complex

#### Cytoplasmic 3' to 5' mRNA turnover requires the Ski proteins and the exosome

Deletion of either of the SKI2, SKI3, SKI7 or SKI8 genes was found to block 3' to 5' degradation (Anderson and Parker, 1998; van Hoof et al., 2000b), and conditional knock-outs of SKI6/RRP41 and RRP4 produced similar phenotypes, suggesting that these six proteins operate along the same pathway. Since Rrp41 and Rrp4 had been previously reported as subunits of the exosome complex (Mitchell et al., 1997), this results annotated

the exosome as the catalytic component of the 3' to 5' degradation pathway and identified the Ski proteins as required cofactors.

Ski2, Ski3 and Ski8 form a stable complex *in vivo* in the yeast cytoplasm (Brown et al., 2000; Synowsky and Heck, 2008). SKI7, the last of the original Superkiller genes, encodes a homolog of translational guanosine triphosphate hydrolases (GTPases) like eRF3 and EF1- $\alpha$  (Benard et al., 1999; Atkinson et al., 2008). Its N-terminal region was shown to co-immunoprecipitate with the Ski2-Ski3-Ski8 complex and with exosome subunits (presumably Rrp4 and Csl4) (Wang et al., 2005; Araki et al., 2001; van Hoof et al., 2002). Deletion of the Ski7 N-terminus *in vivo* interferes with cytoplasmic 3' to 5' decay. In contrast, the C-terminal GTPase domain of Ski7 is dispensable for exosome-mediated mRNA turnover (Araki et al., 2001; van Hoof et al., 2000b).

### **The Ski2-Ski3-Ski8 complex and Ski7 are essential for cytoplasmic mRNA quality control**

Apart from its role in mRNA turnover, the Ski2-Ski3-Ski8 complex is required for at least three distinct mRNA quality control pathways that feed into the cytoplasmic exosome (Fig. 2.2). First, NMD targets transcripts with premature stop codons through concerted action of the Upf1-2-3 complex and stalled ribosomes (reviewed in Chang et al., 2007; Conti and Izaurralde, 2005). Recruitment of other surveillance factors eventually releases the stalled mRNA which is subsequently degraded from the 5' end (Xrn1) and the 3' end (exosome/Ski7/Ski2-Ski3-Ski8) (Takahashi et al., 2003; Mitchell et al., 2003).

Second, transcripts that cause the ribosome to stall, e.g. due to unresolvable secondary structure, are eliminated by NGD. Two dedicated translation factors, Dom34 and Hbs1, are crucial to this pathway. Dom34 (homologous to eRF1) mimicks tRNA (Lee et al., 2007) and binds along with the translational GTPase Hbs1 in the A-site of the stalled ribosome (Becker et al., 2011; Chen et al., 2010). While the endonuclease activity that releases the stalled transcript remains elusive, the exosome and Ski proteins were found responsible for the degradation of the resulting 5' fragment and Xrn1 for elimination of the corresponding 3' fragment (Doma and Parker, 2006).

Third, transcripts that lack a stop codon altogether are targeted by NSD. NSD substrates are readily degraded by the exosome in a Ski2-Ski3-Ski8- and Ski7-dependent fashion (Frischmeyer et al., 2002; van Hoof et al., 2002). This pathway depends on the Ski7 N-terminal region but also requires the C-terminal GTPase domain (Frischmeyer et al., 2002). This prompted a model according to which ribosomes that are stalled on read-

through messages recruit Ski7 (possibly together with an eRF1-homolog) and thus induce exosome- and Ski2-Ski3-Ski8-dependent mRNA decay. In contrast to NMD and NGD, the 5' to 3' degradation machinery is dispensable for NSD (Frischmeyer et al., 2002). To date all known exosome-mediated 3' to 5' decay routes in the cytoplasm require Ski7 as well as the Ski2-Ski3-Ski8 complex.

Consistently with their cytoplasmic localization, mutations in the Ski proteins do not affect functions of the nuclear exosome like rRNA processing (van Hoof et al., 2000b; Anderson and Parker, 1998). Taken together, these observations prompted the concept that Ski2-Ski3-Ski8 in concert with Ski7 is a general cofactor of the cytoplasmic exosome.

## 2.4.2 Towards the architecture of the *S. cerevisiae* Ski2-Ski3-Ski8 complex

### **Ski2 is a putative ATP-dependent RNA helicase of the DExH-box family**

Ski2 has eluded biochemical and structural characterization so far, and knowledge about its function mainly comes from extrapolation of data concerning related helicases like yeast Mtr4 or the archaeal Hel308. Ski2 is a SF2 helicase, hallmark of which are two RecA-like domains that contain a set of at least seven conserved motifs that mediate binding to nucleotides or RNA (Fig. 2.5, for review see Pyle, 2008; Jankowsky and Fairman, 2007). While all SF2 enzymes bind nucleic acids and hydrolyze ATP, their molecular functionality can vary greatly in terms of processivity, directionality and unwinding activity (translocation-dependent or not). Ski2 and Mtr4 are most closely related to each other, and together with Hel308 they have traditionally been classified as members of the family of DExH-box RNA helicases (Pyle, 2008), bearing the eponymous Asp-Glu-X-His motif (X being any amino acid) within the first RecA domain.

X-ray structures of *A. fulgidus* Hel308 (Büttner et al., 2007) and of yeast Mtr4 (Jackson et al., 2010; Weir et al., 2010) have revealed the common architecture of the DExH-box family (Fig. 2.6). These structures confirmed the canonical RecA domains and identified a C-terminal helical domain formed by a winged helix (WH) and the so-called ratchet domain (Büttner et al., 2007). The helical domain packs against both RecA-like domains opposite of their RNA-binding motifs. This arrangement creates a funnel through which the nucleic acid is threaded during translocation (Fig. 2.6). A conserved  $\beta$ -hairpin wedges between guide and passenger strand, and translocation on the guide strand presumably induces unwinding of double stranded nucleic acids. ATP-dependent duplex unwinding

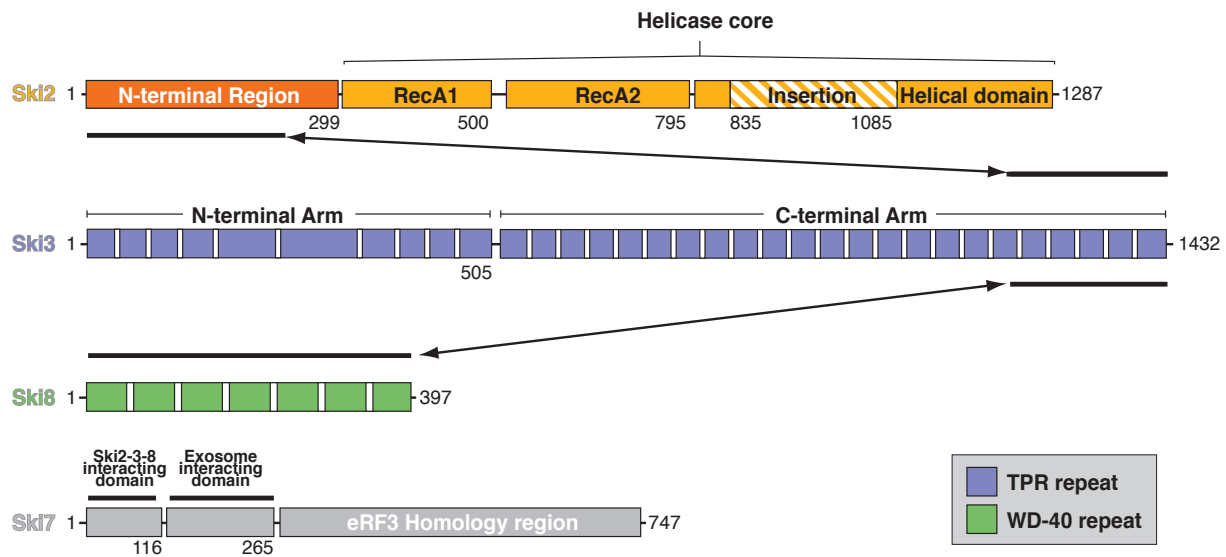


**Figure 2.5** | Domain structure of *Ski2*, *Ski3*, *Ski8* and *Ski7*. *Ski2* is colored in shades of yellow and orange, *Ski3* in blue, *Ski8* in green and *Ski7* in gray (This color scheme is maintained throughout the manuscript). The domain boundaries are extracted from the structural information obtained in this study. Black bars and arrows indicate interacting domains.

with 3' to 5' directionality has been demonstrated for Mtr4 (Bernstein et al., 2008) and can be expected for Ski2 as well.

Recently, a refinement to the classification of SF2 helicases was proposed (Fairman-Williams et al., 2010), according to which the DExH-box family is split into the DEAH-type and the Ski2-like groups with Ski2 and Mtr4 belonging to the latter. While this new classification is based on phylogenetic and functional data, recent work has revealed structural similarities between members of both groups, blurring the proposed borders. For instance, the DEAH-type Rrp43 (Walbott et al., 2010; He et al., 2010) and the Ski2-like Mtr4 (Jackson et al., 2010; Weir et al., 2010) both share the WH and ratchet domains as well as the unwinding  $\beta$ -hairpin.

Apart from the well-conserved helicase domains, Ski2 contains two regions of unknown function (Fig. 2.5). First, a poorly conserved N-terminal region (residues 1 - 299) that is followed by the RecA domains. Second, a long insertion (residues 835 - 1085) within the WH domain. Mtr4 contains an insertion at an equivalent position (Fig. 2.6, lower panel), but this domain is not conserved with Ski2 in terms of primary sequence. In Mtr4, this region was shown to fold in to a KOW domain that is connected to the helicase core through a helical stalk. The domain, dubbed arch domain (Jackson et al., 2010), is located

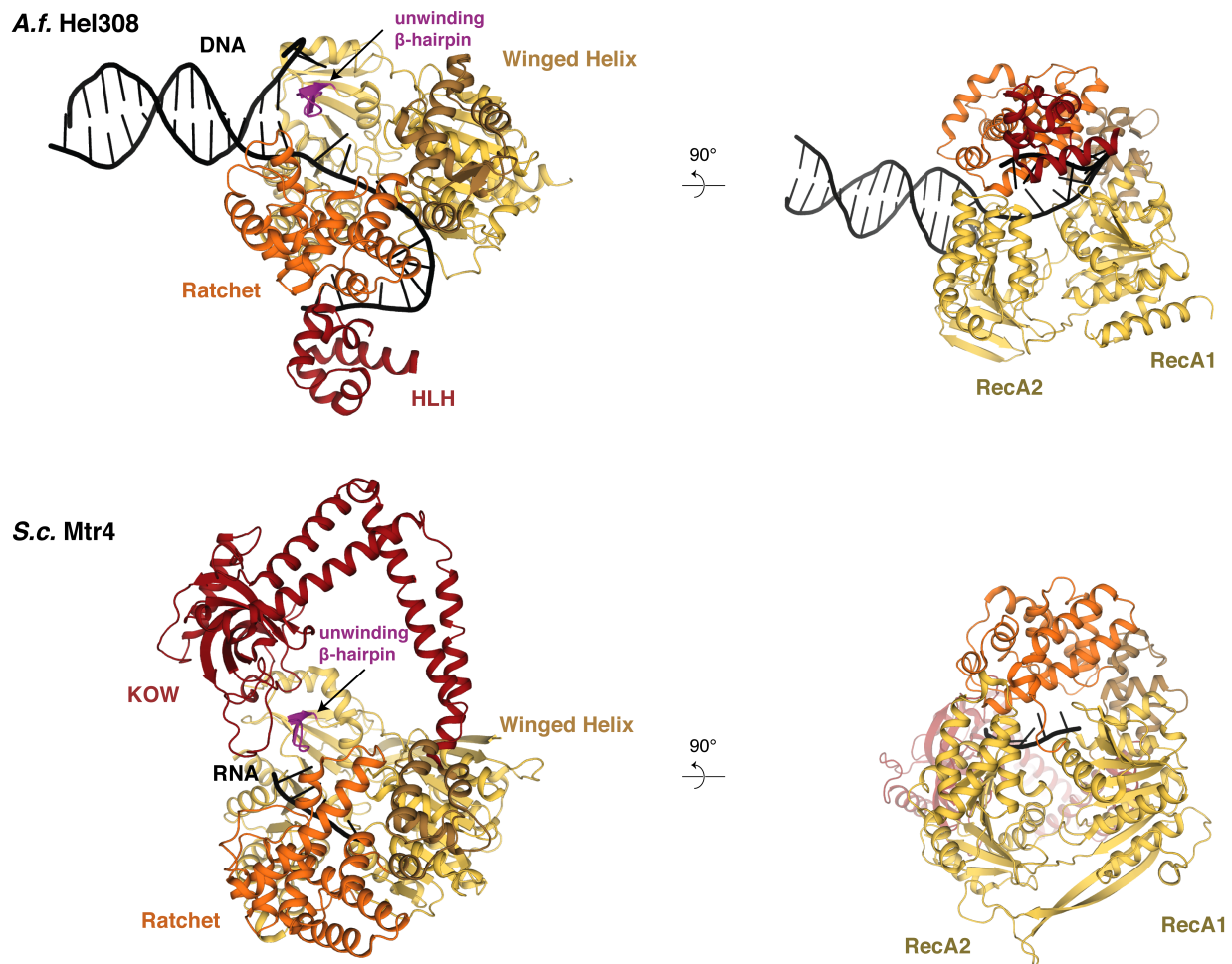


**Figure 2.6** | The molecular architecture of DExH-box helicases. The upper panel shows the crystal structure of *A. fulgidus* Hel308 bound to a partially unwound DNA duplex (shown in black) (Büttner et al., 2007). Both RecA domains are colored in yellow, the WH domain in dark yellow and the ratchet domain in orange. The WH and ratchet domains form a helical domain that packs against both RecA domains. A C-terminally inserted helix-loop-helix (HLH) motif is colored in red and an unwinding  $\beta$ -hairpin in magenta. The lower panel displays the crystal structure of *S. cerevisiae* Mtr4 (Weir et al., 2010). The RecA, WH and ratchet domains are conserved with *A. fulgidus* Hel308 and are colored accordingly. The inserted KOW domain is shown in red.

above the RNA entry site into the helicase core (Weir et al., 2010). It binds structured RNAs *in vitro* (Weir et al., 2010) and is required for 5.8S rRNA processing *in vivo* (Jackson et al., 2010). Given that the insertion in Ski2 and the KOW domain in Mtr4 occur are well conserved positions in the protein, it can be speculated that Ski2 contains a similar domain.

### **Ski3 and Ski8 are predicted to be structural proteins**

Ski3 is a large protein (1432 residues) that is predicted to contain several tetratricopeptide (TPR) motifs (Fig. 2.5). However, number and position of the TPRs vary according to the algorithms used for prediction. In general, a single TPR motif is formed by two helices that pack against each other in an antiparallel fashion (Hirano et al., 1990; Sikorski et al., 1990; Das et al., 1998). TPRs typically occur as arrays of several contiguous motifs. Since the individual repeats within an array are rotated by about 60°, the resulting solenoid has a superhelical shape. TPRs are known as protein-protein interaction motifs, and to date no other ligands than (poly-)peptides have been identified (for review see Zeytuni and Zarivach, 2012). TPR proteins are thus thought of as typical scaffold proteins that organize large protein complexes. Indeed, this role has been highlighted by several structures of TPR-mediated protein assemblies (Zhang et al., 2010; Lapouge et al., 2000; Paczkowski et al., 2012) and has been proposed for Ski3, too.

The previously determined crystal structure of Ski8 (Madrona and Wilson, 2004; Cheng et al., 2004) shows that it contains seven Trp-Asp 40 (WD40) repeats that fold into a seven-bladed  $\beta$ -propeller (Figs. 2.5 and 2.7). The seven blades form a disc-like structure with top and bottom surfaces that are connected by a narrow constriction. While  $\beta$ -propeller proteins sometimes display intrinsic enzymatic activities (e.g. as hydrolases or reductases), they act more frequently as ligand-binding domains or mediators of protein-protein interactions (reviewed in Chen et al., 2011). As no enzymatic activity had been demonstrated for Ski8, a structural role for Ski8 has been proposed in the context of the Ski2-Ski3-Ski8 complex. In line with this hypothesis, mutations on a conserved hydrophobic cage at the top surface of Ski8 have been shown to interfere with binding of Ski8 *in vivo* (Cheng et al., 2004), pointing to a potential interface within the Ski2-Ski3-Ski8 complex. Mass-spectrometry analysis of endogenous samples from yeast indicate a 1:1:2 stoichiometry for Ski2-Ski3-Ski8 complex with two copies of the Ski8 subunit (Synowsky and Heck, 2008). Nevertheless, the function of Ski8 within the complex as well as the necessity for two copies of this subunit remain unclear.

### **Ski8 is also part of a meiotic DNA recombination complex**

In yeast, Ski8 has a second role apart from its function in mRNA degradation. During meiosis, DNA double-strand break (DSB) formation is the first step in crossing over of homologous chromatids, a process that eventually leads to genetic diversification. The catalytic activity of DSB initiation has been pinned down to the protein Spo11, a relative

of subunit A from archaeal topoisomerase VI (topo VI-A) that is well conserved in higher eukaryotes (Keeney et al., 1997; Bergerat et al., 1997; Nichols et al., 1999). Spo11 does not exert its activity alone but functions in a large protein complex (for review see Cole et al., 2010). During meiosis, yeast Ski8 localizes to the nucleus where it directly associates with Spo11, which is required for the cleavage activity of Spo11 (Arora et al., 2004; Tesse et al., 2003). Other subunits are then recruited to the Spo11-Ski8 dimer, but the exact order and architecture of this DSB-initiation complex is unknown. In a transesterification reaction, a conserved catalytic tyrosine residue in Spo11 covalently attaches to the target DNA strand, and this process eventually establishes the DSB. After removal of Spo11 from the DNA, the 5' ends are resected and single stranded overhangs recruit the canonical DSB repair machinery, leading to a productive crossover. Alternatively, synthesis-dependent strand annealing restores the initial chromatid configuration (non-crossover) (reviewed in Cole et al., 2010).

How and why Ski8 has to interact with Spo11 for initiation of this process remains largely unknown because detailed biochemical and structural information are missing. However, residues in the C-terminus of Spo11 (Arora et al., 2004) and on the top surface of Ski8 (Cheng et al., 2004) have been linked with the formation of the Spo11-Ski8 complex. Interestingly, a similar “moonlighting” function of Ski8 has been reported in hu-

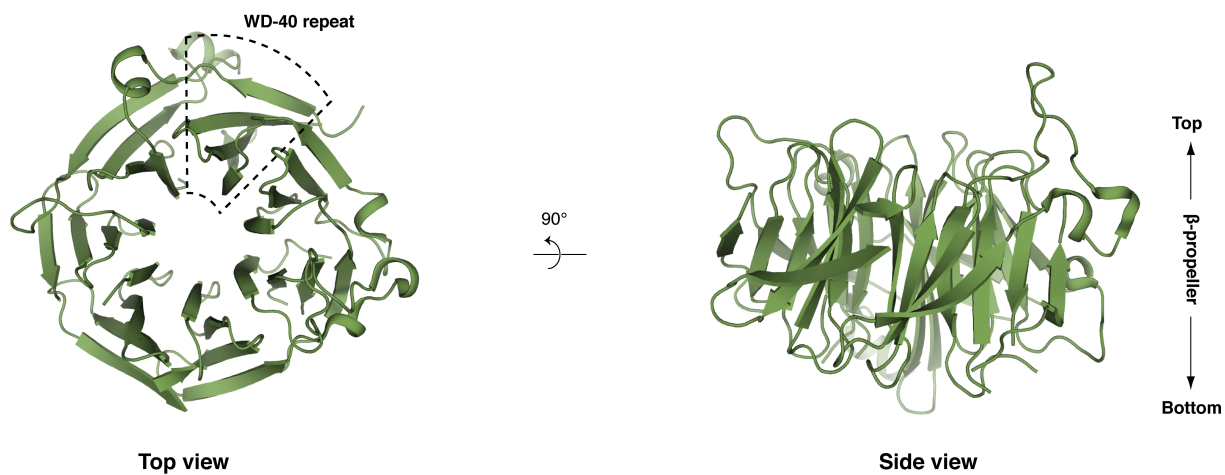


**Figure 2.7** | The crystal structure of *S. cerevisiae* Ski8 (1S4U, Cheng et al., 2004). The structure is shown in top and side views that are related as indicated. One of the seven blades of the  $\beta$ -propeller is indicated, as well as the location of top and bottom surfaces.

mans. Here, the Ski8 homolog Wdr61 was shown to also participate in the Paf1 complex that links transcription elongation with histone modification (Zhu et al., 2005).

### Domain interactions within the Ski2-Ski3-Ski8 complex and with Ski7

While structural and biochemical characterization of the Ski2-Ski3-Ski8 complex is limited to the crystal structure of Ski8, some information concerning the complex architecture is available from yeast-two-hybrid and co-immunoprecipitation experiments (see also Fig. 2.5) (Wang et al., 2005; Brown et al., 2000). First, the interaction of Ski2 and Ski8 depends on the presence of Ski3, consistent with the notion of Ski3 as a scaffold for the complex. Second, the N-terminus of Ski2 (residues 1 - 279) is required and sufficient for interaction with Ski3 *in vivo* (Wang et al., 2005). Third, the C-terminus of Ski3 (residues 1206 - 1432) mediates binding to Ski8 (Wang et al., 2005). This agrees well with the observation that a conserved hydrophobic patch on the top surface of Ski8 (Fig. 2.7) is required for interaction with Ski3 *in vivo* (Cheng et al., 2004). Co-immunoprecipitation experiments indicate that Ski7 interacts directly with Ski3 but not with Ski2 (Wang et al., 2005). The interaction site resides in the Ski7 N-terminus (residues 1 - 96), while the Ski7 sub-N-terminus (80 - 264) mediates binding to the exosome (Araki et al., 2001).

#### 2.4.3 Conservation of the Ski2-Ski3-Ski8 complex and Ski7 in higher eukaryotes

The Ski2-Ski3-Ski8 complex subunits are conserved in higher eukaryotes. For instance, homologs of the yeast genes SKI2 (twister/SKI2), SKI3 (CG8777 / SKI3) and SKI8 (CG3909) are present in flies (Seago et al., 2001; Orban and Izaurralde, 2005). These homologs appear to be functional, too. For example, the 5' fragments generated by the RNAi silencing mechanism in *D. melanogaster* are degraded by the exosome, and this pathway requires the SKI2, SKI3 and SKI8 gene products (Orban and Izaurralde, 2005). These results indicate that *Drosophila* SKI2, SKI3 and SKI8 are in fact orthologs of their yeast relatives, and that the function of the Ski2-Ski3-Ski8 complex in mRNA decay may be conserved in higher eukaryotes.

In humans, homologs of SKI2 (SKI2W), SKI3 (TTC37) and SKI8 (WDR61) exist (Dangel et al., 1995; Lee et al., 1995), and recombinant Ski2w protein shows ATP hydrolase (ATPase) activity in an RNA-dependent manner (Dangel et al., 1995). Another study shows that Ski2w, Ttc37, and Wdr61 proteins form a stable complex (designated the

“hSki” complex) *in vivo* in the cytoplasm and nucleus of human cells, and that the human Ski8 homolog Wdr61 also forms part of the Paf1 complex (Zhu et al., 2005), a multi-subunit assembly that orchestrates histone modification with transcription elongation (for review see Tomson and Arndt, 2012). The same study also speculates that the Paf1 complex physically interacts with the hSki complex and thus links transcription elongation to mRNA surveillance (Zhu et al., 2005).

In contrast to the core Ski complex proteins, a Ski7 homolog has not been identified to date in higher eukaryotes. In fact, phylogenetic studies have identified Ski7 only in the genus *Saccharomyces* where it appears to have emerged by a gene duplication event from the eRF3/Hbs1 family (Atkinson et al., 2008). How the Ski2-Ski3-Ski8 complex is recruited to the exosome in species lacking Ski7 remains unclear.

Collectively, these results from fly and human show that the Ski2-Ski3-Ski8 complex has been conserved in higher eukaryotes. They further suggest that, despite the loss of Ski7, the Ski2-Ski3-Ski8 complex most likely has maintained its function in mRNA turnover and quality control during evolution and possibly gained functional plasticity.

## 2.5 Scope of this work

The requirement of the Ski proteins for exosome-mediated degradation of mRNAs in the cytoplasm has been demonstrated. However, a thorough molecular understanding of the Ski2-Ski3-Ski8 complex as well as its mode of activation of the exosome remain elusive. No biochemical and structural information is available except for the crystal structure of Ski8 (Cheng et al., 2004; Madrona and Wilson, 2004). The notion that Ski2 activates the exosome by ATP-dependent remodeling of structured RNAs or RNPs lacks experimental support and remains a hypothesis.

Thus, the present work aims to contribute to the understanding of the molecular biology of the Ski2-Ski3-Ski8 complex in exosome-mediated mRNA decay, using a structural and biochemical approach. Particular questions to be addressed are: What is the role of the individual subunits within the complex? Is the helicase activity of Ski2 regulated through its partner proteins? Can we gain mechanistic insights into interactions of RNA with the Ski2-Ski3-Ski8 complex, Ski7 and the exosome, and can these insights help to understand how the Ski proteins activate the cytoplasmic exosome?

## 3 Results

### 3.1 Crystal Structure of the *S. cerevisiae* Ski2 heli- case

This article was published in 2012 in **RNA** (Issue 18(1), pages 124-134). The supplemental material is attached at the end of the article (pages 39-40). Figures and tables of the manuscript are referred to by “3.1.X”, where X follows the numbering within the manuscript.

# The crystal structure of *S. cerevisiae* Ski2, a DExH helicase associated with the cytoplasmic functions of the exosome

FELIX HALBACH, MICHAELA RODE, and ELENA CONTI<sup>1</sup>

Department of Structural Cell Biology, Max-Planck-Institute of Biochemistry, D-82152 Martinsried, Germany

## ABSTRACT

Ski2 is a cytoplasmic RNA helicase that functions together with the exosome in the turnover and quality control of mRNAs. Ski2 is conserved in eukaryotes and is related to the helicase Mtr4, a cofactor of the nuclear exosome involved in the processing and quality control of a variety of structured RNAs. We have determined the 2.4 Å resolution crystal structure of the 113 kDa helicase region of *Saccharomyces cerevisiae* Ski2. The structure shows that Ski2 has an overall architecture similar to that of Mtr4, with a core DExH region and an extended insertion domain. The insertion is not required for the formation of the Ski2–Ski3–Ski8 complex, but is instead an RNA-binding domain. While this is reminiscent of the Mtr4 insertion, there are specific structural and biochemical differences between the two helicases. The insertion of yeast Mtr4 consists of a  $\beta$ -barrel domain that is flexibly attached to a helical stalk, contains a KOW signature motif, and binds *in vitro*-transcribed tRNA<sub>i</sub><sup>Met</sup>, but not single-stranded RNA. The  $\beta$ -barrel domain of yeast Ski2 does not contain a KOW motif and is tightly packed against the helical stalk, forming a single structural unit maintained by a zinc-binding site. Biochemically, the Ski2 insertion has broad substrate specificity, binding both single-stranded and double-stranded RNAs. We speculate that the Ski2 and Mtr4 insertion domains have evolved with different properties tailored to the type of transcripts that are the substrates of the cytoplasmic and nuclear exosome.

**Keywords:** RNA degradation; exosome; helicase; structure

## INTRODUCTION

The exosome is a conserved and essential macromolecular complex that degrades RNA substrates processively from the 3' end (Mitchell et al. 1997). In the eukaryotic nucleus, the exosome is involved in the maturation of ribosomal RNAs, small nuclear RNAs, and small nucleolar RNAs (Allmang et al. 1999; van Hoof et al. 2000a; Houalla et al. 2006). It functions in the turnover of pre-mRNAs and cryptic unstable transcripts (Bousquet-Antonelli et al. 2000; Hilleren et al. 2001; Wyers et al. 2005). It is also required in quality-control mechanisms that target aberrant nuclear RNAs such as hypomodified tRNA<sub>i</sub><sup>Met</sup> (Kadaba et al. 2004; Vanacova et al. 2005). In the cytoplasm, the exosome is involved in bulk mRNA turnover (Anderson and Parker 1998; van Hoof et al. 2000b) and also participates in surveillance pathways for the degradation of aberrant mRNAs that contain a premature stop codon (Lejeune

et al. 2003; Mitchell and Tollervey 2003; Takahashi et al. 2003; Gatfield and Izaurralde 2004) or lack one altogether (van Hoof et al. 2002).

The 10-subunit core of the eukaryotic exosome is identical in the nuclear and cytoplasmic compartments (for review, see Lorentzen et al. 2008a; Lykke-Andersen et al. 2009). Nine subunits form a barrel-like structure (Exo-9) with a prominent central channel (Liu et al. 2006). The structure of Exo-9 is similar to that of the archaeal exosome and bacterial PNPase, but lacks the catalytic activity that is characteristic of these prokaryotic complexes (Büttner et al. 2005; Lorentzen et al. 2005, 2007). The nuclease activity of the core exosome complex is conferred by the tenth subunit, Rrp44 (Liu et al. 2006; Dziembowski et al. 2007; Lebreton et al. 2008; Schaeffer et al. 2009; Schneider et al. 2009). Both Rrp44 and the catalytically inactive Exo-9 subunits are essential in yeast. The Exo-9 subcomplex modulates the activity of Rrp44 (Liu et al. 2006; Dziembowski et al. 2007; Lorentzen et al. 2008b) and binds RNA substrates, guiding them through the central channel to reach the exoribonuclease active site (Bonneau et al. 2009). The Exo-9 structure is also thought to recruit peripheral factors, such as the nuclear ribonuclease Rrp6 (Liu et al. 2006; Cristodero

<sup>1</sup>Corresponding author.

E-mail [conti@biochem.mpg.de](mailto:conti@biochem.mpg.de).

Article published online ahead of print. Article and publication date are at <http://www.rnajournal.org/cgi/doi/10.1261/rna.029553.111>.

et al. 2008) and the cytoplasmic protein Ski7 in yeast (Araki et al. 2001; Dziembowski et al. 2007).

These peripheral factors associate with the core exosome to form an outer shell that is compartment specific (for review, see Lebreton and Seraphin 2008). In the nucleus, the exosome functions together with the helicase Mtr4, which associates with a poly(A) polymerase (Trf4/Trf5) and a zinc finger protein (Air1/Air2) to form the TRAMP complex (LaCava et al. 2005). In the cytoplasm, the exosome functions together with the Ski complex (Anderson and Parker 1998). The Ski (Superkiller) proteins were originally identified from recessive mutations that exacerbated the “killer” phenotype, that is, the ability of yeast strains containing a dsRNA virus to produce a toxin that kills other strains (Toh-E and Wickner 1979; Ridley et al. 1984; Johnson and Kolodner 1995). These studies showed that the Superkiller mutations resided in a helicase (Ski2), a tetratricopeptide-repeat (TPR) protein (Ski3), and a WD40 protein (Ski8) in addition to the cytoplasmic 5′–3′ exoribonuclease (Xrn1). The Ski2, Ski3, and Ski8 proteins were later found to associate in a complex in vivo (Brown et al. 2000). The Ski complex has been implicated in many 3′–5′ cytoplasmic degradation pathways mediated by the exosome, including normal RNA turnover (Anderson and Parker 1998; van Hoof et al. 2000b; Araki et al. 2001), nonsense-mediated decay (Mitchell and Tollervey 2003), nonstop decay (van Hoof et al. 2002), and RNA interference (Orban and Izaurralde 2005). The Ski and exosome complexes interact not only genetically, but also physically via the yeast Ski7 protein (Araki et al. 2001).

The presence of a helicase in both the Ski and TRAMP complexes is intriguing. These exosome-associated helicases are thought to contribute to substrate recognition, to unwind secondary structure elements in the nucleic acids, or to remove bound proteins, and eventually to present favorable single-stranded RNA substrates to the exosome (Lebreton and Seraphin 2008; Houseley and Tollervey 2009). The parallel between the nuclear and cytoplasmic regulators of the exosome is further compounded by the fact that Ski2 and Mtr4 share significant sequence similarity (~35% sequence identity in the predicted helicase region). Previous structural work has shown that Mtr4 has a helicase core similar to that found in other members of the DExH family (Jackson et al. 2010; Weir et al. 2010), including the archaeal DNA helicase Hel308 (Büttner et al. 2007) and the splicing helicase Prp43 (He et al. 2010; Walbott et al. 2010). In addition, Mtr4 features a 200 aa insertion that contains a helical stalk and a  $\beta$ -barrel domain. The latter is structurally and functionally similar to KOW domains, which were shown to bind structured RNAs in ribosomal proteins (Kyrpides et al. 1996; Selmer et al. 2006; Zhang et al. 2009). Consistently, the KOW domain of yeast Mtr4 is required for 5.8S rRNA processing in vivo (Jackson et al. 2010) and binds transcribed tRNA<sub>i</sub><sup>Met</sup> in vitro (Weir et al. 2010). Thus, the specific structural features of Mtr4

are in line with its biological functions in ribosomal RNA processing and quality control (de la Cruz et al. 1998; van Hoof et al. 2000a). Sequence alignments and secondary structure predictions suggest that Ski2 has a helicase and an insertion domain similar to those in Mtr4. However, the potential RNA substrates that Ski2 encounters in the cytoplasm are different from those that are recognized by Mtr4 in the nucleus. This raises the question as to whether Ski2 has specific features as compared with Mtr4. To address this question, we have analyzed the structural and biochemical properties of Ski2 from *Saccharomyces cerevisiae*.

## RESULTS AND DISCUSSION

### Structure determination of the 113 kDa helicase region of yeast Ski2

To initiate the biochemical and structural characterization of Ski2, we expressed and purified the full-length (f.l.) *S. cerevisiae* ortholog (residues 1–1287) from insect cells. Ski2 is predicted to have a low-complexity N-terminal region that has previously been shown to interact with Ski3 by yeast two-hybrid and coimmunoprecipitation analyses (Wang et al. 2005). Limited proteolysis of f.l. Ski2 in combination with N-terminal sequencing and mass spectrometry indicated the presence of a protease-resistant fragment of ~113 kDa that lacked the N-terminal 295 residues and included the predicted helicase region (data not shown). We therefore engineered a construct of yeast Ski2 encompassing residues 296–1287 (designated Ski2- $\Delta$ N) (Fig. 1A). Yeast Ski2- $\Delta$ N was obtained from expression in insect cells and crystallized in the presence of adenosine 5′-( $\beta,\gamma$ -imido)triphosphate (AMPPNP), a nonhydrolyzable ATP analog.

The crystal structure of Ski2- $\Delta$ N was solved to 2.4 Å resolution by the multiwavelength anomalous diffraction (MAD) method using a gold derivative (see Table 1 for data collection and refinement statistics). The DExH helicase core of Ski2- $\Delta$ N could be built and refined almost in its entirety (with the exception of a disordered region between residues 542 and 606) and included electron density for an AMPPNP molecule. An additional domain could be identified that was inserted between residues 830 and 1086, consisting of a helical part and a globular region. However, the electron density for the globular domain, in particular, was weak and did not allow us to trace the polypeptide chain with an unambiguous amino acid register. The structure of Ski2- $\Delta$ N bound to AMPPNP was refined to 2.4 Å resolution, with  $R_{\text{work}}$  of 23.8%,  $R_{\text{free}}$  of 27.5%, and good stereochemistry (Table 1). We proceeded by engineering and crystallizing the region corresponding to the inserted domain (residues 835–1085, designated Ski2-insert). The structure of Ski2-insert was determined de novo by the single anomalous diffraction (SAD) method using a crystal derivatized with gold. Crystals of Ski2-insert contained five

Halbach et al.

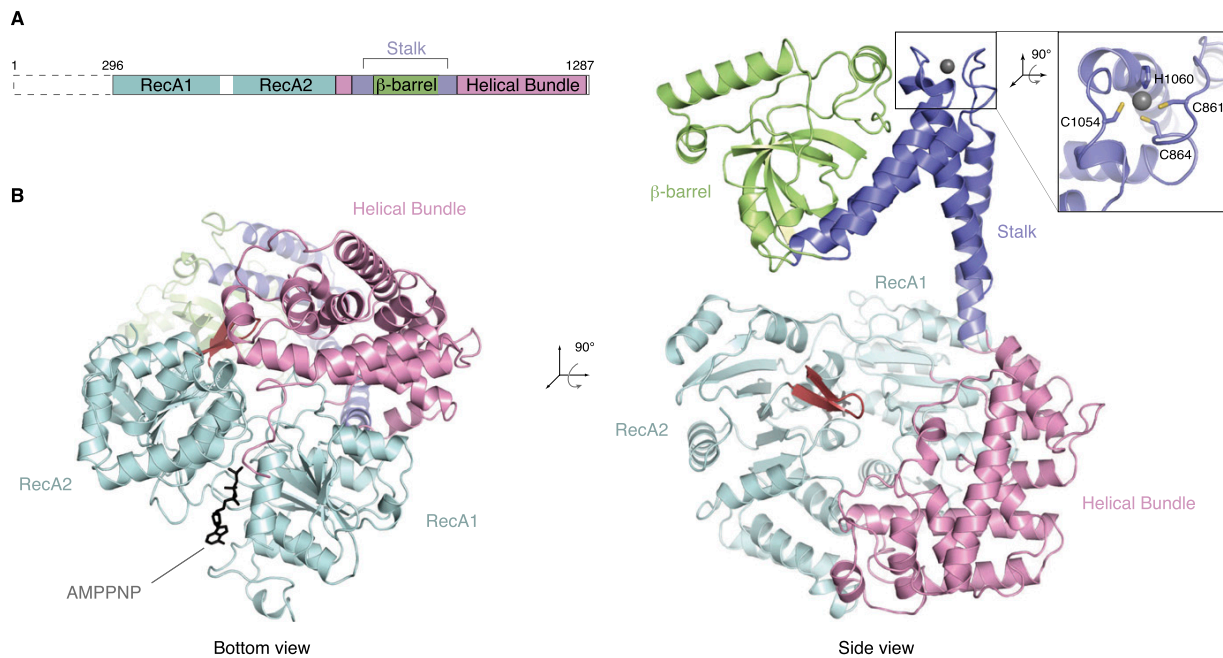


**FIGURE 1.** Ski2 consists of a DEXH helicase core and a protruding insertion domain. (A) Schematic representation of the domain organization of Ski2. The N-terminal low-complexity region not included in the crystal structure is indicated by a dashed box (residues 1–295 in *S. cerevisiae*), and the helicase region is shown with the domains in different colors as in the crystal structure below. (B) The *S. cerevisiae* Ski2- $\Delta$ N crystal structure (lacking the N-terminal 295 residues). This composite model was generated from the Ski2- $\Delta$ N and the Ski2-insert crystal structures (see text). The two views are related by a 90° rotation as indicated. In the DEXH core, the RecA domains are colored in cyan and the helical bundle domain in light pink. The unwinding  $\beta$ -hairpin is highlighted in red, and AMPPNP (black) is depicted in stick representation. The stalk helices and the  $\beta$ -barrel in the insertion domain are shown in blue and green, respectively. A zinc ion present in the stalk region is shown as a gray sphere. A close-up shows the CCCH-type coordination of the zinc ion.

independent molecules in the asymmetric unit. After density modification procedures, the electron density of Ski2-insert was continuous and allowed unambiguous model building. The structure of Ski2-insert was refined at 3.25 Å resolution, with  $R_{\text{work}}$  of 23.6% and  $R_{\text{free}}$  of 25.7% (Table 1). The model of Ski2-insert was then placed into the electron density of Ski2- $\Delta$ N with relatively minor rigid-body adjustments to give a composite model as is discussed below.

### Ski2 contains a conserved DEXH core

Ski2- $\Delta$ N contains two distinct structural features: a compact DEXH helicase core and an elongated insertion (Fig. 1B). The helicase core of Ski2 is similar to that previously described for other DEXH proteins, including the DNA helicase Hel308 (Büttner et al. 2007), the splicing helicase Prp43 (He et al. 2010; Walbott et al. 2010), and the exosome helicase Mtr4 (Jackson et al. 2010; Weir et al. 2010). Briefly, the core consists of a circular arrangement of two RecA domains (RecA1 and RecA2) and a helical bundle (Fig. 1B, left). The two RecA domains contain the characteristic helicase signature motifs that mediate substrate binding and ATP hydrolysis (for review, see Pyle 2008). Also conserved is the unwinding  $\beta$ -hairpin in the RecA2

domain (residues 741–752, in red in Fig. 1B). This  $\beta$ -hairpin is characteristic of DEXH-box helicases and has been shown in the Hel308 structure to wedge between the two strands of a DNA duplex that is being unwound at the 5' end as it approaches the DEXH core (Supplemental Fig. 1A; Büttner et al. 2007).

In the AMPPNP-bound structure of Ski2- $\Delta$ N, the two RecA domains face each other in a closed conformation (Fig. 1B, left). The conformation is similar to that of other DEXH proteins determined in the presence of nucleic acids. For instance, both RecA domains of Ski2 superpose to those of the Mtr4-ADP-RNA structure (Weir et al. 2010), with a root mean square deviation (RMSD) of 1.3 Å over 373 C $\alpha$  atoms. The overall orientation of the two RecA domains in Ski2 and other DEXH proteins is restrained by the interaction with the helical bundle. AMPPNP binds between the two RecA domains with the adenosine base sandwiched by Phe328 of RecA1 and Arg767 of RecA2 (Supplemental Fig. 1B). The phosphates of AMPPNP are arranged around motif I in a canonical conformation, but electron density for the  $\gamma$ -phosphate is weak. This may be caused by the absence of magnesium, which would be required to properly coordinate the phosphate groups, but was not present in the crystallization condition of Ski2- $\Delta$ N.

**TABLE 1.** Crystallographic data collection, phasing, and refinement statistics for the Ski2-ΔN and Ski2-insert structures

Crystal (Data set)	Ski2-ΔN (4A4Z)				Ski2-insert (4A4K)	
	Native	Au (peak)	Au (inflection)	Au (remote)	Native	Au (peak)
Space group	P2 <sub>1</sub> 2 <sub>1</sub> 2 <sub>1</sub>				C2	
Cell dimensions a, b, c (Å)	82.8, 118.6, 129.5	84.6, 119.8, 129.7			230.5, 123.1, 153.2	229.2, 124.9, 149.4
α, β, γ (°)	90, 90, 90	90, 90, 90			90, 131.1, 90	90, 130.7, 90
Molecules/asymmetric unit	1				5	
Data collection						
Wavelength (Å)	0.988	1.037	1.040	0.995	0.999	1.040
Resolution (Å)	119–2.40 (2.53–2.4)	120–2.80 (2.95–2.8)	130–2.80 (2.95–2.8)	130–2.80 (2.95–2.8)	96–3.25 (3.43–3.25)	96–4.2 (4.43–4.20)
R <sub>sym</sub>	6.0 (60.0)	7.6 (58.6)	7.7 (68.8)	11.2 (102)	9.3 (66.1)	8.5 (76.9)
I/σI	17.0 (3.1)	16.5 (3.0)	16.7 (2.8)	19.2 (3.1)	8.4 (1.5)	14.8 (3.3)
Completeness (%)	99.9 (100)	100 (100)	100 (100)	100 (100)	99.6 (99.9)	99.9 (100)
Multiplicity	5.5	3.8	3.8	7.8	2.9	4.5
Phasing						
Phasing Power	0.3		0.3	0.3	n.a	
Mean figure of merit	0.37			0.29		
Refinement						
Resolution	39–2.40				57–3.25	
No. unique reflection	50,434				50,773	
R <sub>work</sub> /R <sub>free</sub> (%)	23.8/27.5				23.6/25.7	
Real space correlation coefficient	0.73				0.76	
B-factors						
Protein	66.5				113.1	
Solvent	48.3				89.7	
Stereochemistry						
RMSD bond lengths (Å)	0.003				0.002	
RMSD bond angles (°)	0.64				0.36	
Ramachandran outliers (%)	0.2				0.0	
Ramachandran favored (%)	96.1				97.0	

The highest resolution shell is shown in parenthesis. The figure of merit numbers are given as a mean value over all resolution shells. The real-space correlation coefficient was calculated for the final refined model against a simulated annealing composite omit map, and the stereochemistry of the refined models was analyzed with the *MolProbity* webserver (Chen et al. 2010).

### An insertion domain protrudes from the Ski2 DExH core

The DExH core of Ski2 has an insertion of about 250 residues that occurs in the middle of the helical bundle domain (Fig. 1A). The insertion forms an elongated structure that protrudes from the core, extending by ~50 Å from the unwinding β-hairpin that marks the position of the 5' end of RNA bound to the DExH core (Fig. 1B, right; Supplemental Fig. 1A). The insertion folds into two pairs of antiparallel helices (α1–α4 and α2–α3), which connect to a distal β-barrel domain (Fig. 2A). The insertion is a rather flexible feature of the structure. First, the crystallographic temperature factors increase significantly as compared with the core (60 Å<sup>2</sup> for the DExH core, 120 Å<sup>2</sup> for helices α1–α4, 145 Å<sup>2</sup> for helices α2–α3, and 130 Å<sup>2</sup> for the barrel). Second, we observe domain movements when comparing the insertion domain in the two structures that

we determined: Superposition of the helices α1–α4 in the Ski2-ΔN and Ski2-insert structures results in a rotation of ~15° in the position of helices α2–α3 and the β-barrel (Supplemental Fig. 1C). Despite the flexibility, the electron density is well defined in the structure of Ski2-insert (Supplemental Fig. 1D).

In contrast to the DExH core, the insertion is poorly conserved even among yeast species (Supplemental Fig. 2). Yet, it is a characteristic feature of exosome helicases: in Mtr4 an insertion occurs at an equivalent position in the sequence and with a comparable topology of secondary structure elements (Fig. 2A,B). The structure of the helical stalk of Ski2 is similar to that of Mtr4 in that it forms an L-like shape with the α1–α4 and α2–α3 pairs of helices roughly perpendicular to each other. In the case of yeast Ski2, the two pairs of helices are connected by a zinc-binding CCCH-type motif (Fig. 1B, right). Although no zinc was present in the purification or crystallization

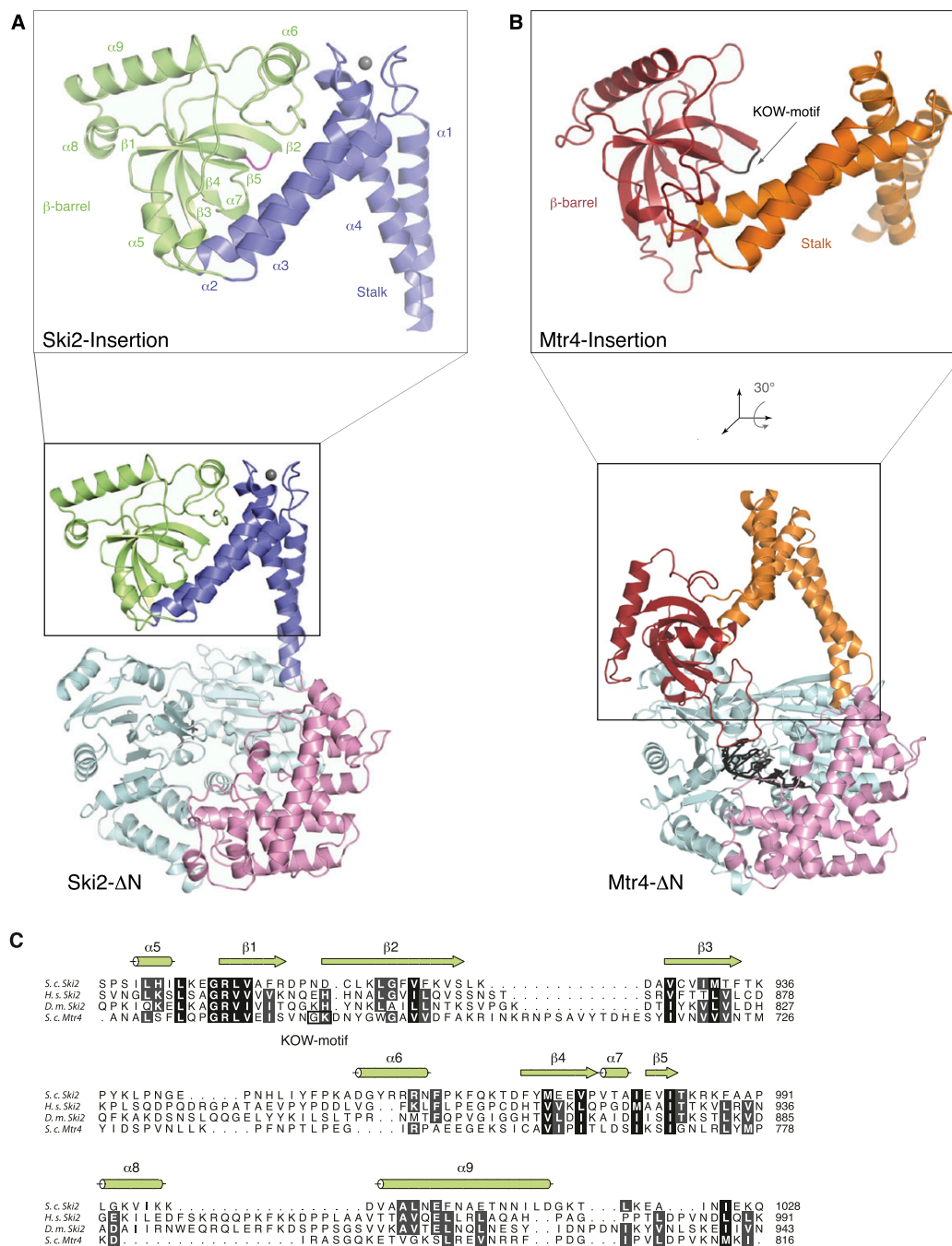


**FIGURE 2.** The exosome helicases Ski2 and Mtr4 have a similar architecture. (A) The structure of yeast Ski2- $\Delta$ N as shown in Figure 1B, with the same color scheme as in Figure 1. The close-up view shows the insertion domain with the secondary structure elements labeled. The  $\beta$ 1- $\beta$ 2 loop is highlighted in magenta. (B) The structure of yeast Mtr4- $\Delta$ N (pdb code 2xgj) is shown in the same orientation as Ski2- $\Delta$ N in A, after optimal superposition of the DExH core. The domains in the DExH core are colored as in Ski2- $\Delta$ N, the stalk is shown in orange, and the  $\beta$ -barrel in red. For the close-up view, the insertion domain has been reoriented as indicated so that the  $\beta$ -barrel is in the same orientation as the Ski2  $\beta$ -barrel in A. The  $\beta$ 1- $\beta$ 2 loop in the  $\beta$ -barrel containing the KOW signature motif is depicted in black. (C) A structure-based sequence alignment of the  $\beta$ -barrel domains of *S. cerevisiae* (*S.c.*) Ski2 and Mtr4. The secondary structure elements of Ski2 are indicated. The alignment includes Ski2 sequences from *Homo sapiens* (*H.s.*) and *Drosophila melanogaster* (*D.m.*). Conservation is indicated in shades of gray and the KOW motif of Mtr4 is indicated by a black box. Sequence conservation between Ski2 and Mtr4 is low in the insertion region and mostly restricted to structural residues that define the  $\beta$ -barrel. A comprehensive sequence alignment is shown in Supplemental Figure 2.

buffers, additional electron density is present at the center of a coordination sphere formed by Cys861, Cys864, Cys1054, and His1060. The density is consistent with a zinc ion, the presence of which was confirmed by X-ray fluorescence (data not shown). This zinc-binding site has a structural role in forming the hinge region that connects the stalk and the  $\beta$ -barrel domain. The four residues that coordinate the zinc ion are conserved in Ski2 orthologs in fungi, but not, for example, in metazoans (Supplemental Fig. 2), where other intramolecular interactions might serve a similar structural role.

The core structure of the  $\beta$ -barrel domain of Ski2 is also similar to that of Mtr4. The corresponding  $\beta$ -strands superpose with an RMSD of 2.6 Å, while the connecting loops vary in sequence, length, and conformation. The evolutionarily conserved residues are mostly restricted to positions on the  $\beta$ -strands pointing into the hydrophobic core (Fig. 2C). A key difference between the Ski2 and Mtr4  $\beta$ -barrels is located in the loop connecting strands  $\beta$ 1 and  $\beta$ 2. The  $\beta$ 1– $\beta$ 2 loop of yeast Mtr4 contains a KOW-domain signature motif (Gly686 and Lys687), a surface feature that is characteristic of domains involved in binding structured RNAs in ribosomal proteins such as bacterial L24 and eukaryotic L26 (Kypides et al. 1996; Selmer et al. 2006; Zhang et al. 2009). The KOW motif is not present in the corresponding  $\beta$ 1– $\beta$ 2 loop of Ski2. In addition, this loop is not accessible to solvent (Fig. 2A). The barrel and the stalk of Ski2 interact via an extensive intramolecular interface (Fig. 2A; Supplemental Fig. 1D), suggesting that they form a single structural unit. These structural differences are also reflected in the biochemical properties of the two domains: while the  $\beta$ -barrel of Mtr4 is stable when expressed and purified in isolation (Weir et al. 2010), we could only obtain expression of a soluble  $\beta$ -barrel-containing fragment of Ski2 when including the  $\alpha$ 2– $\alpha$ 3 helices and the zinc-binding site (data not shown).

### The Ski2 insertion contributes to RNA binding

The overall structural similarity between the two exosome helicases suggests that the insertion of Ski2 functions analogously to that of Mtr4 in terms of contributing a second RNA-binding site in addition to the one expected in the DExH core. To experimentally test whether the Ski2 insertion participates in RNA binding, we used electrophoretic mobility shift assays (EMSA) and compared the RNA-binding properties of Ski2 in the presence and absence of the insertion domain (Ski2- $\Delta$ N and Ski2- $\Delta$ N- $\Delta$ insert) (Fig. 3A). The Ski2- $\Delta$ N- $\Delta$ insert mutant was engineered by replacing residues 835–1085 with a linker sequence (Gly-Ser-Arg-Gly) and behaved like Ski2- $\Delta$ N in biochemical purifications. A single-stranded poly(A) 40-mer RNA (ssA40) bound strongly to Ski2- $\Delta$ N, but markedly less well to Ski2- $\Delta$ N- $\Delta$ insert (Fig. 3A, left). A similar pattern was detected when using a double-stranded 27-mer (ds27) as

substrate (Fig. 3A, right). We conclude that the insertion domain increases the affinity of Ski2 for RNA. Consistently, the insertion alone (Ski2-insert, residues 835–1085) showed robust binding to single-stranded and double-stranded RNAs (ss40 and ds27) (Fig. 3B). The Ski2 insertion was also able to bind unmodified tRNA<sup>Met</sup> *in vitro* (Fig. 3C), pointing to the broad substrate-binding properties of this domain. This contrasts to the specialized KOW domain of Mtr4, which binds unmodified tRNA<sup>Met</sup> (Weir et al. 2010), but does not show significant binding to single-stranded RNA (Fig. 3B).

As discussed above, the KOW sequence motif is not present in the equivalent  $\beta$ 1– $\beta$ 2 loop in the Ski2-insertion. We thus asked which surface features of the Ski2 insert are involved in the interaction with RNA. Calculation of an electrostatic surface potential revealed a prominent positively charged patch on the opposite side of the  $\beta$ 1– $\beta$ 2 loop, stretching from the hinge region to the tip of the domain (Fig. 3D, top). This surface patch is partly organized by hydrogen bonds between the conserved Arg903 and the carbonyl groups of two adjacent loops, which are characterized by several positively charged residues (Fig. 3D, bottom). The central arginine residue is also present in yeast Mtr4 (Arg678), while the specific features of the loops diverge between Ski2 and Mtr4 (Fig. 2C). To perturb the positively charged surface patch of the Ski2 insertion, we mutated Arg903 to a glutamic acid. We purified the Ski2-insert R903E mutant with a similar protocol as the wild-type Ski2-insert and compared their binding properties using EMSA assays (Fig. 3E). We found that binding to single-stranded RNA was impaired in the Ski2-insert R903E mutant, while binding to double-stranded RNA was not affected. These results indicate that the charged surface patch on the Ski2  $\beta$ -barrel domain is the major binding site for single-stranded RNA. They also suggest the presence of a different or more complex binding site for the recognition of double-stranded RNAs. We conclude that the insertion domain of Ski2 binds both single-stranded and structured RNA substrates. It increases the RNA-binding capabilities of the helicase by providing a second interaction site in addition to that of the DExH core.

### The Ski2 insertion is not required to form the Ski complex

We next tested whether the insertion of Ski2 is required to mediate protein–protein interactions with the other subunits of the Ski complex. The core of the Ski complex is formed by the interaction of Ski2 with a large TPR protein (Ski3) and a small WD40 protein (Ski8). Yeast two-hybrid and coimmunoprecipitation data suggest that the N-terminal region of Ski2 mediates binding to Ski3, which in turn interacts with Ski8 (Wang et al. 2005). In line with these data, coexpression of f.l. Ski2, Ski3, and Ski8 in insect

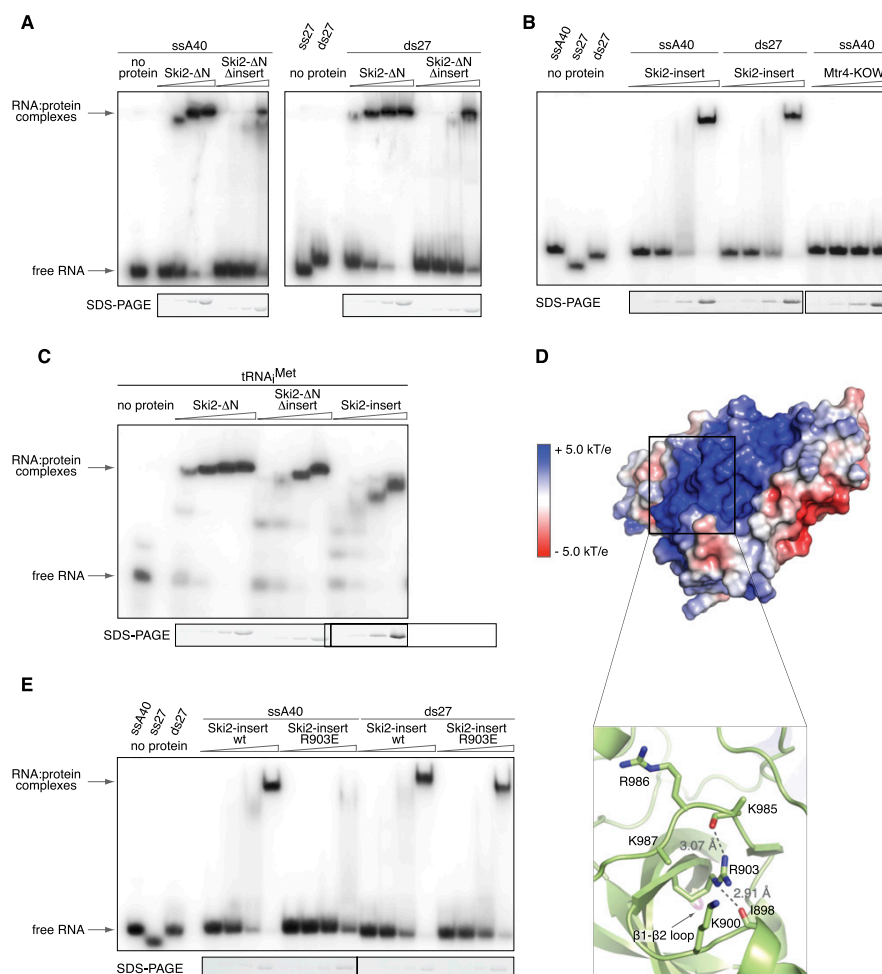


**FIGURE 3.** The insertion domain of Ski2 binds single- and double-stranded RNA substrates. (A) RNA binding to fragments of Ski2 that contain the DEXH core with and without the insertion domain (Ski2- $\Delta$ N and Ski2- $\Delta$ N- $\Delta$ insert, respectively). Electrophoretic mobility shift assays (EMSA) were carried out with a single-stranded poly(A) 40-mer (*left*) or double-stranded 27-mer (*right*) that were labeled at the 5' end with [ $^{32}$ P]phosphate. Identical concentrations (0.25  $\mu$ M, 0.75  $\mu$ M, 2.25  $\mu$ M, 6.75  $\mu$ M) were used for both Ski2- $\Delta$ N and Ski2- $\Delta$ N- $\Delta$ insert and all other proteins in this figure. (*Bottom*) A Coomassie-stained SDS-PAGE of the protein sample used in the corresponding lanes of the gel-shift assay. Deletion of the insertion domain significantly decreases the affinity for single-stranded and double-stranded RNA. (B) EMSAs as described above with single-stranded (ssA40) and double-stranded RNA (ds27) using the Ski2 insertion domain (residues 835–1085). As compared with the Mtr4 KOW domain (residues 667–818), which fails to bind single-stranded RNA at this condition, the Ski2 insertion binds single- and double-stranded RNA with comparable affinity. (C) EMSAs show that the Ski2 insertion binds *in vitro*-transcribed tRNA<sup>Met</sup> with an apparently comparable affinity to that for single- or double-stranded RNA. (D) An electrostatic surface potential analysis reveals a prominent positively charged patch on the surface of the Ski2  $\beta$ -barrel. The domain is shown in a similar orientation to that used in Figure 2A, but without the  $\alpha$ 1 and  $\alpha$ 4 helices (which have been omitted for clarity). Positive electrostatic potential is shown in blue, negative potential in red. The close-up view at *bottom* shows how the conserved Arg903 organizes the positively charged surface by coordinating two loops with several basic residues (indicated). The side-chains of Lys985 and Lys987 are disordered. Hydrogen bonds are indicated by dashed lines together with distances. (E) EMSAs suggest that mutation of Arg903 to glutamic acid impairs binding of the Ski2-insert to single-stranded RNA (A40) but does not affect interaction with double-stranded RNA (ds27).

cells resulted in a stable ternary complex that eluted as a single peak in size-exclusion chromatography (Fig. 4A). Removal of the insertion in Ski2 did not affect complex formation: Ski2- $\Delta$ insert comigrated with Ski3 and Ski8 in size-exclusion chromatography (Fig. 4A). We next tested whether the insertion of Ski2 is required to bind Ski7, an outer-layer protein of the Ski complex that mediates the

interaction with the exosome (Araki et al. 2001; Wang et al. 2005). In *in vitro* pull-down experiments with purified proteins, *f.l.* GST-Ski7 efficiently precipitated both the Ski2-Ski3-Ski8 and the Ski2 $\Delta$ insert-Ski3-Ski8 complexes, but not Ski2-insert alone (Fig. 4B). We conclude that the Ski2 insertion domain is not required for the formation of the Ski complex.

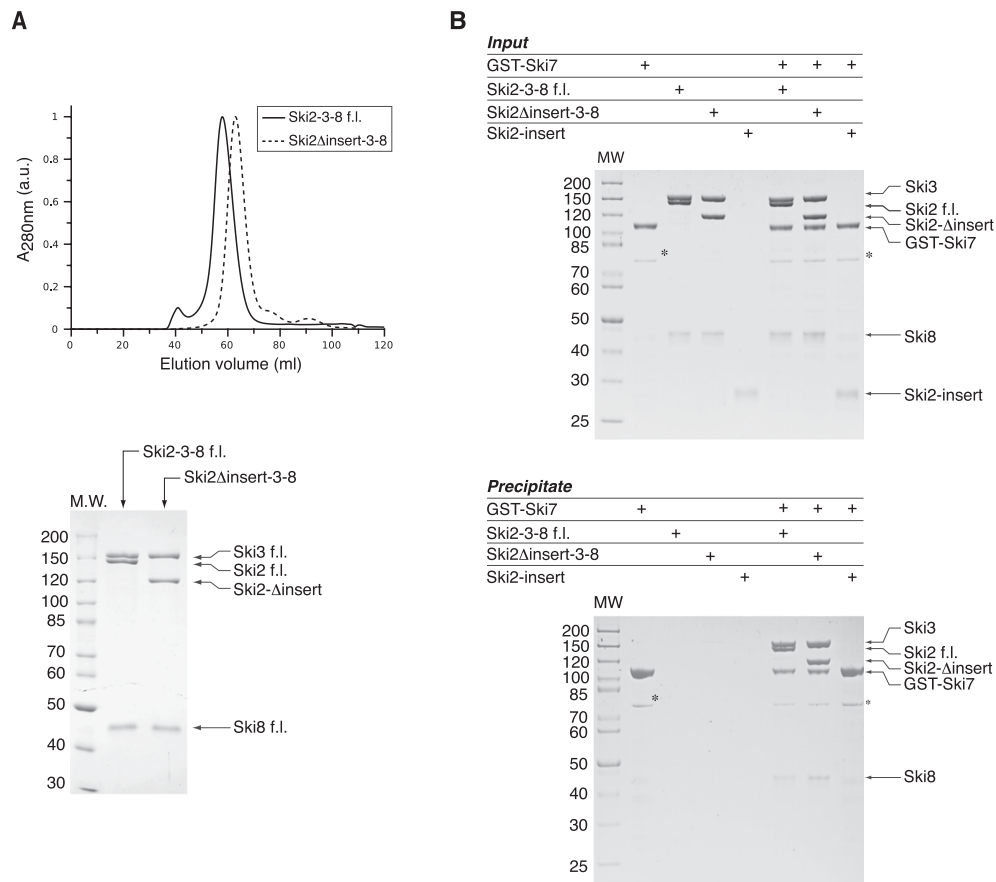


**FIGURE 4.** The Ski2 insertion domain is not required for the protein–protein interactions of the Ski complex. (A) Analytical gel-filtration of f.l. Ski2–Ski3–Ski8 and Ski2Δinsert–Ski3–Ski8 complexes. Both complexes were copurified and then injected on an analytical size-exclusion chromatography column (*top*). Peak fractions were analyzed by SDS-PAGE (*bottom*). All three components comigrated in the case of both complexes, indicating that deletion of the insertion domain of Ski2 does not impair Ski complex formation. (B) Pull-down experiments with GST-tagged f.l. Ski7 (residues 1–747) and untagged f.l. Ski2–Ski3–Ski8 and Ski2Δinsert–Ski3–Ski8 complexes. Input samples (*top*) and samples precipitated on glutathione–Sepharose beads (*bottom*) were analyzed by SDS-PAGE. The proteins corresponding to the bands are indicated on the *right* side of both panels. Both complexes were efficiently precipitated by GST–Ski7, while the insertion alone (Ski2-insert) did not bind to the bait. (\*) A contamination in the GST–Ski7 sample.

## CONCLUSIONS

The two main regulators of exosome activity, the cytosolic Ski and the nuclear TRAMP complexes, contain related RNA helicases. The Ski2 and Mtr4 helicases have a similar architecture with two distinct structural modules: a helicase core and an insertion region. The helicase core is typical of the DExH family of helicases, and is expected to mediate ATP-dependent RNA unwinding and remodeling activities. The insertion contains a long stalk and a  $\beta$ -barrel domain. Removal of the insertion in Ski2 and Mtr4 does not compromise the formation of the respective complexes with Ski3 and Ski8 and with Trf4–Air2 (Weir et al. 2010), but significantly reduces the RNA-binding properties of the two helicases. The insertion domains of both Ski2 and Mtr4 bind RNA *in vitro*. Their position above the entry site of the

RNA-binding channel in the helicase core suggests that they contribute to recruiting RNA substrates to the unwinding site.

Despite these overarching similarities, the  $\beta$ -barrel domains of Mtr4 and Ski2 have specific structural and functional differences. In yeast Mtr4, the  $\beta$ -barrel domain has a KOW signature motif, is involved in 5.8S rRNA maturation *in vivo* (Jackson et al. 2010), binds unmodified tRNA<sup>Met</sup> (Weir et al. 2010), and discriminates against single-stranded RNA *in vitro*. In Ski2, the  $\beta$ -barrel domain does not exhibit a preference for binding structured RNAs, but is rather promiscuous in its RNA-binding properties. The  $\beta$ -barrel of Ski2 does not contain a KOW motif in the corresponding loop ( $\beta$ 1– $\beta$ 2). Mutagenesis studies suggest that binding of the Ski2  $\beta$ -barrel to single-stranded RNA is mediated by the opposite surface, which features several positively charged residues. We speculate that the  $\beta$ -barrel domains of Ski2

and Mtr4 have specialized to reflect the type of transcripts that are presented to the exosome by the two helicases. This specialization contributes to the differential processing of substrates by the cytoplasmic and nuclear exosome.

## MATERIALS AND METHODS

### Protein purification

Ski2 full length (1–1287) and Ski2- $\Delta$ N (296–1287) were expressed in Hi5 insect cells from recombinant baculoviruses. Coding sequences including an N-terminal 6xHis-tag, followed by a 3C protease site, were subcloned into a pFastBac1 vector (Invitrogen). Generation of bacmids and viruses as well as protein expression was done according to standard procedures. Cells were lysed osmotically after resuspending the pellet in a buffer containing 10 mM Tris-Cl (pH 7.4), 10 mM sodium chloride, 2 mM magnesium chloride, and 1 mM  $\beta$ -mercaptoethanol. The cleared lysate was supplemented with 250 mM sodium chloride and 20 mM imidazole, and loaded on a Ni-NTA-sepharose column. The protein was eluted by an imidazole gradient to 300 mM, and the eluate was further purified on a heparin-Sepharose column. The His-tag was cleaved using 3C protease. The cleaved protein was collected as flow-through from a second Ni-NTA column and subjected to a final size-exclusion step in 10 mM HEPES (pH 7.4), 200 mM sodium chloride, and 1 mM  $\beta$ -mercaptoethanol. Full-length Ski2–Ski3–Ski8 and Ski2 $\Delta$ insert–Ski3–Ski8 complexes were obtained by coexpression of corresponding Ski2 constructs with full-length Ski3 and Ski8 in insect cells. Purification of complexes was essentially carried out as described above.

Wild-type Ski2-insert (residues 835–1085) was cloned in a modified pBR322 vector containing an N-terminal 6xHis tag, followed by a 3C protease site. Proteins were expressed in *E. coli* BL21 (DE3) Gold pLysS at 18°C after induction with 0.1 mM IPTG. Cells were resuspended in a buffer containing 20 mM Tris-Cl (pH 7.5), 500 mM sodium chloride, 20 mM imidazole, and 1 mM  $\beta$ -mercaptoethanol, and lysed by sonication. The soluble fraction was loaded on a Ni-NTA column and His-tagged protein was eluted with buffer supplemented with 300 mM imidazole and dialyzed in a low-salt buffer for cleavage of the His-tag with 3C protease. The cleaved protein was further purified with a Q-Sepharose column and a final size-exclusion column in 10 mM HEPES (pH 7.5), 200 mM sodium chloride, and 1 mM  $\beta$ -mercaptoethanol. The Ski2-insert mutant R903E was purified in the same manner.

Full-length Ski7 (residues 1–747) was expressed in *E. coli* BL21 (DE3) Gold pLysS at 18°C from a construct containing an N-terminal GST-tag. Cells were resuspended in a buffer containing 20 mM Tris-Cl (pH 7.4), 500 mM sodium chloride, 2 mM magnesium chloride, and 1 mM  $\beta$ -mercaptoethanol. After sonication, the soluble lysate was bound to GSH-Sepharose beads (GE Healthcare), washed, and eluted with loading buffer supplemented with 20 mM glutathione. The protein was dialyzed in loading buffer containing 5 mM EDTA and subjected to size-exclusion chromatography in 20 mM Tris-Cl (pH 7.4), 200 mM sodium chloride, 2 mM magnesium chloride, and 1 mM  $\beta$ -mercaptoethanol.

### Crystallization

Ski2- $\Delta$ N was concentrated to 15 mg/mL, and AMPNP was added to a final concentration of 0.5 mM. Initial hits were typically

obtained in 15% (w/v) PEG 3350 and 0.1 M HEPES (pH 7.0) by vapor diffusion experiments in sitting drops at 4°C. Iterative microseeding in 3% (w/v) PEG 3350, 5% (v/v) ethylene glycol, and 0.1 M HEPES (pH 7.0) at a protein concentration of 20 mg/mL improved crystal size and diffraction quality. Gold-derivatized Ski2- $\Delta$ N crystals were obtained by soaking native crystals for 6 h in mother liquor containing 10 mM gold cyanide. Prior to flash freezing in liquid nitrogen, crystals were briefly soaked in mother liquor that was stepwise supplemented with ethylene glycol to a final concentration of 25% (v/v).

Crystals of Ski2-insert were grown by vapor-diffusion at 4°C in two different conditions, resulting in the same crystal form. The protein was concentrated to 40 mg/mL and mixed 1:1 (v/v) with 3.5 M sodium formate and 0.1 M MES (pH 6.5) (condition 1, native data set) or with 16% (w/v) PEG 3350, and 0.14 M sodium iodide (condition 2, derivative data set) (Table 1). Gold-derivatization was carried out as described above. Prior to flash freezing in liquid nitrogen, the crystals were briefly soaked in mother liquor containing 25% (v/v) glycerol.

### Structure solution

Data were collected at 100 K at Swiss Light Source and processed using XDS (Kabsch 2010) and SCALA (Evans 2006). The Ski2- $\Delta$ N crystals contain one molecule per asymmetric unit. Phases were obtained with a three-wavelength multiple-anomalous dispersion experiment on gold-derivatized crystals. The PHENIX suite (Adams et al. 2010) was used for substructure solution, phasing, and density modification. An initial model was built automatically with BUCCANEER (Cowtan 2006) and extended manually in COOT (Emsley et al. 2010). Structure refinement against native data was carried out with phenix.refine (Adams et al. 2010).

For the structure of Ski2-insert, phases were determined from a single wavelength anomalous dispersion experiment and essentially calculated as described above. Five gold-derivatization sites were found, corresponding to five molecules in the asymmetric unit. Density modification was carried out using fivefold non-crystallographic symmetry averaging. The backbone was built manually in the experimental electron density. The initial model was extended by subsequent rounds of manual building and refinement against the native data. The structures of Ski2- $\Delta$ N and Ski2-insert were combined to a final model as outlined in the results section. Maximum likelihood coordinate error estimates of the final refined models were 0.76 Å for Ski2- $\Delta$ N and 0.94 Å for Ski2-insert.

### Electrophoretic mobility shift assays (EMSA)

Single-stranded RNA oligos were purchased (biomers.net) and tRNA<sub>i</sub><sup>Met</sup> was in vitro transcribed and purified as described (Weir et al. 2010). RNA substrates were 5'-labeled with [<sup>32</sup>P]phosphate by polynucleotide kinase treatment. Double-stranded 27-mer RNA oligos were generated by adding a 1.2-fold molar excess of unlabeled complementary strand to the labeled RNA oligo (5'-CCCCAC CACCAUCACUAAAAAAAAA-3'), followed by incubation at 95°C for 5 min and annealing by slow cooling. For a typical EMSA reaction, 0.5 pmol of substrate was mixed with the indicated amounts of protein and 1 U of RiboLock RNase inhibitor (Fermentas). 10x buffer was added to final concentrations of 20

mM HEPES (pH 7.5), 50 mM potassium acetate, 5 mM magnesium acetate, 0.1% (v/v) NP-40, and 2 mM dithiothreitol. Reactions were carried out in a volume of 10  $\mu$ L with a final salt concentration of 75 mM sodium chloride and 50 mM potassium chloride in all samples. Samples were incubated at 4°C for 30 min and separated on a native 6% (w/v) polyacrylamide gel. Gels were analyzed by phosphorimaging.

### Pull-down assays

GST-tagged prey protein (4  $\mu$ g) was mixed with equal molar amounts of bait protein. Buffer was added to a volume of 200  $\mu$ L and final concentrations of 10 mM HEPES (pH 7.5), 75 mM sodium chloride, 2 mM magnesium acetate, 0.1% (v/v) NP-40, 1 mM dithiothreitol, and 12.5% (v/v) glycerol (buffer A). A total of 40  $\mu$ L of a 50% (v/v) suspension of GSH-Sepharose beads (GE Healthcare) were added, and the reaction was incubated for 30 min at 4°C. Beads were washed three times with buffer A before eluting the precipitated protein. Samples were analyzed on a 4%–12% (w/v) Bis-Tris polyacrylamide gradient gel (Invitrogen).

### DATA DEPOSITION

The coordinates and the structure factors have been deposited in the Protein Data Bank with accession codes 4a4z (Ski2- $\Delta$ N) and 4a4k for (Ski2-insert).

### SUPPLEMENTAL MATERIAL

Supplemental material is available for this article.

### ACKNOWLEDGMENTS

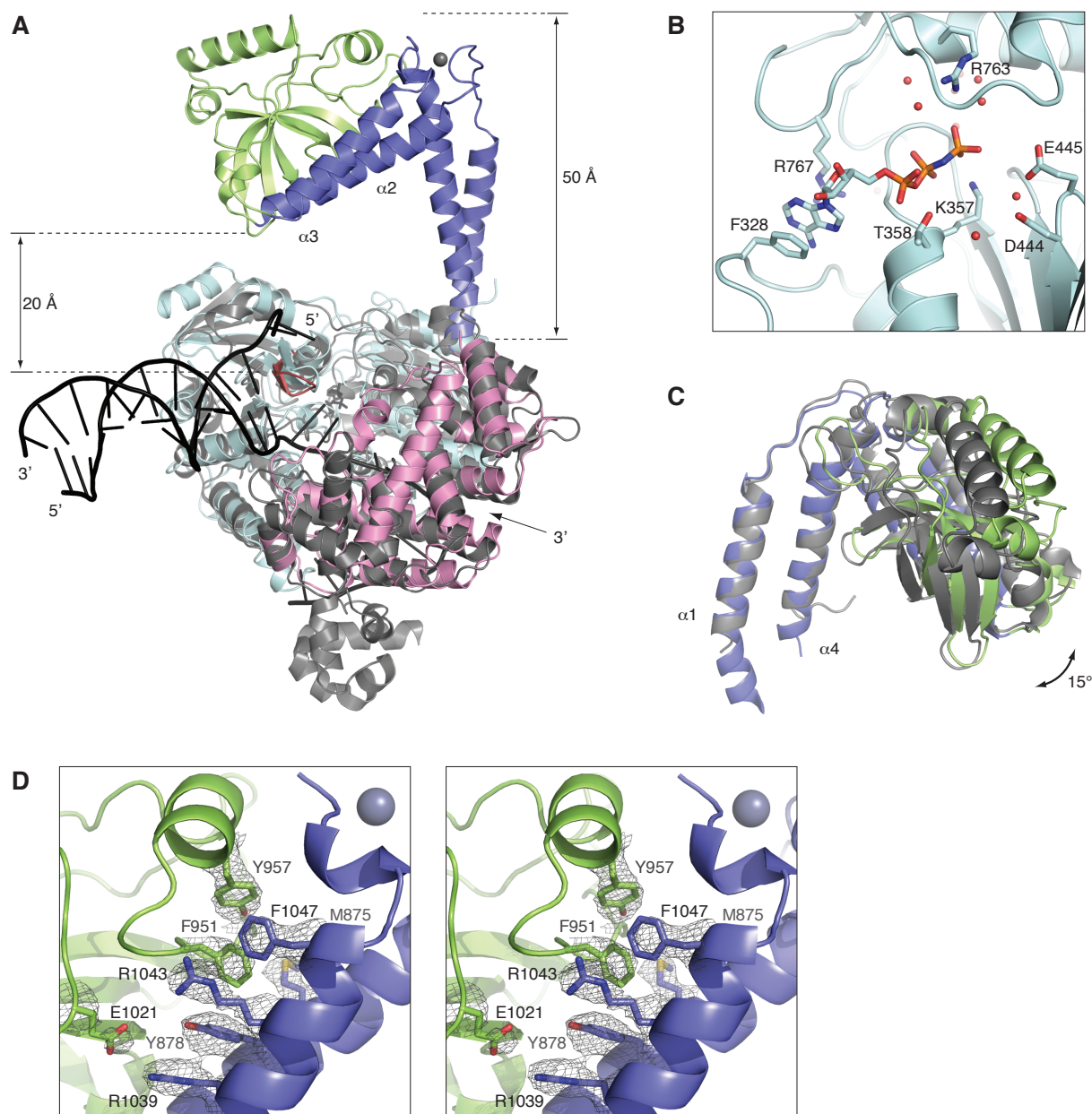
We thank Jérôme Basquin, Karina Valer-Saldaña, and Sabine Pleyer at the MPI-Martinsried crystallization facility, and the staff of the PX beamlines at the Swiss Light Source (Villigen) for assistance during data collection. We also thank Peter Brick and members of our laboratory for suggestions and critical reading of the manuscript. This study was supported by the Boehringer Ingelheim Fonds to F.H.; by the Max Planck Gesellschaft, the Sonderforschungsbereich SFB646, the Gottfried Wilhelm Leibniz Program of the Deutsche Forschungsgemeinschaft (DFG), and the Center for Integrated Protein Science Munich (CIPSM) to E.C.

Received July 27, 2011; accepted October 25, 2011.

### REFERENCES

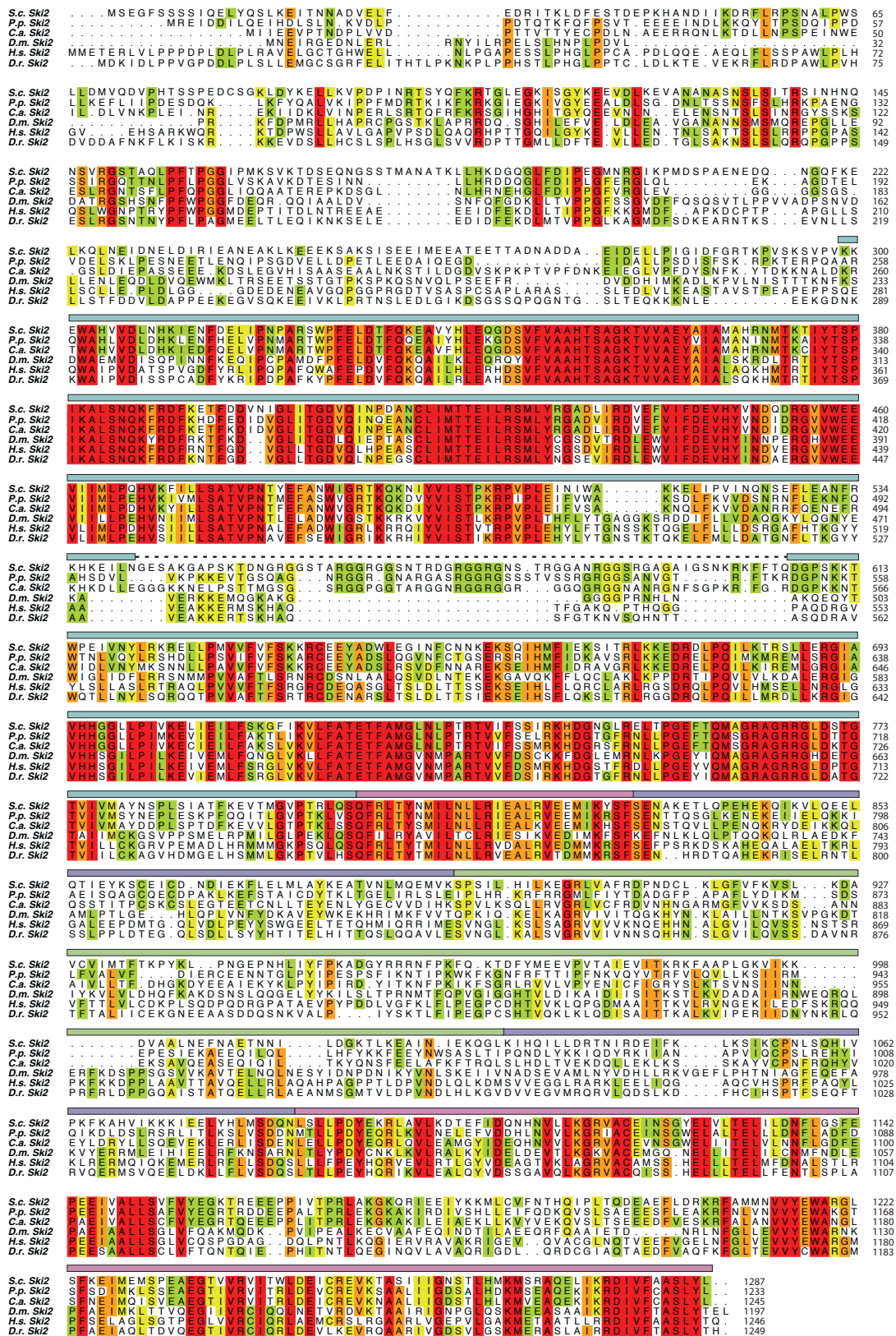
- Adams PD, Afonine PV, Bunkóczi G, Chen VB, Davis IW, Echols N, Headd JJ, Hung LW, Kapral GJ, Grosse-Kunstleve RW, et al. 2010. PHENIX: a comprehensive Python-based system for macromolecular structure solution. *Acta Crystallogr D Biol Crystallogr* **66**: 213–221.
- Allmang C, Kufel J, Chanfreau G, Mitchell P, Petfalski E, Tollervey D. 1999. Functions of the exosome in rRNA, snoRNA and snRNA synthesis. *EMBO J* **18**: 5399–5410.
- Anderson JS, Parker RP. 1998. The 3' to 5' degradation of yeast mRNAs is a general mechanism for mRNA turnover that requires the SKI2 DEVH box protein and 3' to 5' exonucleases of the exosome complex. *EMBO J* **17**: 1497–1506.
- Araki Y, Takahashi S, Kobayashi T, Kajihō H, Hoshino S, Katada T. 2001. Ski7p G protein interacts with the exosome and the Ski complex for 3'-to-5' mRNA decay in yeast. *EMBO J* **20**: 4684–4693.
- Bonneau F, Basquin J, Ebert J, Lorentzen E, Conti E. 2009. The yeast exosome functions as a macromolecular cage to channel RNA substrates for degradation. *Cell* **139**: 547–559.
- Bousquet-Antonelli C, Presutti C, Tollervey D. 2000. Identification of a regulated pathway for nuclear pre-mRNA turnover. *Cell* **102**: 765–775.
- Brown JT, Bai X, Johnson AW. 2000. The yeast antiviral proteins Ski2p, Ski3p, and Ski8p exist as a complex in vivo. *RNA* **6**: 449–457.
- Büttner K, Wenig K, Hopfner KP. 2005. Structural framework for the mechanism of archaeal exosomes in RNA processing. *Mol Cell* **20**: 461–471.
- Büttner K, Nehring S, Hopfner KP. 2007. Structural basis for DNA duplex separation by a superfamily-2 helicase. *Nat Struct Mol Biol* **14**: 647–652.
- Chen VB, Arendall WB III, Headd JJ, Keedy DA, Immormino RM, Kapral GJ, Murray LW, Richardson JS, Richardson DC. 2010. MolProbity: all-atom structure validation for macromolecular crystallography. *Acta Crystallogr D Biol Crystallogr* **66**: 12–21.
- Cowtan K. 2006. The Buccaneer software for automated model building. 1. Tracing protein chains. *Acta Crystallogr D Biol Crystallogr* **62**: 1002–1011.
- Cristodero M, Bottcher B, Diepholz M, Scheffzek K, Clayton C. 2008. The *Leishmania tarentolae* exosome: purification and structural analysis by electron microscopy. *Mol Biochem Parasitol* **159**: 24–29.
- de la Cruz J, Kressler D, Tollervey D, Linder P. 1998. Dob1p (Mtr4p) is a putative ATP-dependent RNA helicase required for the 3' end formation of 5.8S rRNA in *Saccharomyces cerevisiae*. *EMBO J* **17**: 1128–1140.
- Dziembowski A, Lorentzen E, Conti E, Séraphin B. 2007. A single subunit, Dis3, is essentially responsible for yeast exosome core activity. *Nat Struct Mol Biol* **14**: 15–22.
- Emsley P, Lohkamp B, Scott WG, Cowtan K. 2010. Features and development of Coot. *Acta Crystallogr D Biol Crystallogr* **66**: 486–501.
- Evans P. 2006. Scaling and assessment of data quality. *Acta Crystallogr D Biol Crystallogr* **62**: 72–82.
- Gatfield D, Izaurralde E. 2004. Nonsense-mediated messenger RNA decay is initiated by endonucleolytic cleavage in *Drosophila*. *Nature* **429**: 575–578.
- He Y, Andersen GR, Nielsen KH. 2010. Structural basis for the function of DEAH helicases. *EMBO Rep* **11**: 180–186.
- Hilleren P, McCarthy T, Rosbash M, Parker R, Jensen TH. 2001. Quality control of mRNA 3'-end processing is linked to the nuclear exosome. *Nature* **413**: 538–542.
- Houalla R, Devaux F, Fatica A, Kufel J, Barrass D, Torchet C, Tollervey D. 2006. Microarray detection of novel nuclear RNA substrates for the exosome. *Yeast* **23**: 439–454.
- Houseley J, Tollervey D. 2009. The many pathways of RNA degradation. *Cell* **136**: 763–776.
- Jackson RN, Klauer AA, Hintze BJ, Robinson H, van Hoof A, Johnson SJ. 2010. The crystal structure of Mtr4 reveals a novel arch domain required for rRNA processing. *EMBO J* **29**: 2205–2216.
- Johnson AW, Kolodner RD. 1995. Synthetic lethality of *sep1* (*xrn1*) *ski2* and *sep1* (*xrn1*) *ski3* mutants of *Saccharomyces cerevisiae* is independent of killer virus and suggests a general role for these genes in translation control. *Mol Cell Biol* **15**: 2719–2727.
- Kabsch W. 2010. XDS. *Acta Crystallogr D Biol Crystallogr* **66**: 125–132.
- Kadaba S, Krueger A, Trice T, Krecic AM, Hinnebusch AG, Anderson J. 2004. Nuclear surveillance and degradation of hypomodified initiator tRNA<sup>Met</sup> in *S. cerevisiae*. *Genes Dev* **18**: 1227–1240.

- Kyrpides NC, Woese CR, Ouzounis CA. 1996. KOW: a novel motif linking a bacterial transcription factor with ribosomal proteins. *Trends Biochem Sci* **21**: 425–426.
- LaCava J, Houseley J, Saveanu C, Petfalski E, Thompson E, Jacquier A, Tollervey D. 2005. RNA degradation by the exosome is promoted by a nuclear polyadenylation complex. *Cell* **121**: 713–724.
- Lebreton A, Seraphin B. 2008. Exosome-mediated quality control: substrate recruitment and molecular activity. *Biochim Biophys Acta* **1779**: 558–565.
- Lebreton A, Tomecki R, Dziembowski A, Seraphin B. 2008. Endonucleolytic RNA cleavage by a eukaryotic exosome. *Nature* **456**: 993–996.
- Lejeune F, Li X, Maquat LE. 2003. Nonsense-mediated mRNA decay in mammalian cells involves decapping, deadenylation, and exonucleolytic activities. *Mol Cell* **12**: 675–687.
- Liu Q, Greimann JC, Lima CD. 2006. Reconstitution, activities, and structure of the eukaryotic RNA exosome. *Cell* **127**: 1223–1237.
- Lorentzen E, Walter P, Fribourg S, Evguenieva-Hackenberg E, Klug G, Conti E. 2005. The archaeal exosome core is a hexameric ring structure with three catalytic subunits. *Nat Struct Mol Biol* **12**: 575–581.
- Lorentzen E, Dziembowski A, Lindner D, Seraphin B, Conti E. 2007. RNA channelling by the archaeal exosome. *EMBO Rep* **8**: 470–476.
- Lorentzen E, Basquin J, Conti E. 2008a. Structural organization of the RNA-degrading exosome. *Curr Opin Struct Biol* **18**: 709–713.
- Lorentzen E, Basquin J, Tomecki R, Dziembowski A, Conti E. 2008b. Structure of the active subunit of the yeast exosome core, Rrp44: diverse modes of substrate recruitment in the RNase II nuclease family. *Mol Cell* **29**: 717–728.
- Lykke-Andersen S, Brodersen DE, Jensen TH. 2009. Origins and activities of the eukaryotic exosome. *J Cell Sci* **122**: 1487–1494.
- Mitchell P, Tollervey D. 2003. An NMD pathway in yeast involving accelerated deadenylation and exosome-mediated 3' → 5' degradation. *Mol Cell* **11**: 1405–1413.
- Mitchell P, Petfalski E, Shevchenko A, Mann M, Tollervey D. 1997. The exosome: a conserved eukaryotic RNA processing complex containing multiple 3' → 5' exoribonucleases. *Cell* **91**: 457–466.
- Orban TI, Izaurralde E. 2005. Decay of mRNAs targeted by RISC requires XRN1, the Ski complex, and the exosome. *RNA* **11**: 459–469.
- Pyle AM. 2008. Translocation and unwinding mechanisms of RNA and DNA helicases. *Annu Rev Biophys* **37**: 317–336.
- Ridley SP, Sommer SS, Wickner RB. 1984. Superkiller mutations in *Saccharomyces cerevisiae* suppress exclusion of M<sub>2</sub> double-stranded RNA by L-A-HN and confer cold sensitivity in the presence of M and L-A-HN. *Mol Cell Biol* **4**: 761–770.
- Schaeffer D, Tsanova B, Barbas A, Reis FP, Dastidar EG, Sanchez-Rotunno M, Arraiano CM, van Hoof A. 2009. The exosome contains domains with specific endoribonuclease, exoribonuclease and cytoplasmic mRNA decay activities. *Nat Struct Mol Biol* **16**: 56–62.
- Schneider C, Leung E, Brown J, Tollervey D. 2009. The N-terminal PIN domain of the exosome subunit Rrp44 harbors endonuclease activity and tethers Rrp44 to the yeast core exosome. *Nucleic Acids Res* **37**: 1127–1140.
- Selmer M, Dunham CM, Murphy FV IV, Weixlbaumer A, Petry S, Kelley AC, Weir JR, Ramakrishnan V. 2006. Structure of the 70S ribosome complexed with mRNA and tRNA. *Science* **313**: 1935–1942.
- Takahashi S, Araki Y, Sakuno T, Katada T. 2003. Interaction between Ski7p and Upf1p is required for nonsense-mediated 3'-to-5' mRNA decay in yeast. *EMBO J* **22**: 3951–3959.
- Toh-E A, Wickner RB. 1979. A mutant killer plasmid whose replication depends on a chromosomal “superkiller” mutation. *Genetics* **91**: 673–682.
- van Hoof A, Lennertz P, Parker R. 2000a. Yeast exosome mutants accumulate 3'-extended polyadenylated forms of U4 small nuclear RNA and small nucleolar RNAs. *Mol Cell Biol* **20**: 441–452.
- van Hoof A, Staples RR, Baker RE, Parker R. 2000b. Function of the Ski4p (Csl4p) and Ski7p proteins in 3'-to-5' degradation of mRNA. *Mol Cell Biol* **20**: 8230–8243.
- van Hoof A, Frischmeyer PA, Dietz HC, Parker R. 2002. Exosome-mediated recognition and degradation of mRNAs lacking a termination codon. *Science* **295**: 2262–2264.
- Vanacova S, Wolf J, Martin G, Blank D, Dettwiler S, Friedlein A, Langen H, Keith G, Keller W. 2005. A new yeast poly(A) polymerase complex involved in RNA quality control. *PLoS Biol* **3**: e189. doi: 10.1371/journal.pbio.0030189.
- Walbott H, Mouffok S, Capeyrou R, Lebaron S, Humbert O, van Tilbeurgh H, Henry Y, Leulliot N. 2010. Prp43p contains a processive helicase structural architecture with a specific regulatory domain. *EMBO J* **29**: 2194–2204.
- Wang L, Lewis MS, Johnson AW. 2005. Domain interactions within the Ski2/3/8 complex and between the Ski complex and Ski7p. *RNA* **11**: 1291–1302.
- Weir JR, Bonneau F, Hentschel J, Conti E. 2010. Structural analysis reveals the characteristic features of Mtr4, a DEXH helicase involved in nuclear RNA processing and surveillance. *Proc Natl Acad Sci* **107**: 12139–12144.
- Wyers F, Rougemaille M, Badis G, Rousselle JC, Dufour ME, Boulay J, Regnault B, Devaux F, Namane A, Seraphin B, et al. 2005. Cryptic Pol II transcripts are degraded by a nuclear quality control pathway involving a new poly(A) polymerase. *Cell* **121**: 725–737.
- Zhang W, Dunkle JA, Cate JH. 2009. Structures of the ribosome in intermediate states of ratcheting. *Science* **325**: 1014–1017.



### Supplemental Figure 1

(A) Superposition of the Ski2- $\Delta$ N structure and the archaeal Hel308 bound to a partially unwound DNA duplex (protein shown in grey, DNA in black and the unwinding  $\beta$ -hairpin in red. PDB code 2p6r). The two structures are compared after superposition of their RecA domains. The Ski2 insertion domain is located above the 5' end of the nucleic acid bound to the DExH box core. Minimum and maximum distances between the DExH core and the insertion domain are indicated. (B) Close-up view of the ATP-binding site of Ski2. AMPPNP is shown in stick-representation and the residues involved in nucleotide-binding are indicated. Water molecules are shown as red spheres. (C) Flexibility of the Ski2 insertion domain as indicated by the superposition of the domains from the crystal structure of Ski2- $\Delta$ N (shown in blue and green) and Ski2-insert (shown in grey). The superposition was aligned to the  $\alpha$ 1- $\alpha$ 4 region of the stalk, and amplitude and direction of the flexing are indicated. (D) Stereo-view of the hydrophobic interface that is formed by the  $\beta$ -barrel and the  $\alpha$ 2- $\alpha$ 3 helices of the Ski2 insertion domain. The refined electron density is shown for a representative set of residues.



### Supplemental Figure 2

A multiple sequence alignment of eukaryotic Ski2 orthologs (white indicates variable residues, red strictly conserved ones). The domain assignment is shown as derived from the Ski2- $\Delta$ N structure using the color scheme introduced in Figure 1. A dashed line marks a region that is not observed in the crystal structure. S.c., *S. cerevisiae*, P.p., *P. pastoris*, C.a., *C. albicans*, D.m., *D. melanogaster*, D.r., *D. rerio*, H.s., *H. sapiens*.



## **3.2 The Ski complex: Crystal structure and substrate channeling to the exosome**

This article was published in 2013 in **Cell** (Issue 154, pages 814-826). The supplemental material is attached at the end of the article (pages 56-64). Figures and tables of the manuscript are referred to by “3.1.X”, where X follows the numbering within the manuscript.

Cell

# The Yeast Ski Complex: Crystal Structure and RNA Channeling to the Exosome Complex

Felix Halbach,<sup>1</sup> Peter Reichelt,<sup>1</sup> Michaela Rode,<sup>1</sup> and Elena Conti<sup>1,\*</sup><sup>1</sup>Department of Structural Cell Biology, Max Planck Institute of Biochemistry, Am Klopferspitz 18, 82152 Martinsried/Munich, Germany

\*Correspondence: conti@biochem.mpg.de

<http://dx.doi.org/10.1016/j.cell.2013.07.017>

## SUMMARY

The Ski complex is a conserved multiprotein assembly required for the cytoplasmic functions of the exosome, including RNA turnover, surveillance, and interference. Ski2, Ski3, and Ski8 assemble in a tetramer with 1:1:2 stoichiometry. The crystal structure of an *S. cerevisiae* 370 kDa core complex shows that Ski3 forms an array of 33 TPR motifs organized in N-terminal and C-terminal arms. The C-terminal arm of Ski3 and the two Ski8 subunits position the helicase core of Ski2 centrally within the complex, enhancing RNA binding. The Ski3 N-terminal arm and the Ski2 insertion domain allosterically modulate the ATPase and helicase activities of the complex. Biochemical data suggest that the Ski complex can thread RNAs directly to the exosome, coupling the helicase and the exoribonuclease through a continuous RNA channel. Finally, we identify a Ski8-binding motif common to Ski3 and Spo11, rationalizing the moonlighting properties of Ski8 in mRNA decay and meiosis.

## INTRODUCTION

RNA degradation is involved in the processing, turnover, and surveillance of virtually all RNAs in eukaryotic cells and is thus a central process for gene expression (reviewed in Houseley and Tollervey, 2009). A conserved multiprotein complex, the exosome, is the main nuclease that degrades RNAs in the 3'-to-5' direction (reviewed in Lebreton and Séraphin, 2008; Lykke-Andersen et al., 2009). The 400 kDa core complex of the eukaryotic exosome is formed by ten subunits (Exo-10) (Mitchell et al., 1997). Nine subunits are catalytically inert (Dziembowski et al., 2007; Liu et al., 2006) but form a conserved channel that threads single-stranded RNA substrates to the processive exoribonuclease in the complex, Rrp44 (Bonneau et al., 2009; Makino et al., 2013; Wasmuth and Lima, 2012). All Exo-10 subunits are essential in yeast and form a stable assembly present in both the nucleus and the cytoplasm (Allmang et al., 1999; Mitchell et al., 1997).

Auxiliary factors have been identified that bind and regulate the exosome in a compartment-specific manner (reviewed in Houseley et al., 2006; Lebreton and Séraphin, 2008; Lykke-Andersen et al., 2009; Vanacova and Stefl, 2007). Among these, important exosome regulators are RNA helicases that are specifically localized either to the cytoplasm (Ski2) (Anderson and Parker, 1998; Brown et al., 2000) or to the nucleus (Mtr4) (de la Cruz et al., 1998). Ski2 and Mtr4 share a similar overall fold (Halbach et al., 2012; Jackson et al., 2010; Weir et al., 2010) and are also similar in that they participate in protein complexes. Mtr4 functions both in isolation and in the context of the TRAMP complex (LaCava et al., 2005; van Hoof et al., 2000a; Vanáčová et al., 2005; Wyers et al., 2005). Ski2 associates with Ski3 and Ski8 to form the so-called Ski complex (Anderson and Parker, 1998; Brown et al., 2000).

The Ski complex is evolutionarily conserved and has been shown to participate in many cytoplasmic pathways of the exosome in both yeast and metazoan cells, including 3'-to-5' mRNA turnover (Anderson and Parker, 1998; Araki et al., 2001; van Hoof et al., 2000b), nonstop decay (van Hoof et al., 2002), nonsense-mediated decay (Mitchell and Tollervey, 2003), and RNAi (Orban and Izaurralde, 2005). In *S. cerevisiae*, *SKI2*, *SKI3*, and *SKI8* mutants are synthetically lethal with a deletion of *SKI1/XRN1* (Anderson and Parker, 1998; Johnson and Kolodner, 1995), the 5'-to-3' exoribonuclease that operates redundantly with the exosome (Gameau et al., 2007). An additional protein, Ski7, physically links the Ski and exosome complexes (Araki et al., 2001). Interestingly, genetic data indicate that Ski8 is unique among all Ski proteins in that it also moonlights in a separate process: meiotic DNA recombination (Arora et al., 2004).

The Ski complex is predicted to harbor a single enzymatic activity embedded in the helicase core of Ski2. Ski3 and Ski8 contain tetratricopeptide repeats (TPRs) and WD40 repeats, respectively. These structural motifs typically mediate protein-protein interactions (D'Andrea and Regan, 2003; Stimimann et al., 2010). Native mass spectrometry analysis has revealed that the endogenous complex from yeast contains one copy of Ski2 and Ski3 and two copies of Ski8 (Synowsky and Heck, 2008). How and why the Ski complex is organized in a 1:1:2 stoichiometry and why Ski2 interacts with Ski3 and Ski8 to perform its functions are unknown. In addition, it remains unclear how the Ski complex cooperates with the exosome. In this manuscript, we report a combination of biochemical and structural studies that address these questions.

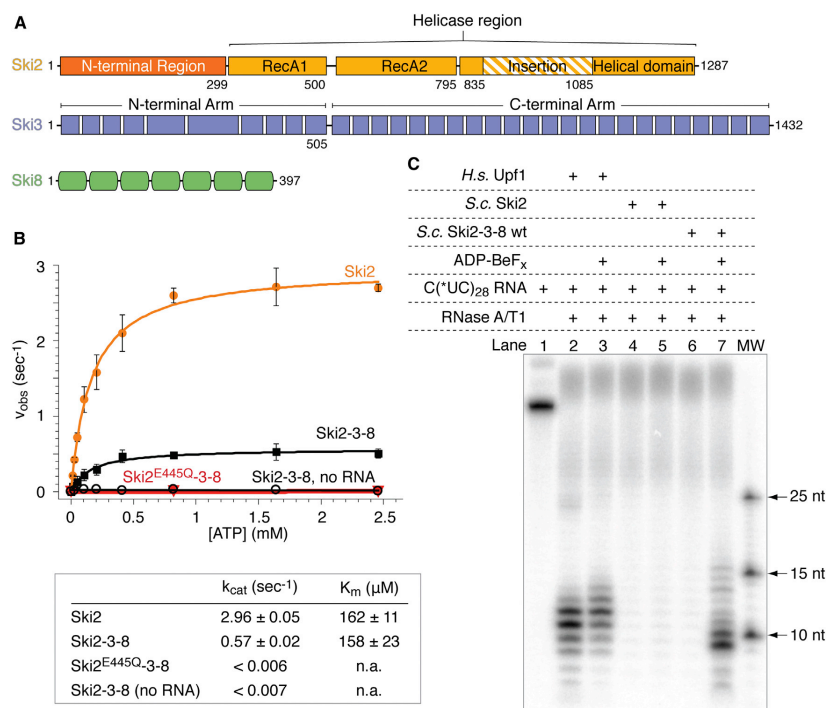


**Figure 1. Ski3 and Ski8 Modulate the RNA-Binding and ATPase Properties of Ski2**

(A) Domain structure of the subunits of the *S. cerevisiae* Ski complex is presented. The N-terminal region of Ski2 is shown in orange, the helicase region in yellow, and the insertion domain in yellow dashes. Ski3 is in blue with the individual TPR motifs indicated as boxes. Ski8 is colored green, and rounded rectangles indicate the WD40 motifs. Residue numbers and domain boundaries are derived from the structural analysis reported here.

(B) ATPase activity of the indicated samples was measured using a coupled enzyme assay. Initial ATPase rates (mole of ADP produced per second and per mole of Ski2) are plotted against the ATP concentration (top). Protein and U<sub>25</sub> RNA concentrations were 30 nM and 0.5  $\mu$ M, respectively. Data were fitted according to Michaelis-Menten kinetics, and the derived kinetic parameters are shown in the table in the lower panel. Error bars represent  $\pm$  1 SD from three independent experiments. n.a., not applicable.

(C) RNase protection patterns of Ski2 and Ski2-3-8 are shown. A single-stranded C(<sup>32</sup>U)<sub>28</sub> RNA internally labeled with <sup>32</sup>P at the uridine  $\alpha$ -phosphate was incubated with proteins and nucleotides as indicated and treated with RNase A/T1, and the reaction products were analyzed by denaturing PAGE. RNA fragments of 9 to 10 nt length accumulated in the presence of ADP-beryllium fluoride with the Ski2-3-8 complex but not with Ski2 in isolation. The human Upf1 helicase was included as a control (Chakrabarti et al., 2011). MW, molecular weight.

## RESULTS AND DISCUSSION

### Ski3 and Ski8 Modulate the Biochemical Properties of Ski2

*S. cerevisiae* Ski2 is a 146 kDa multidomain protein. The N-terminal region is required and sufficient for the interaction with Ski3 and Ski8 in vivo (Wang et al., 2005). The C-terminal helicase region contains the catalytic core typical of the DEXH family of RNA-dependent ATPases as well as an insertion domain with RNA-binding properties (Halbach et al., 2012) (Figure 1A). Ski3 is a 164 kDa protein with 24 predicted TPRs, as estimated by profile-based sequence analysis (Karpenahalli et al., 2007).

Ski8 folds into a  $\beta$  propeller protein of 44 kDa formed by seven WD40 repeats (Cheng et al., 2004; Madrona and Wilson, 2004). To investigate whether the enzymatic properties of Ski2 are modulated by binding to Ski3 and Ski8, we purified recombinant *S. cerevisiae* Ski2 and Ski2-Ski3-Ski8 (hereafter referred to as Ski2-3-8) from baculovirus-infected insect cells. Notably, the Ski complex could only be purified by coexpression because Ski3 proved to be insoluble when expressed in isolation.

We characterized the ATPase activity of Ski2 using a spectrophotometric enzyme-coupled assay (Bradley and De La Cruz, 2012). As expected for an RNA-dependent ATPase, Ski2 was inactive in the absence of RNA ( $k_{cat} < 0.007$  s<sup>-1</sup>) but showed

**Table 1. Data Collection and Refinement Statistics for Native and Selenomethionine-Substituted Ski2<sup>Δinsert-3-8</sup> Crystals**

Data Set	Native	SeMet (Peak)
Space group	P2 <sub>1</sub> ,2 <sub>1</sub> ,2 <sub>1</sub>	P2 <sub>1</sub> ,2 <sub>1</sub> ,2 <sub>1</sub>
Cell dimension a (Å)	183.4	184.0
Cell dimension b (Å)	200.4	200.0
Cell dimension c (Å)	340.2	341.2
Molecules/asymmetric unit	2	2
Data Collection		
Wavelength (Å)	0.9788	0.9788
Resolution (Å)	3.7 (3.9–3.7)	4.6 (4.85–4.6)
R <sub>merge</sub>	0.14 (0.91)	0.21 (1.27)
I/σI	5.8 (1.4)	19.6 (4.5)
Completeness (%)	99.1 (99.2)	100 (100)
Multiplicity	3.3	26.0
CC <sub>1/2</sub>	0.99 (0.46)	1.0 (0.92)
Refinement		
Number of unique reflections	132,408	
R <sub>work</sub> /R <sub>free</sub> (%)	23.1/26.5	
Average B factors (Å <sup>2</sup> )	116.8	
Number of atoms (nonhydrogen)	43,020	
Stereochemistry		
Rmsd bond lengths (Å)	0.005	
Rmsd bond angles (°)	0.81	
Ramachandran outliers (%)	0.3	
Ramachandran favored (%)	95.5	

Values for the highest-resolution shell are given in parentheses. Structure validation was carried out using MolProbity (Chen et al., 2010). See also Figure S1.

ATPase activity in the presence of a U<sub>25</sub> RNA oligo ( $k_{\text{cat}} \sim 3 \text{ s}^{-1}$ ) (Figure 1B). These values are comparable to those previously reported for the Mtr4 helicase using a similar assay (Bernstein et al., 2010). When in complex with Ski3 and Ski8, the ATPase rate of Ski2 decreased 5-fold, whereas the  $K_M$  for ATP remained essentially unchanged (Figure 1B). The ATPase activity of the Ski2-3-8 complex was abolished by a single-point mutation in the Ski2 DEXH core (Glu445 to Gln), confirming that the catalytic site resides exclusively in Ski2 (Figure 1B). We conclude that Ski2 is a less efficient ATPase when bound to Ski3 and Ski8.

We next employed RNase protection assays to investigate the extent of RNA-protein interactions. Protein samples incubated with an internally labeled single-stranded C<sup>(+)UC</sup><sub>28</sub> RNA oligo were treated with RNase A/T1, and the protected RNA fragments were analyzed by denaturing PAGE. No RNase protection was observed with Ski2 in isolation, neither in the presence nor in the absence of ATP analogs (Figure 1C, lanes 4 and 5). In the case of Ski2-3-8, fragments of 9 to 10 nt accumulated in the presence of nucleotide analogs that mimic the ground state of the ATPase reaction (ADP-beryllium fluoride, Figure 1C, compare lanes 6 and 7). We conclude that the association with Ski3 and Ski8 stabilizes RNA binding to Ski2. The finding that Ski3 and Ski8 increase RNA binding and decrease the ATPase activity of Ski2 suggests that, in addition to the N-terminal region,

the helicase core of Ski2 is also involved in and/or regulated by the association with Ski3 and Ski8. To understand the underlying mechanisms, we determined the crystal structure of a core Ski complex.

#### Overall Structure of the Yeast Ski2<sup>Δinsert-3-8</sup> Complex

Attempts to crystallize the full-length yeast Ski complex were not successful. We had previously reported that the flexible insertion domain of Ski2 is dispensable for formation of Ski2-3-8 (Halbach et al., 2012). Removal of this domain (residues 835–1,085 replaced by a Gly-Ser-Arg-Gly linker, designated Ski2<sup>Δinsert</sup>) enabled us to obtain crystals of the complex suitable for structure determination. The structure of Ski2<sup>Δinsert-3-8</sup> was determined at 3.7 Å resolution using selenomethionine-based single-wavelength anomalous diffraction (SAD) combined with molecular replacement (using the coordinates of Ski2<sup>ΔN-Δinsert</sup> [Halbach et al., 2012] and of Ski8 [Cheng et al., 2004]). Despite the moderate resolution, we could build and refine the structure to an R<sub>free</sub> of 26.5% and an R<sub>work</sub> of 23.1%, with good stereochemistry (Table 1). The accurate tracing of the polypeptide chains was aided by a combination of factors: the quality of the electron density map after averaging and B factor sharpening (DeLaBarre and Brunger, 2006), the position of the labeled methionines as sequence markers, and the regular topology of TPRs (Figure S1A available online). The atomic models of the two Ski2<sup>Δinsert-3-8</sup> complexes present in the asymmetric unit of the crystals include essentially the complete polypeptides. Notable exceptions are two long (and poorly conserved) loops in Ski3 and Ski2 (residues 340–398 and residues 542–606, respectively) and the linker between the N-terminal and helicase regions of Ski2 (residues 207–300), which were either disordered or partially built as a polyalanine model (Figure S1B).

The crystal structure of Ski2<sup>Δinsert-3-8</sup> reveals a tetrameric assembly, with one molecule of Ski2 and two molecules of Ski8 arranged around Ski3 (Figure 2A). Ski3 forms a TPR solenoid consisting of two arms of similar length (~140 Å) and roughly perpendicular to each other, resulting in an L-shaped molecule. The N-terminal region of Ski2 wraps around the C-terminal arm of Ski3. The helicase region of Ski2 docks to a central surface of Ski3 and contacts both molecules of Ski8. One Ski8 subunit has an outer, peripheral position in the complex (hereby referred to as Ski8<sub>OUT</sub>), whereas the other Ski8 subunit is located more centrally within the complex (referred to as Ski8<sub>IN</sub>) (Figure 2A).

#### Ski3 Is a Solenoid of 33 TPR Motifs and Forms the Scaffold of the Ski Complex

Canonical TPR motifs consist of 34 residues with a characteristic pattern of small and large hydrophobic side chains (Hirano et al., 1990; Sikorski et al., 1990). TPRs fold into two antiparallel  $\alpha$  helices (termed A and B) and usually occur in arrays of up to 16 repeats (Das et al., 1998). Consecutive repeats typically pack side-by-side with an ~50° rotation, giving rise to superhelical solenoids with a concave and a convex surface. The Ski2<sup>Δinsert-3-8</sup> crystal structure reveals that the entire polypeptide chain of Ski3 forms an array of 33 contiguous TPR motifs. Nevertheless, the N-terminal and

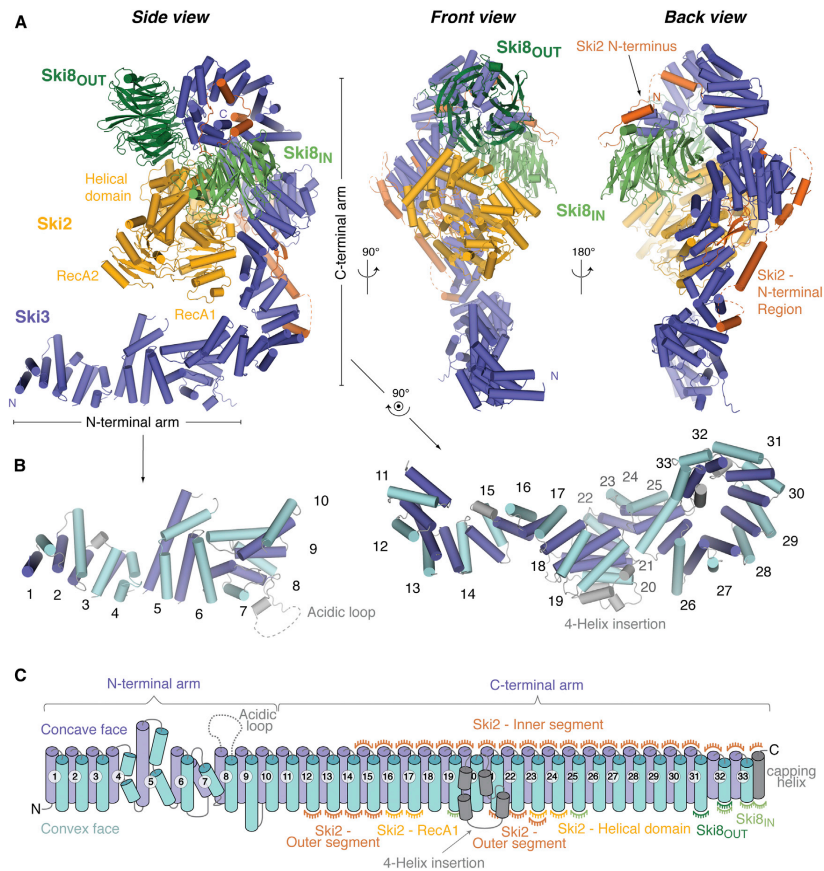


**Figure 2. The Ski Complex Is a Tetramer Organized around the TPR Protein Ski3**

(A) The crystal structure of the *S. cerevisiae* Ski2<sup>insert-3-8</sup> complex is shown in side, front, and back views. The N-terminal and helicase regions of Ski2 are colored in orange and yellow, respectively. Ski3 is depicted in blue and the two Ski8 subunits in green (Ski8<sub>OUT</sub> is in dark green; Ski8<sub>IN</sub> is in light green). The N- and C-terminal arms of Ski3 are indicated. Structures in this and all other figures were generated using the program PyMOL (Schrodinger, 2010).

(B) Ski3 contains 33 TPRs and can be subdivided into an N-terminal arm (TPRs 1–10, left) and a C-terminal arm (TPRs 11–33, right). Individual TPR motifs are numbered from the N to the C-terminus, and the A and B helices of each repeat are colored in blue and cyan, respectively. Elements other than TPRs (the four-helix insertion in TPR 20 and the C-terminal-capping helix) are shown in gray.

(C) A schematic shows the topology of the secondary structure elements in Ski3 (colored as in B). Interfaces to other subunits are mapped to the individual TPRs by half-circles that are established as above.

See also Figure S2.

C-terminal arms of this solenoid have different structural and functional characteristics.

The N-terminal arm of Ski3 encompasses TPRs 1–10 and points into solution (Figures 2A and 2B, left). This part of the molecule contains noncanonical repeats, featuring a split B helix (TPRs 4 to 5) or large interrepeat angles (TPRs 6 to 7) (Figure 2C).

TPRs 4–7 disrupt the regular stacking of the flanking canonical repeats (TPRs 1–3 and 8–10). This arrangement generates an overall extended structure with significant flexibility. Superposition of the two independent copies of the complex in the asymmetric unit of the crystals shows movements of the N-terminal arm of up to 20 Å (Figure S2A), whereas the rest of

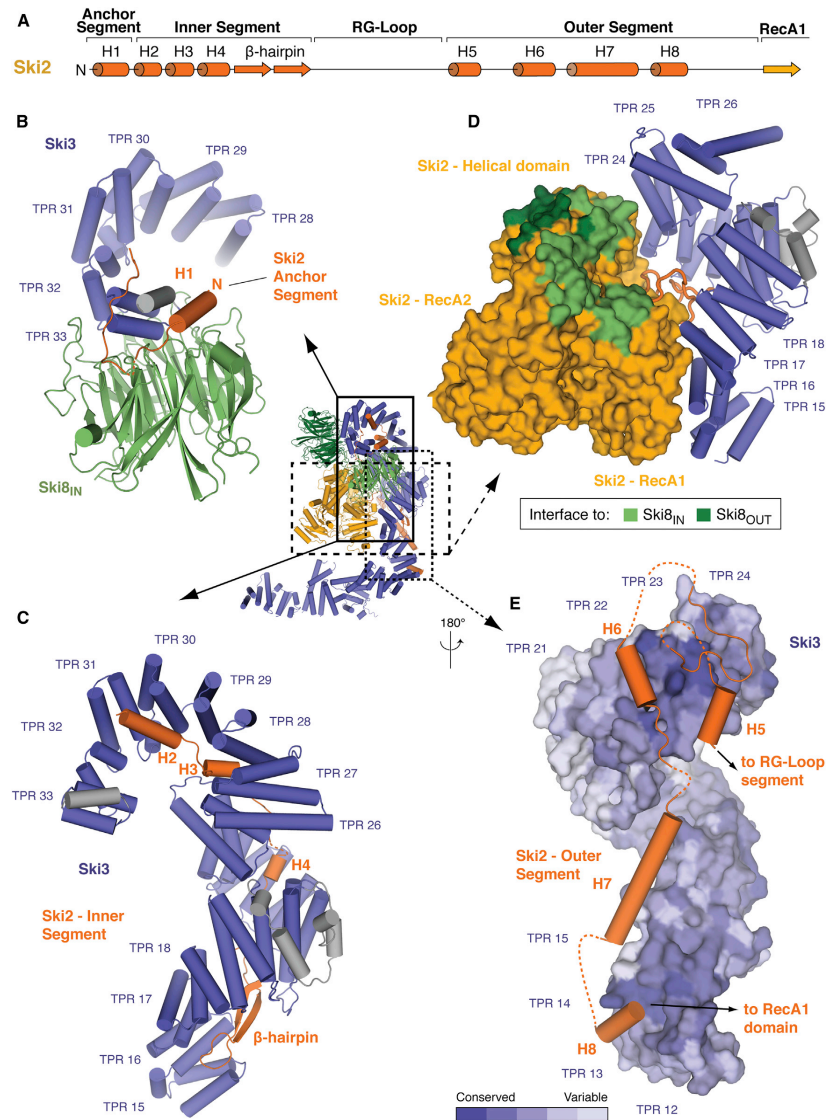


**Figure 3. Interactions of the N-Terminal and Helicase Regions of Ski2 with Ski3 and Ski8**  
 (A) A cartoon of the domain organization in the Ski2 N-terminal region is illustrated. Four separate segments (anchor, inner, RG, and outer segments) have been identified from the structure. Secondary structure elements are indicated as cylinders ( $\alpha$  helices) or arrows ( $\beta$  strands).  
 (B–E) Close-up views of the four segments in the N-terminal region of Ski2 and their interactions with Ski3, Ski8<sub>N</sub>/Ski8<sub>OUT</sub>, and the helicase core of Ski2 are shown. The central panel shows the position of the individual close-up views within the complex. For clarity, only the directly involved regions of the molecules are shown.  
*(legend continued on next page)*

the complex remains rigid. The N-terminal arm of Ski3 is not involved in interactions with Ski2<sup>Δinsert</sup> or Ski8 (Figure 2A). Nevertheless, TPRs 1–3 feature a prominent cluster of conserved positively charged surface residues (Figure S2B), pointing to a potential functional site.

The C-terminal arm of Ski3 consists of TPRs 11–33 and a single C-terminal capping helix that stacks against TPR 33 (Figure 2B, right panel, and Figure 2C). The C-terminal arm is built exclusively from canonical TPR motifs and adopts a supercoiled conformation with three and a half superhelical turns. An atypical structural feature is a yeast-specific intrarepeat insertion at TPR 20 (residues 871–913), which folds into four helices that pack against the outer surface of the solenoid. The C-terminal arm of Ski3 provides the binding sites for Ski2<sup>Δinsert</sup>, Ski8<sub>IN</sub>, and Ski8<sub>OUT</sub> (Figure 2A).

#### The N-Terminal Region of Ski2 Winds into and around the C-Terminal Arm of Ski3

The N-terminal region of Ski2 (residues 1–300) interacts with TPRs 12–33 of Ski3, stretching over a distance of about 130 Å and burying a surface of about 6,200 Å<sup>2</sup> (Figures 2A and 2C). This region contains four Ski3-interacting segments that we refer to as the Ski2 “anchor,” “inner,” “RG,” and “outer” segments (Figure 3A). The anchor segment of Ski2 (residues 1–40) forms an  $\alpha$  helix (H1) that complements the single C-terminal capping helix of Ski3, creating a pseudo-TPR motif (Figure 3B). The anchor segment also contacts the Ski8<sub>IN</sub> subunit, mainly via polar interactions. Next, the inner segment of Ski2 (residues 41–128) binds at the concave surface of Ski3, spanning three superhelical turns with extensive interactions (Figure 3C). The inner segment is mostly inaccessible to solvent and forms an integral part of the hydrophobic core of Ski3. Within this segment, helices H2 and H3 dock to the groove of TPRs 26–31, helix H4 binds in the groove of the adjacent TPRs 20–25, and the  $\beta$  hairpin winds through TPRs 15–19. Consistently with the important role of the last superhelical turn of Ski3 in binding the anchor and inner segments of Ski2 in the structure, deletion of a region of Ski3 that with hindsight corresponds to TPRs 28–33 was shown to cause lethality in a yeast strain lacking *XRN1* (Wang et al., 2005).

The following RG segment of Ski2 (residues 129–164) lacks secondary structure elements but adopts a globular fold (Figure 3D). In contrast to the rest of the N-terminal region of Ski2, the RG segment is well conserved, particularly at an Arg-Gly sequence motif (residues 149–150, see below). This segment wedges in the groove between TPRs 17 to 18 and 22–23 of Ski3 and also contacts the helicase region of Ski2. The RG segment is thus sandwiched between Ski3 and the Ski2 helicase core. Finally, the outer segment of Ski2 (residues 165–300) folds into four helices (H5–H8) that bind the convex surface of the Ski3 superhelix, traversing the superhelical groove between TPRs 15 and 21 (Figure 3E). This segment is exposed to solvent and was generally poorly defined in the electron density (Fig-

ure S1B). Although the outer segment is variable in sequence, the corresponding binding surface of Ski3 is well conserved (Figures 3E and S3A). Other conserved hot spots on the C-terminal arm of Ski3 mediate binding to the helicase region of Ski2 (Figures S3A and S3B).

#### The Ski2 Helicase Core Is Centrally Positioned by Extensive Contacts to Ski3 and Ski8

In the structure, the last residue of the Ski2 N-terminal region is about 60 Å apart from the first residue of the Ski2 helicase region, separated by a disordered linker. The helicase region of Ski2 contains two RecA domains and a helical domain (Figures 1A and 2A) that are characteristic of the DExH family of helicases. Briefly, the RecA1 and RecA2 domains face each other, juxtaposing the motifs that mediate RNA binding and ATP hydrolysis (Figure S3C) (Pyle, 2008). The helical domain flanks RecA1 and RecA2, creating an overall globular structure with a central RNA channel. The global conformation of the domains and the local conformation of the active site motifs are essentially the same in comparison to the other DExH structures (Halbach et al., 2012; Jackson et al., 2010; Weir et al., 2010), superposing with a root-mean-square deviation (rmsd) of less than 1.6 Å over more than 80% of the C $\alpha$  atoms (Figure S3C).

The helicase region of Ski2 makes extensive contacts with Ski3 and Ski8 via the RecA1 and helical domains, whereas the RecA2 domain is mostly exposed to solvent (Figure 2A, left, and Figure 2C). RecA1 binds the Ski8<sub>IN</sub> subunit and TPRs 16 to 17 of Ski3 (Figures 2C and 3D). The helical domain of Ski2 binds Ski8<sub>IN</sub>, Ski8<sub>OUT</sub>, and TPRs 23 to 24 of Ski3. Both the RecA1 and the helical domains pack against the RG segment of Ski2. Thus, the helicase region of Ski2 is positioned centrally in the complex by contacts with the N-terminal region of Ski2, with Ski3 and the two Ski8 subunits. Ski8<sub>IN</sub> and Ski8<sub>OUT</sub> contribute more than 60% of the buried surface area of the DExH core (~2,400 Å<sup>2</sup> in total).

#### The Two Ski8 Subunits Recognize Two Separate Q-R-x-x- $\Phi$ Motifs in Ski3

The structures of Ski8<sub>IN</sub> and Ski8<sub>OUT</sub> in the complex and of Ski8 in isolation (Cheng et al., 2004; Madrona and Wilson, 2004) are nearly identical, with the exception of an acidic loop (residues 332–356) that adopts different conformations. The Ski8  $\beta$  propeller has the characteristic top, side, and bottom surfaces of WD40 domains (Stirnimann et al., 2010). Ski8<sub>IN</sub> interacts at the top with Ski3 TPR 33 and the Ski2 N-terminal region and at the side with the Ski2 helicase region and TPRs 19 and 26 of Ski3 (burying ~1,000 Å<sup>2</sup> of surface area) (Figures 2A and 2C). Ski8<sub>OUT</sub> interacts at the top with TPR 31 of Ski3 and at the side with the Ski2 helicase region (~400 Å<sup>2</sup> buried surface). Remarkably, the A helices of TPRs 31 and 33 both contain a Q-R-x-x- $\Phi$  motif (x being any amino acid and  $\Phi$  being an aromatic residue) that binds the top surfaces of Ski8<sub>OUT</sub> and Ski8<sub>IN</sub> with similar interactions (Figures 4A and 4B). The glutamine and arginine residues

shown in each panel, and only selected elements are labeled. In (D), the helicase core of Ski2 is shown in surface representation, with the light and dark green colors representing the areas of Ski2 that interact with the inner and outer Ski8 subunits. In (E), Ski3 is shown as a surface representation colored according to sequence conservation (dark blue indicates conserved residues; light blue represents variable residues). See also Figure S3.

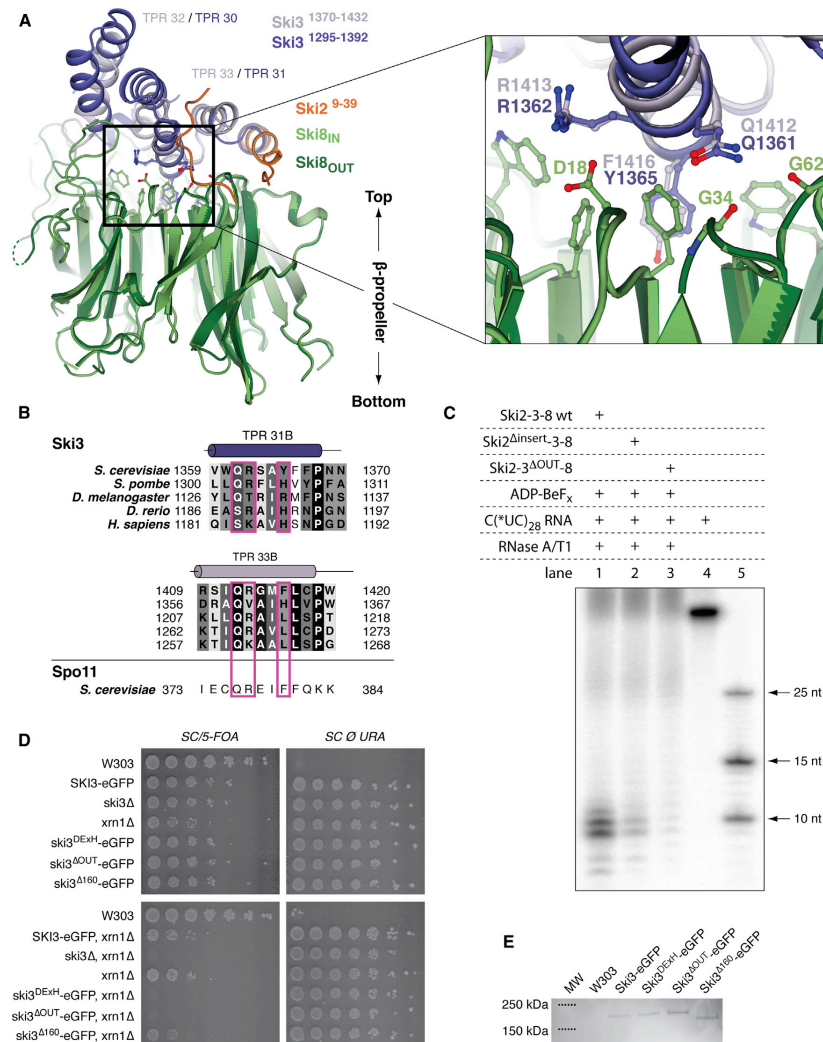


**Figure 4. The Two Ski8 Subunits Bind to Two Separate Q-R-x-x-Φ Motifs in Ski3**

(A) Superposition of Ski8<sub>IN</sub> (light green) and Ski8<sub>OUT</sub> (dark green) with their respective binding regions in Ski3 (TPRs 32 and 33 indicated in light blue, and TPRs 30 and 31 in dark blue) is shown. The top and bottom surfaces of the β propeller are indicated. The close-up view in the right panel shows how each Ski3 Q-R-x-x-Φ motif is recognized by Ski8.

(B) Alignment of Q-R-x-x-Φ motifs (boxed in magenta) from representative Ski3 sequences is shown. Residue numbers are indicated, and conservation is given in shades of gray (black indicates conserved; white represents variable). The alignment includes the Q-R-x-x-Φ motif present in the Ski8-binding protein Spo11.

(C) RNase protection assay with complexes containing structure-based mutants in Ski3 (Ski3<sup>ΔOUT</sup>) or Ski2 (Ski2<sup>Δinsert</sup>) as described in the text. The assays were carried out as described in Figure 1C. Lane 5 shows a molecular weight marker. See also Figure S4.

(legend continued on next page)



of the motifs form polar and electrostatic contacts with specific loops of Ski8. The aromatic residue of the motif inserts into the central hydrophobic cavity at the top of Ski8. Consistent with the structure, mutation of nonpolar amino acids that line the central cavity in Ski8 has previously been shown to abolish the interaction with Ski3 *in vivo* (Cheng et al., 2004).

Site-directed mutagenesis has shown that the hydrophobic top surface of Ski8 mediates binding not only to Ski3 but also to Spo11 (Cheng et al., 2004). Spo11 is a nuclear topoisomerase-like protein and interacts with Ski8 to initiate double-strand breaks during meiotic recombination (Arora et al., 2004). Mutations in Spo11 have been identified that impair the interaction with Ski8 *in vivo* (Gln376 or Arg377/Glu378) (Arora et al., 2004). Strikingly, these residues map to a Q-R-x-x- $\Phi$  motif in the C terminus of Spo11 (residues 376–380) (Figure 4B). Homology modeling of yeast Spo11 based on the similarity with an archaeal topoisomerase of known structure (Bergerat et al., 1997; Nichols et al., 1999) predicts that the Q-R-x-x- $\Phi$  motif is part of an  $\alpha$  helix that aligns remarkably well to the corresponding Ski8-binding motifs of Ski3 (Figure S4A). Ski8 is therefore likely to recognize Ski3 and Spo11 by a similar mechanism.

#### The Ski8 Subunits Contribute Differently to the Structure and Activity of the Ski Complex

To assess the relative contributions of the inner and outer Ski8 subunits in the Ski complex, we engineered mutations in the two Q-R-x-x- $\Phi$  motifs of Ski3. These mutants are predicted to impair the binding to either Ski8<sub>IN</sub> (Ski3 Q1412A/R1413D/F1416D mutant, referred to as Ski3<sup>ΔIN</sup>) or to Ski8<sub>OUT</sub> (Ski3 Q1361A/R1362D/Y1365D mutant, Ski3<sup>ΔOUT</sup>). Coexpression of Ski2, Ski3<sup>ΔIN</sup>, and Ski8 resulted in an insoluble sample, reflecting an important role of the inner subunit for the structural integrity of the complex. In contrast, coexpression of Ski2, Ski3<sup>ΔOUT</sup>, and Ski8 yielded a soluble complex that lacked a significant amount of Ski8 as compared to wild-type Ski2-3-8 (Figure S4B), consistent with the dissociation of Ski8<sub>OUT</sub>. In RNase protection experiments, Ski2-3<sup>ΔOUT</sup>-8 impaired the accumulation of the 9 to 10 nt RNA fragments characteristic of the wild-type complex (Figure 4C). We conclude that the outer Ski8 subunit is not essential for the structural integrity of the complex but plays an important role *in vitro* in modulating the RNA-binding properties of Ski2.

To analyze the effect of the Ski3<sup>ΔOUT</sup> mutation *in vivo*, we integrated wild-type *SKI3* or *ski3*<sup>ΔOUT</sup> as C-terminal EGFP fusions at the endogenous locus in a W303 diploid yeast strain in which one of the chromosomal copies of *SKI3* had been deleted. To assess growth defects in the absence of *XRN1*, we also generated an *XRN1/xrn1*Δ diploid strain. After sporulation and tetrad dissection, haploids were mated accordingly to generate *ski3*Δ/*xrn1*Δ, *ski3*<sup>ΔOUT</sup>EGFP/*xrn1*Δ, and *SKI3*-EGFP/*xrn1*Δ strains (Figures 4D, S4C, and S4D). Consistent with previous reports, deletion of *XRN1* resulted in a slow growth phenotype (*SKI3*/

*xrn1*Δ, Figure 4D), and disruption of *SKI3* and *XRN1* was synthetically lethal (*ski3*Δ/*xrn1*Δ, Figure 4D) (Johnson and Kolodner, 1995; Larimer and Stevens, 1990). In the *ski3*<sup>ΔOUT</sup>-EGFP/*xrn1*Δ strain, the mutant protein was expressed at levels comparable to wild-type Ski3-EGFP as judged by western blot (Figure 4E), but cells showed a synthetic growth defect (Figure 4D). We conclude that Ski8<sub>OUT</sub> has an important physiological function. In the structure, Ski8<sub>OUT</sub> contacts the helical domain of Ski2. We tested the effect of disrupting another contact to the helical domain of Ski2 by engineering a mutation in Ski3 at TPRs 23 to 24 (P1050R, Q1046A, H1078A, Ski3<sup>DEXH</sup>). A *ski3*<sup>DEXH</sup>/*xrn1*Δ strain generated as described above had a severe growth defect, similar to *ski3*<sup>ΔOUT</sup>-EGFP/*xrn1*Δ and to *ski3*Δ/*xrn1*Δ (Figures 4D and S4C). These results suggest that the interaction and/or position of the ATPase core of Ski2 on the Ski3-Ski8 scaffold is important for function.

#### Ski8 and the Ski3 C-Terminal Arm Extend the RNA-Binding Path of Ski2

To understand the contribution of the Ski proteins to RNA binding, we extrapolated the RNA-binding path of the helicase in the complex using the available structural information. The structure of Ski2<sup>Δinsert</sup>-3-8 was superposed with those of Ski2<sup>ΔN</sup> bound to AMPPPNP (Halbach et al., 2012) and Mtr4<sup>ΔN</sup> bound to ADP and an A<sub>5</sub> RNA oligo (Weir et al., 2010), resulting in a composite model of the full-length Ski complex (Figure 5A). As in Mtr4, RNA is expected to enter the helicase at the top of the DEXH core (near the insertion domain, Figure 5A, panel 1), to span the internal channel between the RecA and helical domains (Figure 5A, panel 2), and to exit with the 3' end at the bottom of the DEXH core (Figure 5A, panel 3). The composite model shows that the 5' end of the RNA is accessible to solvent, whereas the 3' end is buried (Figure 5A, panels 1 and 3). The RG segment of Ski2 packs below RecA1 (Figure 5A, panel 2), with the RG motif pointing into the RNA exit channel. The conserved RG loop is positioned adjacent to the canonical motifs that line the RNA path in the helicase region (Figures 5A, panel 2, and Figure S5A). Ski3 and Ski8<sub>IN</sub> are placed below Ski2, effectively extending the internal channel (Figure 5A, panel 3). Thus, the RG segment of Ski2, Ski3, and Ski8<sub>IN</sub> appears to cooperatively form an exit site for the RNA 3' end that emerges from the DEXH core of Ski2, rationalizing the stabilization of RNA binding upon complex formation (Figure 1C). In contrast, Ski8<sub>OUT</sub> is far from the RNA-binding path, suggesting that its contribution to RNA binding is indirect.

#### The Ski2 Insertion and the Ski3 N-Terminal Arm Allosterically Regulate Ski2 Helicase Activity

Upon assaying the biochemical properties of the Ski complex, we found that removal of the insertion domain of Ski2 resulted in a significant increase of both ATPase and helicase activities as compared to the wild-type Ski2-3-8 complex (Figures 5B, 5C, and S5B). In the case of Ski2 in isolation, however, the

(D) Growth assay of wild-type and mutant yeast strains is shown. Endogenous *SKI3* was replaced by wild-type or mutant *SKI3*-EGFP fusions in a strain where endogenous *XRN1* was present (top) or deleted (bottom). All strains (except wild-type) also carried an *XRN1*-URA3 plasmid. For the growth assay, cells were grown to early exponential phase and spotted in serial dilutions onto 5-fluoroorotic acid (5-FOA) medium or control plates. Medium containing 5-FOA selects for cells that have lost the URA3-*XRN1* plasmid. For controls and yeast strains, see Figures S4C and S4D. SC, synthetic complete medium; URA, uracil.

(E) EGFP-tagged proteins were by immunoprecipitation from soluble lysate of the yeast strains shown in (D) and analyzed by anti-GFP western blotting.

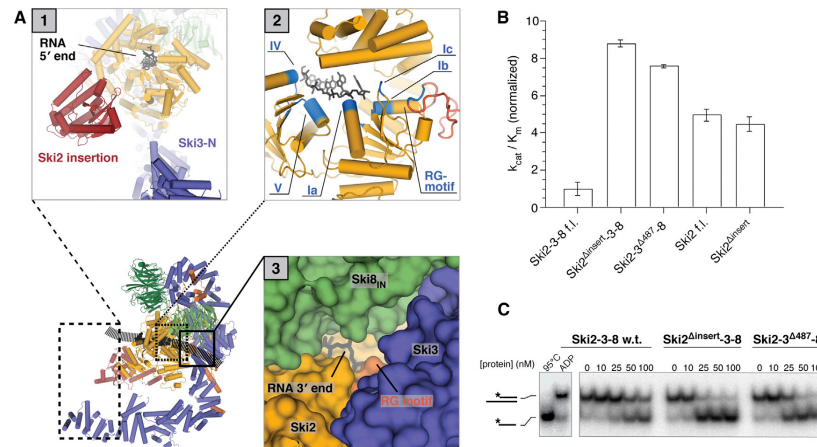


**Figure 5. RNA-Binding Path and Regulation in the Ski Complex**

(A) Model of the full-length Ski complex based on the superposition of the Ski2<sup>Δinsert</sup>-3-8 structure with Ski2<sup>ΔN</sup>-AMPPNP (4A4Z) and of Mtr4<sup>ΔN</sup>-ADP-A5 (2XGJ) is shown. The three close-up views (panels 1–3) show important features in the RNA-binding path: the “lid” formed by the Ski insertion and the Ski3 N-terminal arm above the RNA 5′ end (panel 1), the RG segment of Ski2 extending the RNA-binding motifs in the DExH core (numbered, panel 2), and Ski3 and Ski8<sub>N</sub> forming an exit channel for the RNA 3′ end (panel 3).

(B) ATPase activities of wild-type and mutant Ski2 and Ski2-3-8 samples are given in terms of  $k_{cat}/K_M$  (normalized to full-length Ski2-3-8). Removal of the insertion domain of Ski2 or of the N-terminal arm of Ski3 derepresses the ATPase activity of Ski2 when bound in the Ski complex. Removal of the insertion domain has no effect on Ski2 in isolation (see Figures 1C and S5B for raw data). Error bars represent  $\pm 1$  SD from three independent experiments.

(C) Unwinding activity of wild-type and mutant Ski complexes is shown. RNA duplexes with a 3′ overhang were incubated with the indicated amounts of protein and separated by native PAGE. Removal of the Ski2 insertion domain or the Ski3 N terminus stimulates the helicase activity of the complex. See also Figure S5.

insertion domain did not significantly alter the rate of ATP hydrolysis (Figures 5B and S5B). These data suggest that binding of Ski3 and/or Ski8 modulates the effect of the insertion domain on Ski2. The model of the full-length Ski complex suggests that the insertion domain of Ski2 is juxtaposed to the N-terminal arm of Ski3 (Figure 5A, panel 1). These two domains are predicted to reside above the RNA entry site of the DExH core and would thus be in a favorable position to modulate the helicase. To test a possible effect of the N-terminal arm of Ski3 on helicase activity, we purified a Ski complex containing the Ski2 insertion domain but lacking the ten N-terminal TPRs (residues 1–487) (Figure S5C). Although the Ski3 N terminus is not required to bind to Ski7 nor for complex formation, its removal resulted in a significant increase in the helicase and ATPase activities of the Ski complex, comparably to the effect observed with the Ski2<sup>Δinsert</sup>-3-8 complex (Figures 5B, 5C, and S5B).

The insertion domain of Ski2 is essential for exosome-mediated functions in yeast (Klauer and van Hoof, 2013). We therefore assessed the importance of the N-terminal arm of Ski3 in vivo. Reasoning that the first three TPR motifs of Ski3 contain a conserved surface patch (Figure S2B) and are predicted from the composite model to approach the globular domain of the Ski2 insertion (Figure 5A, panel 1), we deleted a small region of the N-terminal arm encompassing residues 1–160 (Ski3<sup>Δ160</sup>). A *ski3<sup>Δ160</sup>/xrm1Δ* strain generated as described above impaired

growth (Figures 4D and S4C). The effect was not as severe as in the case of mutations in the C-terminal arm but appears to be specific because the mutant protein was present at a level comparable to the Ski3-EGFP knockin (Figure 4E). We conclude that the N-terminal arm of Ski3 cooperates with the insertion domain of Ski2 to allosterically regulate the helicase activity of the complex. Notably, the insertion domain of the related nuclear helicase Mtr4 has similar properties as compared to the insertion of Ski2: it has a comparable architecture and position, it is not required for the assembly of the TRAMP complex (Weir et al., 2010), and it is important in vivo (Jackson et al., 2010). Whether its insertion domain also regulates Mtr4 allosterically in the context of the TRAMP or higher-order complexes is currently unknown.

#### RNA Channeling from the Ski Complex to the Exosome

Next, we evaluated the RNA-binding path of the Ski complex bound to the exosome. Coimmunoprecipitation studies have shown that in *S. cerevisiae*, the Ski2-3-8 complex interacts with the exosome via the protein Ski7 (Araki et al., 2001; Wang et al., 2005). In GST pull-down assays with purified recombinant proteins, Ski7 interacted directly with Ski2-3-8 (or Ski2<sup>Δinsert</sup>-3-8), with the exosome and concomitantly with both (Figure S6A). Notably, Ski7 did not interact with Ski2 or Ski8 in isolation (Figure S6A). Having established the physical association of both complexes, we next asked how this interaction impacts on

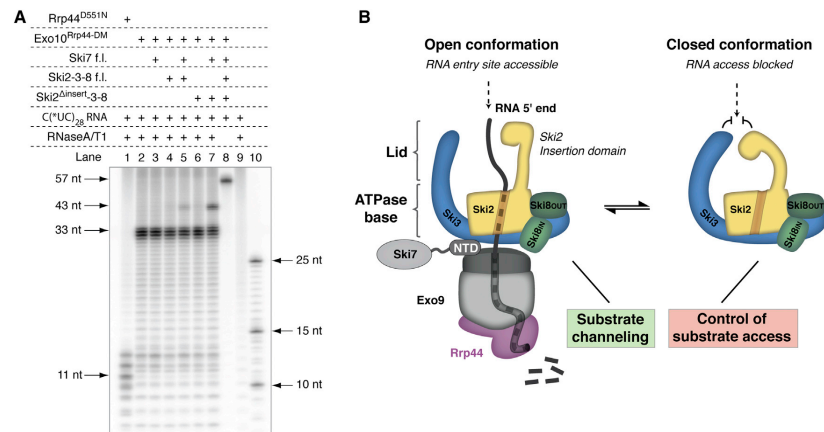


**Figure 6. RNA Channeling in the Exosome-Ski Assembly**

(A) RNase A/T1 protection assays were carried out as described for Figure 1C. The size of the RNA fragments is indicated on the left. Lane 10 shows a molecular weight marker. RNA fragments of 31–33 nt accumulated with Exo-10 (Bonneau et al., 2009). Fragments of 43 to 44 nt accumulated when incubating Exo-10 and Ski2<sup>Δinsert-3-8</sup> in the presence of Ski7. The intensity of the 43 to 44 nucleotide fragments decreased when using the full-length Ski complex. See Figure S6B for a similar assay using a 5'-to-3' exoribonuclease instead. Rrp44-DM indicates the Rrp44 D551N/D171N double mutant.

(B) A model for the substrate channeling in the cytoplasmic exosome-Ski assembly. The exosome is shown with the catalytically inactive core (Exo-9) in gray and the active subunit Rrp44 in pink. The drawing of the Ski complex (Ski2 in yellow, Ski3 in blue and Ski8 in green) is based on the structure reported here. The Ski complex can be described as formed by an ATPase base and a regulatory lid (the N-terminal arm of Ski3 and the insertion domain of Ski2). No structural data for Ski7 (shown in gray) are currently available. The model is based on known interaction data (Figures S5C and S6A). The path of the RNA is shown as a black line, according to individual structures of the exosome (Makino et al., 2013) and of known DEXH box proteins (Büttner et al., 2007; Weir et al., 2010). The overall path is consistent with the results from the RNase protection assays (A and Figure S6B) and with the synergistic effect of the lid domains in gating the entrance of the assembly. See also Figure S6.

the RNA-binding path of the Ski complex. We have previously shown that RNase A/T1 protection assays with Exo-10 reveal an accumulation of fragments of 10 to 11 and 31–33 nt (Bonneau et al., 2009). The latter correspond to the path of the RNA through the central channel of the exosome (Makino et al., 2013). When carrying out RNase A/T1 protection assays of Exo-10 in the presence of full-length Ski7 and Ski2<sup>Δinsert-3-8</sup> complex, we observed an additional band corresponding to RNA fragments of about 43 to 44 nt (Figure 6A, compare lanes 2 and 7). The presence of a 43 to 44 nt fragment is remarkable because it roughly corresponds to the sum of the individual path lengths of the exosome (31–33 nt) and the Ski2-3-8 complex (9 to 10 nt), suggesting that a continuous channel is formed between the Ski and exosome complexes (Figure 6B). Such a continuous channel also predicts that the ATPase base of the Ski complex is in close proximity to the entrance of the exosome channel. Consistently, the interaction of Ski7 with the exosome is known to involve Csl4, a subunit that lines the top of Exo-10 (Schaeffer et al., 2009; van Hoof et al., 2002).

To corroborate these findings, we carried out protection assays using a 5'-to-3' exoribonuclease instead of the endonucleases RNase A/T1. In the 5'-to-3' exoribonuclease assay, Exo-10 protected ~28 nt fragments (Figure S6B), corresponding almost exactly to the path estimated from the RNA-bound Exo-10 structure (Makino et al., 2013). We did not observe accumu-

lation of the 10 to 11 nt fragments typical of the RNase A/T1 assays (Bonneau et al., 2009), suggesting that these short species form by endonucleolytic cleavage at an exposed part of the substrate in Rrp44. This implies that, in Exo-10, there might not be a short, channel-independent RNA path but only the long, channel-dependent path. Addition of Ski2<sup>Δinsert-3-8</sup> resulted in longer (~46 nt) fragments in a Ski7-dependent manner (Figure S6B). These fragments reflect protection of the 5' end beyond the DEXH core, suggesting a possible involvement of the N-terminal arm of Ski3. Notably, the intensity of fragments protected by the Ski-exosome assembly decreased when incubating Exo-10 and Ski7 with full-length Ski2-3-8 instead of Ski2<sup>Δinsert-3-8</sup> both in the RNase A/T1 protection assays (Figure 6A, compare lanes 5 and 7) and in the 5'-to-3' exoribonuclease protection assays (Figure S6B). Altogether, the biochemical data suggest that the insertion domain of Ski2 and the N-terminal arm of Ski3 are involved in gating the entrance of the helicase-nuclease assembly.

### Conclusions

All subunits of the Ski complex are required for exosome-mediated mRNA degradation (Anderson and Parker, 1998). Yet, the enzymatic activity of the complex arises from a single subunit, Ski2, raising the question as to how Ski3 and Ski8 contribute to the function of this assembly. The structural and

biochemical data reported here reveal intricate interaction networks that engage the catalytic and noncatalytic subunits and sophisticated mechanisms that control the ATPase activity of the complex.

Overall, the Ski complex can be thought of as formed by an ATPase base and a regulatory lid (Figure 6B). In the ATPase base, the DExH core of Ski2 is located in a central position, surrounded by the C-terminal arm of Ski3, two Ski8 subunits, and the N-terminal region of Ski2. With the exception of the outer Ski8 subunit, all other nonenzymatic constituents of the base appear to directly extend the RNA channel of Ski2, forming an exit tunnel where the unwound RNA 3' end is expected to emerge. Despite adopting the most peripheral position in the complex and being dispensable for Ski2-Ski3 interaction, the outer Ski8 subunit is important for function *in vivo* and for RNA binding *in vitro*, possibly by restraining the ATPase core in a productive conformation. Most of the DExH core of Ski2 is embedded in protein-protein interactions within the base. However, the RecA2 domain of the helicase is exposed to solvent, rationalizing how the required conformational plasticity of the DExH core in the course of the ATPase cycle can be maintained without disrupting the complex. The regulatory lid that surmounts the ATPase base is the most dynamic part of the complex. The lid is formed by the insertion domain of Ski2 and the N-terminal arm of Ski3. Neither domain is required to assemble the ATPase base, but together they regulate ATPase activity, possibly by gating substrate access to the ATPase base. Binding to Ski3 and Ski8 also allows Ski2 to connect to Ski7 and hence to the exosome complex. Our biochemical results suggest that the Ski complex directly channels single-stranded RNA into the exosome (Figure 6B). This mechanism would couple the helicase and nuclease activities of the complexes, resulting in a direct pipeline for mRNP remodeling and degradation.

The RNA-degrading exosome complex has conceptual similarities to the proteasome, a cellular machinery that breaks down polypeptides (Lorentzen and Conti, 2006; van Hoof and Parker, 1999). The exosome core and the 20S proteasome both possess cylindrical chambers where unfolded substrates are sequestered and degraded. The 20S proteasome associates with a major regulatory complex: the 19S complex (Kish-Trier and Hill, 2013). The 19S complex contains an ATPase base that unfolds polypeptides and injects them into the 20S complex for degradation. It also contains a dynamic lid that recognizes the substrates and transfers them to the ATPase base. In the context of our structural and biochemical data on the Ski complex, the emerging picture is that the conceptual similarities in the degradation mechanisms of exosome and proteasome are likely to extend to their regulatory complexes.

#### EXPERIMENTAL PROCEDURES

See also the [Extended Experimental Procedures](#).

##### Protein Purification

Recombinant *S. cerevisiae* Ski2 and Ski2-3-8 complexes (wild-type and mutants) were purified from insect cells as previously described (Halbach et al., 2012). Ski7 was expressed in *E. coli* and purified as reported earlier (Halbach et al., 2012). The exosome (nine or ten subunit complexes) was reconstituted as published by Makino et al. (2013). Details on constructs,

expression systems, and purification procedures are available in the [Extended Experimental Procedures](#).

##### Crystallization and Structure Solution

Crystallization and structure solution are described in detail in the [Extended Experimental Procedures](#). Briefly, a combination of molecular replacement (using the Ski2 helicase core [4A4Z] and Ski8 [1S4U] as search models) and selenomethionine SAD phases yielded an experimental electron density map that was improved by solvent flattening and phase extension. Manual model building and refinement allowed completion of the model.

##### Biochemical Assays

Steady-state ATPase activity was analyzed using an assay that couples oxidation of NADH to regeneration of ATP (Bradley and De La Cruz, 2012).  $K_M$  and  $K_{cat}$  were derived by fitting the data according to Michaelis-Menten kinetics. Single turnover unwinding assays were carried out essentially as described in Lucius et al. (2003). As substrate, a 17-mer single-stranded RNA was labeled at the 5' end with  $^{32}P$  and annealed with a 1.5 molar excess of a 27-mer RNA (consisting of a complementary sequence and a 3' extension of 10 nt). RNase protection assays have been described in Bonneau et al. (2009). See the [Extended Experimental Procedures](#) for details.

##### Yeast Strains

See the [Extended Experimental Procedures](#) for generation of yeast strains.

##### ACCESSION NUMBERS

The coordinates and structure factors have been deposited in the Protein Data Bank with ID code 4BUJ.

##### SUPPLEMENTAL INFORMATION

Supplemental Information includes [Extended Experimental Procedures](#) and six figures and can be found with this article online at <http://dx.doi.org/10.1016/j.cell.2013.07.017>.

##### ACKNOWLEDGMENTS

We thank the MPI-Biochemistry Core Facility and Crystallization Facility, F. Bonneau for help with biochemical assays, E. Kowalinski, J. Ebert, and D. Makino for exosome samples or plasmids, and S. Chakrabarti for Upf1 samples. We also thank the staff of the Swiss Light Source synchrotron for assistance during data collection and Z. Storchova, S. Jentsch, and the CSH course on yeast genetics for guidance and training in the *in vivo* experiments. We also thank M. Krause for the drawing in Figure 6B and the members of our lab for discussions and for critical reading of the manuscript. This study was supported by the Boehringer Ingelheim Fonds (to F.H.), the Max Planck Gesellschaft, the European Research Council (ERC Advanced Investigator Grant 294371 and ITN RNPnet), and the Deutsche Forschungsgemeinschaft (DFG SFB646, SFB1035, GRK1721, FOR1680, and CIPSM; to E.C.). F.H. purified proteins and conducted crystallization and structure determination as well as all *in vitro* assays. P.R. generated and analyzed yeast strains. M.R. carried out the insect-cell expression. E.C. supervised the project. F.H. and E.C. wrote the manuscript.

Received: October 17, 2012

Revised: May 13, 2013

Accepted: July 12, 2013

Published: August 15, 2013

##### REFERENCES

Allmang, C., Kufel, J., Chanfreau, G., Mitchell, P., Pettfalski, E., and Tollervey, D. (1999). Functions of the exosome in rRNA, snoRNA and snRNA synthesis. *EMBO J.* 18, 5399–5410.

- Anderson, J.S., and Parker, R.P. (1998). The 3' to 5' degradation of yeast mRNAs is a general mechanism for mRNA turnover that requires the SKI2 DEVH box protein and 3' to 5' exonucleases of the exosome complex. *EMBO J.* **17**, 1497–1506.
- Araki, Y., Takahashi, S., Kobayashi, T., Kajih, H., Hoshino, S., and Katada, T. (2001). Ski7p G protein interacts with the exosome and the Ski complex for 3'-to-5' mRNA decay in yeast. *EMBO J.* **20**, 4684–4693.
- Arora, C., Kee, K., Maleki, S., and Keeney, S. (2004). Antiviral protein Ski8 is a direct partner of Spo11 in meiotic DNA break formation, independent of its cytoplasmic role in RNA metabolism. *Mol. Cell* **13**, 549–559.
- Bergerat, A., de Massy, B., Gadelle, D., Varoutas, P.C., Nicolas, A., and Forterre, P. (1997). An atypical topoisomerase II from Archaea with implications for meiotic recombination. *Nature* **386**, 414–417.
- Bernstein, J., Ballin, J.D., Patterson, D.N., Wilson, G.M., and Toth, E.A. (2010). Unique properties of the Mtr4p-poly(A) complex suggest a role in substrate targeting. *Biochemistry* **49**, 10357–10370.
- Bonneau, F., Basquin, J., Ebert, J., Lorentzen, E., and Conti, E. (2009). The yeast exosome functions as a macromolecular cage to channel RNA substrates for degradation. *Cell* **139**, 547–559.
- Bradley, M.J., and De La Cruz, E.M. (2012). Analyzing ATP utilization by DEAD-Box RNA helicases using kinetic and equilibrium methods. *Methods Enzymol.* **511**, 29–63.
- Brown, J.T., Bai, X., and Johnson, A.W. (2000). The yeast antiviral proteins Ski2p, Ski3p, and Ski8p exist as a complex in vivo. *RNA* **6**, 449–457.
- Büttner, K., Nehring, S., and Hopfner, K.P. (2007). Structural basis for DNA duplex separation by a superfamily-2 helicase. *Nat. Struct. Mol. Biol.* **14**, 647–652.
- Chakrabarti, S., Jayachandran, U., Bonneau, F., Fiorini, F., Basquin, C., Domcke, S., Le Hir, H., and Conti, E. (2011). Molecular mechanisms for the RNA-dependent ATPase activity of Upr1 and its regulation by Upr2. *Mol. Cell* **41**, 693–703.
- Chen, V.B., Arendall, W.B., 3rd, Headd, J.J., Keedy, D.A., Immormino, R.M., Kapral, G.J., Murray, L.W., Richardson, J.S., and Richardson, D.C. (2010). MolProbity: all-atom structure validation for macromolecular crystallography. *Acta Crystallogr. D Biol. Crystallogr.* **66**, 12–21.
- Cheng, Z., Liu, Y., Wang, C., Parker, R., and Song, H. (2004). Crystal structure of Ski8p, a WD-repeat protein with dual roles in mRNA metabolism and meiotic recombination. *Protein Sci.* **13**, 2673–2684.
- D'Andrea, L.D., and Regan, L. (2003). TPR proteins: the versatile helix. *Trends Biochem. Sci.* **28**, 655–662.
- Das, A.K., Cohen, P.W., and Barford, D. (1998). The structure of the tetratricopeptide repeats of protein phosphatase 5: implications for TPR-mediated protein-protein interactions. *EMBO J.* **17**, 1192–1199.
- DeLaBarre, B., and Brunger, A.T. (2006). Considerations for the refinement of low-resolution crystal structures. *Acta Crystallogr. D Biol. Crystallogr.* **62**, 923–932.
- de la Cruz, J., Kressler, D., Tollervey, D., and Linder, P. (1998). Dob1p (Mtr4p) is a putative ATP-dependent RNA helicase required for the 3' end formation of 5.8S rRNA in *Saccharomyces cerevisiae*. *EMBO J.* **17**, 1128–1140.
- Dziembowski, A., Lorentzen, E., Conti, E., and Séraphin, B. (2007). A single subunit, Dis3, is essentially sufficient for yeast exosome core activity. *Nat. Struct. Mol. Biol.* **14**, 15–22.
- Garneau, N.L., Wilusz, J., and Wilusz, C.J. (2007). The highways and byways of mRNA decay. *Nat. Rev. Mol. Cell Biol.* **8**, 113–126.
- Halbach, F., Rode, M., and Conti, E. (2012). The crystal structure of *S. cerevisiae* Ski2, a DExH helicase associated with the cytoplasmic functions of the exosome. *RNA* **18**, 124–134.
- Hirano, T., Kinoshita, N., Morikawa, K., and Yanagida, M. (1990). Snap helix with knob and hole: essential repeats in *S. pombe* nuclear protein nuc2+. *Cell* **60**, 319–328.
- Houseley, J., and Tollervey, D. (2009). The many pathways of RNA degradation. *Cell* **136**, 763–776.
- Houseley, J., LaCava, J., and Tollervey, D. (2006). RNA-quality control by the exosome. *Nat. Rev. Mol. Cell Biol.* **7**, 529–539.
- Jackson, R.N., Klauer, A.A., Hintze, B.J., Robinson, H., van Hoof, A., and Johnson, S.J. (2010). The crystal structure of Mtr4 reveals a novel arch domain required for rRNA processing. *EMBO J.* **29**, 2205–2216.
- Johnson, A.W., and Kolodner, R.D. (1995). Synthetic lethality of sep1 (xrn1) ski2 and sep1 (xrn1) ski3 mutants of *Saccharomyces cerevisiae* is independent of killer virus and suggests a general role for these genes in translation control. *Mol. Cell Biol.* **15**, 2719–2727.
- Karpenahalli, M.R., Lupas, A.N., and Söding, J. (2007). TPRpred: a tool for prediction of TPR-, PPR- and SEL1-like repeats from protein sequences. *BMC Bioinformatics* **8**, 2.
- Kish-Trier, E., and Hill, C.P. (2013). Structural biology of the proteasome. *Annu. Rev. Biophys.* **42**, 29–49.
- Klauer, A.A., and van Hoof, A. (2013). Genetic interactions suggest multiple distinct roles of the arch and core helicase domains of Mtr4 in Rrp6 and exosome function. *Nucleic Acids Res.* **41**, 533–541.
- LaCava, J., Houseley, J., Saveanu, C., Petfalski, E., Thompson, E., Jacquier, A., and Tollervey, D. (2005). RNA degradation by the exosome is promoted by a nuclear polyadenylation complex. *Cell* **121**, 713–724.
- Larimer, F.W., and Stevens, A. (1990). Disruption of the gene XRN1, coding for a 5' → 3' exoribonuclease, restricts yeast cell growth. *Gene* **95**, 85–90.
- Lebreton, A., and Séraphin, B. (2008). Exosome-mediated quality control: substrate recruitment and molecular activity. *Biochim. Biophys. Acta* **1779**, 558–565.
- Liu, Q., Greimann, J.C., and Lima, C.D. (2006). Reconstitution, activities, and structure of the eukaryotic RNA exosome. *Cell* **127**, 1223–1237.
- Lorentzen, E., and Conti, E. (2006). The exosome and the proteasome: nano-compartments for degradation. *Cell* **125**, 651–654.
- Lucius, A.L., Maluf, N.K., Fischer, C.J., and Lohman, T.M. (2003). General methods for analysis of sequential "n-step" kinetic mechanisms: application to single turnover kinetics of helicase-catalyzed DNA unwinding. *Biophys. J.* **85**, 2224–2239.
- Lykke-Andersen, S., Brodersen, D.E., and Jensen, T.H. (2009). Origins and activities of the eukaryotic exosome. *J. Cell Sci.* **122**, 1487–1494.
- Madrona, A.Y., and Wilson, D.K. (2004). The structure of Ski8p, a protein regulating mRNA degradation: implications for WD protein structure. *Protein Sci.* **13**, 1557–1565.
- Makino, D.L., Baumgärtner, M., and Conti, E. (2013). Crystal structure of an RNA-bound 11-subunit eukaryotic exosome complex. *Nature* **495**, 70–75.
- Mitchell, P., and Tollervey, D. (2003). An NMD pathway in yeast involving accelerated deadenylation and exosome-mediated 3' → 5' degradation. *Mol. Cell* **11**, 1405–1413.
- Mitchell, P., Petfalski, E., Shevchenko, A., Mann, M., and Tollervey, D. (1997). The exosome: a conserved eukaryotic RNA processing complex containing multiple 3' → 5' exoribonucleases. *Cell* **91**, 457–466.
- Nichols, M.D., DeAngelis, K., Keck, J.L., and Berger, J.M. (1999). Structure and function of an archaeal topoisomerase VI subunit with homology to the meiotic recombination factor Spo11. *EMBO J.* **18**, 6177–6188.
- Orban, T.I., and Izaurralde, E. (2005). Decay of mRNAs targeted by RISC requires XRN1, the Ski complex, and the exosome. *RNA* **11**, 459–469.
- Pyle, A.M. (2008). Translocation and unwinding mechanisms of RNA and DNA helicases. *Annu. Rev. Biophys.* **37**, 317–336.
- Schaeffer, D., Tzanova, B., Barbas, A., Reis, F.P., Dastidar, E.G., Sanchez-Rotunno, M., Arraiano, C.M., and van Hoof, A. (2009). The exosome contains domains with specific endoribonuclease, exoribonuclease and cytoplasmic mRNA decay activities. *Nat. Struct. Mol. Biol.* **16**, 56–62.
- Schrödinger. (2010). The PyMOL Molecular Graphics System, Version 1.5.0.4 (Schrödinger, LLC).
- Sikorski, R.S., Boguski, M.S., Goebel, M., and Hieter, P. (1990). A repeating amino acid motif in CDC23 defines a family of proteins and a new relationship among genes required for mitosis and RNA synthesis. *Cell* **60**, 307–317.

The logo for the journal 'Cell' is displayed in white text on a dark blue rectangular background.

- Stimimann, C.U., Petsalaki, E., Russell, R.B., and Müller, C.W. (2010). WD40 proteins propel cellular networks. *Trends Biochem. Sci.* 35, 565–574.
- Synowsky, S.A., and Heck, A.J. (2008). The yeast Ski complex is a heterotetramer. *Protein Sci.* 17, 119–125.
- Vanacova, S., and Stefl, R. (2007). The exosome and RNA quality control in the nucleus. *EMBO Rep.* 8, 651–657.
- Vanáčová, S., Wolf, J., Martin, G., Blank, D., Dettwiler, S., Friedlein, A., Langen, H., Keith, G., and Keller, W. (2005). A new yeast poly(A) polymerase complex involved in RNA quality control. *PLoS Biol.* 3, e189.
- van Hoof, A., and Parker, R. (1999). The exosome: a proteasome for RNA? *Cell* 99, 347–350.
- van Hoof, A., Lennertz, P., and Parker, R. (2000a). Yeast exosome mutants accumulate 3'-extended polyadenylated forms of U4 small nuclear RNA and small nucleolar RNAs. *Mol. Cell. Biol.* 20, 441–452.
- van Hoof, A., Staples, R.R., Baker, R.E., and Parker, R. (2000b). Function of the ski4p (Csl4p) and Ski7p proteins in 3'-to-5' degradation of mRNA. *Mol. Cell. Biol.* 20, 8230–8243.
- van Hoof, A., Frischmeyer, P.A., Dietz, H.C., and Parker, R. (2002). Exosome-mediated recognition and degradation of mRNAs lacking a termination codon. *Science* 295, 2262–2264.
- Wang, L., Lewis, M.S., and Johnson, A.W. (2005). Domain interactions within the Ski2/3/8 complex and between the Ski complex and Ski7p. *RNA* 11, 1291–1302.
- Wasmuth, E.V., and Lima, C.D. (2012). Exo- and endoribonucleolytic activities of yeast cytoplasmic and nuclear RNA exosomes are dependent on the non-catalytic core and central channel. *Mol. Cell* 48, 133–144.
- Weir, J.R., Bonneau, F., Hentschel, J., and Conti, E. (2010). Structural analysis reveals the characteristic features of Mtr4, a DExH helicase involved in nuclear RNA processing and surveillance. *Proc. Natl. Acad. Sci. USA* 107, 12139–12144.
- Wyers, F., Rougemaille, M., Badis, G., Rouselle, J.C., Dufour, M.E., Boulay, J., Régnault, B., Devaux, F., Namane, A., Séraphin, B., et al. (2005). Cryptic pol II transcripts are degraded by a nuclear quality control pathway involving a new poly(A) polymerase. *Cell* 121, 725–737.

## Supplemental Information



### EXTENDED EXPERIMENTAL PROCEDURES

#### Protein Purification

Full-length Ski2 and Ski2<sup>Δinsert</sup> (residues 835 - 1085 replaced by a Gly-Ser-Arg-Gly linker) were cloned with an N-terminal hexahistidine tag followed by a 3C protease site and subcloned into pFastBac1 vectors (Invitrogen). Proteins were expressed in baculovirus-infected Hi-Five insect cells (Invitrogen) at 26°C for 70 hr. Protein purification was carried out at 4°C or on ice and all buffers were supplemented with 1 mM β-mercaptoethanol. Cells were homogenized in low salt buffer (10 mM Tris-Cl pH 7.4, 10 mM NaCl, 2 mM MgCl<sub>2</sub>), supplemented with NaCl and imidazole to 250 mM and 20 mM, respectively, and lysate was cleared by centrifugation. His-tagged protein was enriched on Ni<sup>2+</sup>-NTA resin (Clontech), eluted with lysis buffer containing 300 mM imidazole and directly loaded on heparin sepharose resin (GE Healthcare). For elution, a gradient from 100 to 1,000 mM NaCl in 20 mM Tris-Cl pH 7.4 was used. The eluate was mixed with 3C protease and dialyzed in 20 mM Tris-Cl pH 7.4, 200 mM NaCl and 3 mM β-mercaptoethanol until complete removal of His-tags. Cleaved proteins were further purified by size-exclusion chromatography (SEC) in 10 mM HEPES pH 7.4 and 200 mM NaCl.

For expression of Ski2<sup>Δinsert</sup>-3-8, a pFL vector (Fitzgerald et al., 2006) was generated containing full-length Ski8 and full-length Ski3 (with an N-terminal hexahistidine tag followed by a 3C protease site) in the multiple cloning site (MCS) 1 and 2, respectively. The complex was then expressed from Hi-Five insect cells infected with two viruses encoding Ski2<sup>Δinsert</sup> (see above) and the dual Ski3<sup>His</sup>-Ski8 cassette. Purification was carried out as described for Ski2<sup>Δinsert</sup> (see above). Selenomethionine-labeled Ski2<sup>Δinsert</sup>-3-8 was expressed in insect cells grown in methionine-free medium (Expression Systems, LLC). L-Selenomethionine (Acros Chemicals) was added 8 hr postinfection to the medium at a final concentration of 100 mg/l. Cells were harvested 60 hr postinfection and the complex was purified as described. Incorporation rates of selenomethionine were estimated by mass-spectrometry to range from 66 to 75%.

Ski2-Ski3<sup>ΔN</sup>-Ski8 complex was expressed and purified as described above. Briefly, a pFL vector was cloned containing f.l. Ski8 and Ski3<sup>ΔN</sup> (residues 488-1432) fused to a 3C-cleavable N-terminal hexahistidine tag. The complex was then expressed in insect cells coinfecting with one virus expressing the Ski3<sup>ΔN+His</sup>-Ski8 cassette and one virus expressing f.l. Ski2. For expression of full-length Ski2-3-8, a f.l. Ski2 expression cassette was subcloned without N-terminal hexahistidine tag into a pFL vector. The cassette was then inserted into the Ski3<sup>His</sup>-Ski8 containing pFL vector via restriction / ligation using the BstZ171 and SpeI restriction sites (Fitzgerald et al., 2006). Full-length Ski2-3-8 complex was then purified from Hi-Five insect cells infected with a single virus containing the triple-expression cassette. Mutants used in this study were generated according to the Quikchange protocol (Stratagene) and expressed as the wild-type Ski2-3-8 complex.

Full-length Ski8 was subcloned with a hexahistidine tag followed by a TEV protease site into a pET-MCN vector (Romier et al., 2006). Protein was expressed in *E. coli* BL21 (DE3) Gold pLysS cells at 18°C for 16 hr after induction with 0.3 mM IPTG. Cells were resuspended in buffer A (20 mM Tris-Cl pH 7.5, 100 mM NaCl, 10 mM imidazole and 1 mM β-mercaptoethanol) broken by sonication and lysate was cleared by centrifugation. His-tagged protein was captured by Ni<sup>2+</sup>-NTA affinity chromatography and eluted with buffer A containing 500 mM imidazole. Eluate was mixed with TEV protease and dialyzed in buffer A until complete removal of the His-tag. The protein was further purified on a monoQ anion-exchange column (GE Healthcare) and subjected to SEC in 10 mM HEPES pH 7.5 and 200 mM NaCl. Ski7, GST-Ski7 (Halbach et al., 2012) and Exo-10 (Bonneau et al., 2009) were purified as described earlier.

#### Crystallization, Structure Determination, and Refinement

Ski2<sup>Δinsert</sup>-3-8 was concentrated to 13.5 mg/ml, supplemented with Tris(2-carboxyethyl)phosphine hydrochloride to 1 mM and mixed 1:1 (v/v) with reservoir solution (1.88 M NH<sub>4</sub>SO<sub>4</sub>, 100 mM Bis-Tris pH 6.0). 1 μl drops were set up in the sitting drop format and equilibrated against 500 μl reservoir solution at 4°C. For mounting, crystals were transferred to mother liquor stepwise supplemented with increasing amounts of glycerol. At the final glycerol concentration of 25% (v/v) the crystals were flash frozen in liquid nitrogen. Selenomethionine-substituted crystals were produced and manipulated in the same way, except that the reservoir solution contained 1.7 M NH<sub>4</sub>SO<sub>4</sub> and 100 mM Bis-Tris pH 5.5. Data were collected at 100 K on the PX-II beamline at Swiss Light Source, Paul-Scherrer Institute, Switzerland.

The data were processed using XDS (Kabsch, 2010) and SCALA (Evans, 2006). A high resolution cut-off for the data was chosen by  $I/\sigma(I) > 1$ , near 100% completeness and particularly by correlation between half-data sets ( $CC_{1/2}$ ) > 50% (Karplus and Diederichs, 2012). A partial solution could be obtained using molecular replacement (MR) with the Ski2 helicase core (residues 299 – 835 and 1,085 – 1,287, PDB code 4A4Z) and Ski8 (residues 1 – 397, 1S4U) and the program PHASER (McCoy et al., 2007). The partial MR solution was combined with experimental phase information from a selenomethionine single anomalous diffraction (SAD) experiment using PHASER. This gave an initial experimental electron density map and allowed location of 112 out of 126 methionine positions in the asymmetric unit. Two copies of the Ski2<sup>Δinsert</sup>-3-8 complex were present in the asymmetric unit and related by a 2-fold noncrystallographic symmetry (NCS) axis. Solvent flattening with 2-fold NCS-averaging was carried out using DM (Cowtan, 1994), and the native data to 3.7 Å were included by phase extension using phenix.autobuild (Adams et al., 2010). Parts of the structure that were previously unknown (Ski2 N-terminal segment, full-length Ski3) were then built manually in the resulting electron density map. Refinement was carried out with phenix.refine (version 1.82, [Adams et al., 2010]). Initial rounds of rigid body refinement were followed by positional refinement, TLS refinement (TLS groups determined using the TLSMD server [Painter and Merritt, 2006]) and group

B-factor refinement (the moderate resolution and the size of the asymmetric unit suggested using B-factor instead of individual B-factor refinement). The refinement additionally used secondary structure and NCS restraints (released during final stages of refinement) while B-factors remained unrestrained. Model building was carried out in COOT (Emsley et al., 2010). For fitting of side-chains, B-factor sharpened electron density maps were used (COOT) that allowed establishing a sequence register consistent with the selenomethionine positions. Iterative cycles of building and refinement improved model completeness and quality of electron density map. The electron density for the Ski8<sub>OUT</sub> subunit in the second NCS copy was partially broken, probably due to lacking crystal contacts. Nonetheless, four peaks in the anomalous difference density map allowed unambiguous placement of Ski8 as a rigid body. In this manuscript we refer to the model as taken from the first NCS copy, which appeared to be generally better ordered. The model-sequence coverage of the final model is indicated in Figure S1B. Data collection and refinement parameters as given in Table 1 are defined as follows:  $R_{merge} = (\sum_{hkl} \sum_j |I_{hklj} - \langle I_{hkl} \rangle|) / (\sum_{hkl} \sum_j \langle I_{hklj} \rangle)$ , where  $\langle I_{hkl} \rangle$  is the average of symmetry-related observations of a unique reflection;  $R_{work,free} = (\sum_{hkl} |F_{hkl}^{obs} - F_{hkl}^{calc}|) / (\sum_{hkl} F_{hkl}^{obs})$ , where  $R_{work}$  and  $R_{free}$  are calculated from the working or the test set of reflections, respectively;  $I/\sigma(I)$  is defined as the average intensity of a group of reflections belonging to a given resolution shell divided by the average standard deviation (sigma) of the same group of reflections.

#### RNase Protection Assays

An internally labeled 57-mer single stranded RNA (5' - C\*(UC)<sub>26</sub> - 3') was generated by in vitro-transcription in presence of  $\alpha$ -<sup>32</sup>P UTP using the MEGAshortscript kit (Ambion) and purified by poly-acrylamide gel electrophoresis. In a typical RNase protection reaction, 10 pmol protein was mixed with 5 pmol internally labeled RNA to a final reaction volume of 20  $\mu$ l (final buffer: 50 mM HEPES pH 7.5, 50 mM NaCl, 5 mM magnesium diacetate, 10% (w/v) glycerol, 0.1% (w/v) NP40, and 1 mM dithiothreitol). Samples were incubated at 4°C for 1 hr and treated with 1  $\mu$ g RNase A and 2.5 U RNase T1 (Fermentas) or with 1 U Terminator 5'-to-3' exoribonuclease (Epicenter Biotechnologies) for 20 min at 20°C. Protected RNA fragments were then extracted twice with phenol:chloroform:isoamyl alcohol (25:24:1, v/v, Invitrogen), precipitated with ethanol, separated on a 20% (w/v) denaturing poly-acrylamide gel and visualized by phosphorimaging.

#### Pull-Down Assays

GST-tagged prey protein (4  $\mu$ g) was mixed with equal molar amounts of bait protein and input samples were taken. Buffer was added to a volume of 200  $\mu$ l and final concentrations of 10 mM HEPES pH 7.5, 75 mM sodium chloride, 2 mM magnesium acetate, 0.1% (v/v) NP-40, 1 mM dithiothreitol and 12.5% (v/v) glycerol (buffer A). 40  $\mu$ l of a 50% (v/v) suspension of GSH-sepharose beads (GE Healthcare) were added and the reaction was incubated for 30 min at 4°C. Beads were washed three times with buffer A before eluting the precipitated protein. Samples were analyzed on a 8.5% (w/v) SDS-poly(acrylamide) gel.

#### Helicase Assay

RNA oligo C<sub>ss</sub>17 (AAGUGAUGGUGGUGGG) was labeled at the 5' position with <sup>32</sup>P by standard polynucleotide kinase treatment and mixed with a 1.5 molar excess of RNA oligo ss27 (CCCCACCACCAUCACUAAAAAAAAA). Annealing was induced by heating to 95°C and slow cooling. For a typical unwinding reaction, 2 nM duplex were mixed with indicated amounts of proteins in a buffer containing 100 mM KCl, 0.1 mM EDTA, 1 mM DTT and 20 mM MES pH 6.0. The reaction was started by adding a mix of ATP (final concentration of 2 mM), MgCl<sub>2</sub> (2 mM) and RNA trap-oligo (C<sub>ss</sub>17, 500 nM). Samples were incubated at 30°C for 30 min and then mixed with quenching buffer (150 mM NaAc, 10 mM EDTA, 0.5% (w/v) SDS, 25% (v/v) glycerol, 0.05% (w/v) xylene cyanol, 0.05% (w/v) bromophenol blue). Samples were separated by native PAGE at 4°C.

#### Yeast Strains

Initially, three working strains were created using the base strain W303 (*MATa/MATa, {leu2-3,112 trp1-1 can1-100 ura3-1 ade2-1 his3-11,15, RAD5}*): a *SKI3* deletion strain, a strain carrying a c-terminally EGFP-tagged *SKI3* and an *XRN1* deletion strain. The *SKI3* deletion strain (*ski3 $\Delta$ ::klURA3*) was obtained by transforming the diploid wild-type W303 with a *klURA3* cassette (Gueldener et al., 2002) targeted to the region upstream and downstream of *SKI3*. The knockout was confirmed by PCR. Diploid cells were sporulated and tetrads were dissected to test for the nonessential nature of the *SKI3* deletion. The EGFP c-terminally tagged strain (*SKI3-EGFP::kanMX4*) was created by transforming a diploid wild-type with a PCR fragment generated from plasmid *pym27* (PCR Toolbox [Janke et al., 2004]). The obtained diploid strain was sporulated and tetrads were analyzed for any grave growth defects due to the inserted tag. The *XRN1* deletion strain (*xrn1 $\Delta$ ::natNT2*) was essentially constructed as described above, except that in a second transformation the *klURA3* cassette was exchanged with a *natNT2* selection marker generated from pFA6a-*natNT2* bearing homologies to the region upstream and downstream of *xrn1 $\Delta$ ::klURA3*. The marker switch was confirmed by PCR and testing for a *nat<sup>R</sup>* and *ura<sup>-</sup>* phenotype. Subsequently the diploid strain was sporulated and tetrad dissected.

For generation of *SKI3* mutants, *SKI3-EGFP* including 500bp upstream and downstream of the ORF was subcloned from the *SKI3-EGFP* strain into a Ycplac33 vector by SmaI linearization cotransformation followed by gap repair. The plasmid was then mutagenized to obtain the *SKI3* mutations as indicated in Figure S4D.

Mutant strains were created from the *ski3 $\Delta$ ::klURA3* strain by gene replacement (Amberg et al., 2006; Gietz and Schiestl, 2007). PCR products bearing the desired mutations were generated from the mutagenized Ycplac33-*SKI3-EGFP::kanMX4* plasmids. Cells were transformed and plated on YPD/G418 plates and subsequently replicated on SC-FOA plates. Cells having a G418<sup>R</sup>

and  $ura^-$  phenotype were sporulated and tetrads dissected. Candidate strains were further analyzed via sequencing to test for the presence of the desired mutation. Generation of the double mutation strains was carried out by crossing the *ski3* mutant strains with the *xrn1 $\Delta$ ::natNT2 / Ycplac33-Xrn1* strain, followed by sporulation and tetrad dissection. Yeasts were grown in standard media supplemented with the appropriate antibiotic or in standard synthetic media to select against auxotrophies.

#### Western Blot Analysis

Yeast strains were grown to midlog phase. Cells were lysed using the Yeast Buster kit (Novagen) and soluble lysate was prepared by centrifugation. After normalizing levels of total protein input, EGFP-tagged protein was enriched by immunoprecipitation with immobilized anti-GFP nanobodies. Samples were analyzed by western blot using a mouse anti-GFP primary antibody (Santa Cruz Biotechnology) and an HRP-conjugated goat anti-mouse secondary antibody (Bio-Rad). Blots were visualized using ECL Advance developer solution (GE Healthcare) and a LAS 4000 imaging system (GE Healthcare).

#### SUPPLEMENTAL REFERENCES

- Adams, P.D., Afonine, P.V., Bunkóczy, G., Chen, V.B., Davis, I.W., Echols, N., Headd, J.J., Hung, L.W., Kapral, G.J., Grosse-Kunstleve, R.W., et al. (2010). PHENIX: a comprehensive Python-based system for macromolecular structure solution. *Acta Crystallogr. D Biol. Crystallogr.* **66**, 213–221.
- Amberg, D.C., Burke, D.J., and Strathern, J.N. (2006). "Quick and dirty" plasmid transformation of yeast colonies. *CSH Protoc.* 2006, pdb.prot4146.
- Cowtan, K. (1994). 'dm': an automated procedure for phase improvement by density modification. *Joint CCP4 and ESF-EACBM Newsletter on Protein Crystallography* **37**, 34–38.
- Emsley, P., Lohkamp, B., Scott, W.G., and Cowtan, K. (2010). Features and development of Coot. *Acta Crystallogr. D Biol. Crystallogr.* **66**, 486–501.
- Evans, P. (2006). Scaling and assessment of data quality. *Acta Crystallogr. D Biol. Crystallogr.* **62**, 72–82.
- Fitzgerald, D.J., Berger, P., Schaffitzel, C., Yamada, K., Richmond, T.J., and Berger, I. (2006). Protein complex expression by using multigene baculoviral vectors. *Nat. Methods* **3**, 1021–1032.
- Gietz, R.D., and Schiestl, R.H. (2007). High-efficiency yeast transformation using the LiAc/SS carrier DNA/PEG method. *Nat. Protoc.* **2**, 31–34.
- Guldener, U., Heinisch, J., Koehler, G.J., Voss, D., and Hegemann, J.H. (2002). A second set of loxP marker cassettes for Cre-mediated multiple gene knockouts in budding yeast. *Nucleic Acids Res.* **30**, e23.
- Janke, C., Magiera, M.M., Rathfelder, N., Taxis, C., Reber, S., Maekawa, H., Moreno-Borchart, A., Doenges, G., Schwob, E., Schiebel, E., and Knop, M. (2004). A versatile toolbox for PCR-based tagging of yeast genes: new fluorescent proteins, more markers and promoter substitution cassettes. *Yeast* **21**, 947–962.
- Kabsch, W. (2010). Xds. *Acta Crystallogr. D Biol. Crystallogr.* **66**, 125–132.
- Kabsch, W., and Sander, C. (1983). Dictionary of protein secondary structure: pattern recognition of hydrogen-bonded and geometrical features. *Biopolymers* **22**, 2577–2637.
- Karplus, P.A., and Diederichs, K. (2012). Linking crystallographic model and data quality. *Science* **336**, 1030–1033.
- Kelley, L.A., and Sternberg, M.J. (2009). Protein structure prediction on the Web: a case study using the Phyre server. *Nat. Protoc.* **4**, 363–371.
- McCoy, A.J., Grosse-Kunstleve, R.W., Adams, P.D., Winn, M.D., Storoni, L.C., and Read, R.J. (2007). Phaser crystallographic software. *J. Appl. Cryst.* **40**, 658–674.
- Painter, J., and Merritt, E.A. (2006). Optimal description of a protein structure in terms of multiple groups undergoing TLS motion. *Acta Crystallogr. D Biol. Crystallogr.* **62**, 439–450.
- Romier, C., Ben Jelloul, M., Albeck, S., Buchwald, G., Busso, D., Celie, P.H., Christodoulou, E., De Marco, V., van Gerwen, S., Knipscheer, P., et al. (2006). Co-expression of protein complexes in prokaryotic and eukaryotic hosts: experimental procedures, database tracking and case studies. *Acta Crystallogr. D Biol. Crystallogr.* **62**, 1232–1242.
- Schneider, C.A., Rasband, W.S., and Eliceiri, K.W. (2012). NIH Image to ImageJ: 25 years of image analysis. *Nat. Methods* **9**, 671–675.



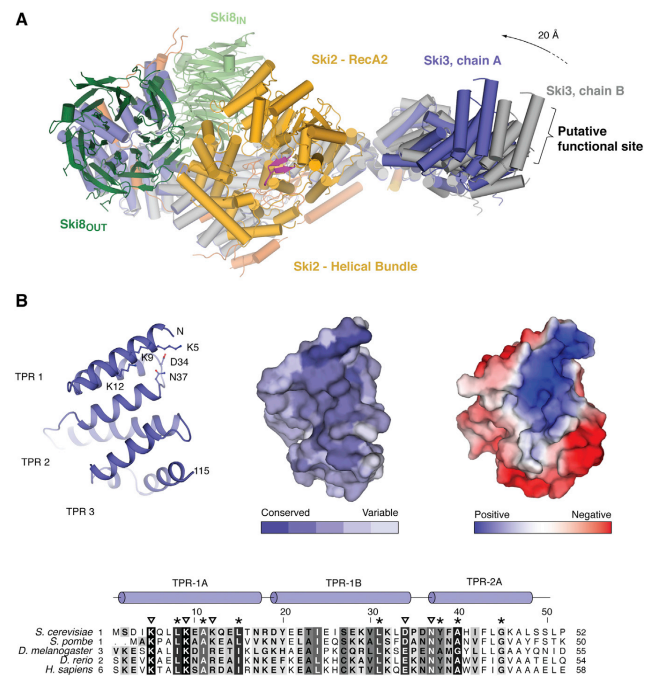


**Figure S2. The N-Terminal Arm of Ski3 Is Flexible and Contains a Conserved Surface Patch, Related to Figure 2**

(A) Superposition of the two copies of the Ski complex in the asymmetric unit of the crystals. One copy is shown in the same colors as in Figure 2A. The second copy is shown in gray. While Ski2, the two Ski8 subunits and the C-terminal arm of Ski3 superpose with an rmsd less than 0.5 Å, the N-terminal arm has two different conformations with a maximum displacement of 20 Å.

(B) In the N-terminal arm, the surface of TPRs 1 - 3 contains a set of conserved, positively-charged residues. The left panel shows the canonical TPR-fold of this domain and the conserved residues are labeled. The central and right panels show the same portion of the molecule as a surface representation colored according to sequence conservation and to electrostatic potential, respectively. An alignment of eukaryotic Ski3 sequences covering the first 1.5 TPR repeats is shown in the lower panel. Conservation is indicated by shades of gray (black, conserved; white, variable), triangles denote surface residues and asterisks denote structural residues.

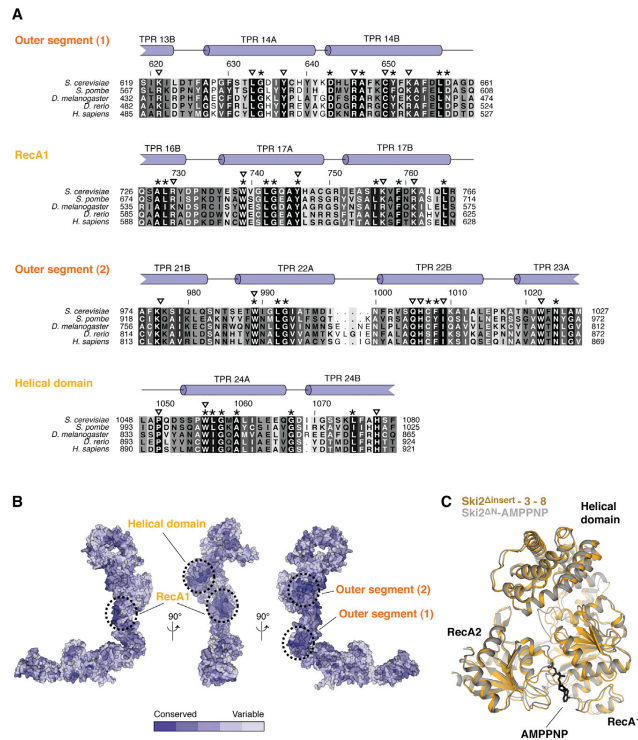


**Figure S3. Binding of the Ski2 Helicase Core to Conserved Sites in Ski3, Related to Figure 3**  
 (A) Sequence alignments of regions in Ski3 that form the interfaces to the Ski2 helicase core, as indicated in (B). The interfaces are well conserved, suggesting that Ski complex in higher eukaryotes may have a similar architecture.  
 (B) Ski3 is shown in surface representation colored according to sequence conservation (dark blue, conserved; light blue, variable). The orientation of the model in the left and middle panels corresponds to those in Figure 2A. The binding sites to the Ski2 core are denoted by dashed circles and the corresponding interacting regions of Ski2 are indicated.  
 (C) A superposition of the Ski2<sup>ΔN</sup>-AMPPNP crystal structure (gray, AMPPNP in black) to the structure of the Ski2 helicase core as found in the Ski2<sup>Δinsert-3-8</sup> complex (yellow).

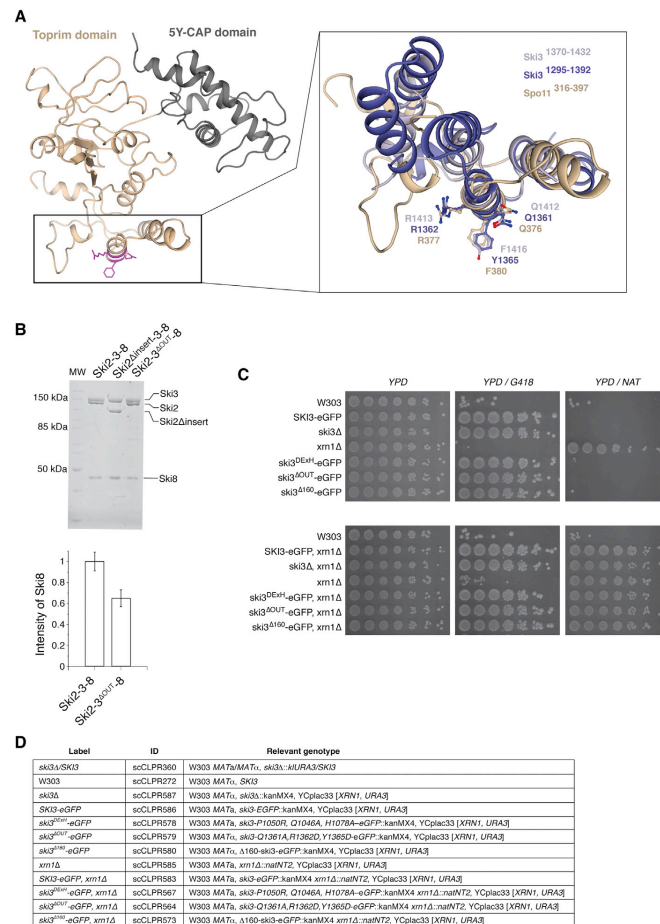


**Figure S4. Mutation of the Q-R-x-x-Φ Motif in Ski3 or Spo11 Impairs Binding to Ski8, Related to Figure 4**

(A) In the left panel, a homology model of yeast Spo11 was generated based on the structure of the related *M. jannaschii* topoisomerase VI-A (PDB code 1D3Y, (Nichols et al., 1999)) using the PHYRE server (Kelley and Sternberg, 2009). The N-terminal 5YCAP domain is colored in gray and the C-terminal toprim domain in beige. The Q-R-x-x-Φ motif in the C terminus of the toprim domain is highlighted in magenta. The right panel shows a close-up view of the Spo11 C terminus including the Q-R-x-x-Φ motif. Additionally, the corresponding helices of Ski3 that bind to Ski8<sub>IN</sub> (TPRs 32/33 in light blue) and Ski8<sub>OUT</sub> (TPRs 30/31 in dark blue) were superposed. The Spo11 homology model superposes well to the experimentally observed Ski8-binding surfaces in Ski3. Remarkably, modeling of Ski8 to the Spo11 Q-R-x-x-Φ motif (not shown) results in a structural model of the Spo11-Ski8 complex without steric clashes.

(B) The upper panel shows an SDS-PAGE of wild-type and mutant Ski2-3-8 complexes used in the RNase protection assay in Figure 4C. The lower panel shows the quantification of complex stoichiometry of the samples in (A). The density of the band corresponding to Ski8 was related to those corresponding to Ski2 and Ski3. The ratios were normalized to the wild-type sample. Densities were measured using the program ImageJ (Schneider et al., 2012). Error bars represent +/- 1 standard deviation from three independent experiments. In the Ski2-3-8<sup>OUT</sup>-8 mutant, the Ski8:(Ski2+Ski3) ratio drops to ~60%, indicating that disruption of the Q-R-x-x-Φ motif in TPR 31 of Ski3 indeed leads to loss of the Ski8<sub>OUT</sub> subunit.

(C) Spotting of the yeast strains shown in Figure 4D to YPD, YPD/G418 and YPD/NAT control plates. Here, in addition to the undiluted sample the dilutions omitted in Figure 4 are shown. NAT, nourseothricin; YPD, yeast extract peptone dextrose.

(D) A table of the yeast strains generated in this study including the relevant genotype.

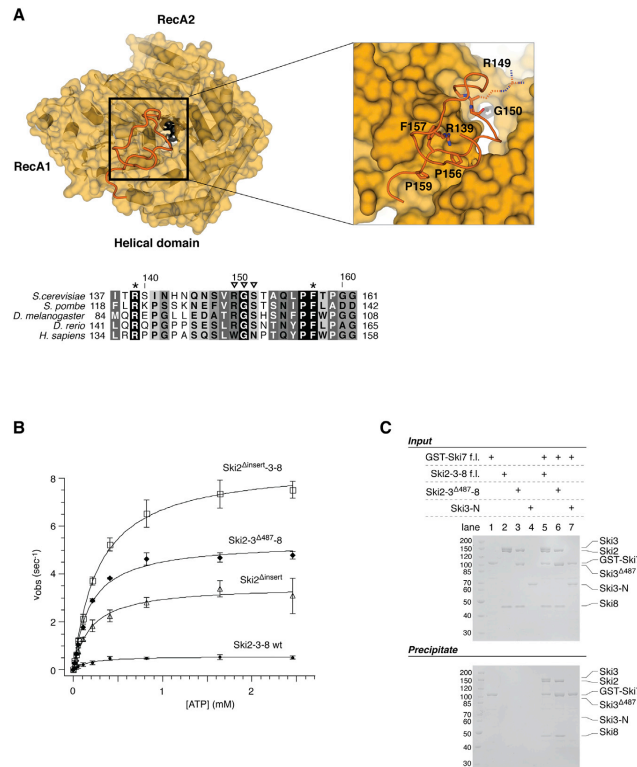


**Figure S5. Properties of the Ski2 RG-Loop Segment and the Ski3 N-Terminal Arm, Related to Figure 5**

(A) Interactions of the RG-loop segment with the Ski2 helicase core. The upper left panel shows a surface representation of the Ski2 helicase core (yellow) and the RG-loop segment in cartoon representation (orange). The upper right panel shows a close-up view as indicated. Relevant residues are highlighted. The side-chain of Arg149 is shown as dashed line as no electron density was observed. In the lower panel, an alignment of RG-loop segment sequences from eukaryotic Ski2 species is given. Conservation is indicated in shades of gray (black, conserved; white, variable). Asterisks denote structural residues and triangles indicate solvent-accessible side-chains.

(B) ATPase activity raw data corresponding to the graph shown in Figure 5B. The initial reaction velocity (mole ADP produced per mole of Ski2 and second) is plotted versus the concentration of ATP (mM). Error bars represent standard deviation from three independent experiments. For data on Ski2, see Figure 1C.

(C) Pull-down assays indicate that the Ski3 N terminus is not involved in interactions within the Ski complex nor with Ski7 (Ski3-N, residues 1 - 521). Input samples separated by SDS-PAGE are shown in the upper panel, samples precipitated with GST-Ski7 in the lower panel.

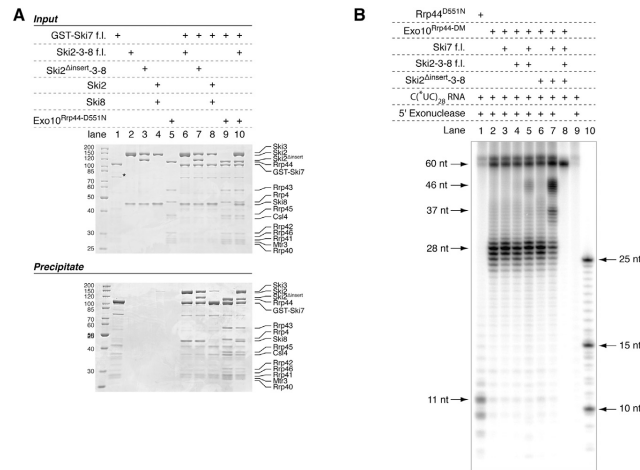


**Figure S6. Ski7 Mediates the Interaction between the Ski2-3-8 and Exosome Complexes In Vitro, Related to Figure 6**

(A) A pull-down experiment was carried out with GST-tagged full-length Ski7 and untagged Exo10, Ski2, Ski8 or Ski2-3-8 proteins. Input samples are shown in the upper panel and precipitated samples in the lower panel. A molecular weight marker was included and the identity of the proteins is indicated. Ski2-3-8 and Exo-10 bind to Ski7 separately (lanes 6 and 9) and simultaneously (lane 10). Ski2 and Ski8 only bind to the Ski7-Exo-10 complex in presence of Ski3 (compare lanes 6 and 8). An asterisk indicates an impurity in the GST-Ski7 preparation.

(B) An RNase protection experiment as shown in Figure 6A except that a processive 5'-to-3' exoribonuclease was used instead of RNase A/T1.

## 4 Discussion

The major achievement of the PhD work at hand was to determine the crystal structures of the Ski2 helicase region (Ski2 $\Delta$ N), the Ski2 insertion domain as well as the Ski2 <sup>$\Delta$ insert-Ski3-Ski8</sup> complex. The assembly of the individual structures yields the first comprehensive structural description of the full-length yeast Ski2-Ski3-Ski8 complex (Fig. 4.1). Additional functional characterization helped to understand the role of the individual subunits and to identify two regulatory mechanisms that may contribute to the regulation of exosome activity.

The following sections discuss the structure and function of the Ski2 helicase region alone (section 4.1) as well as in the context of the Ski2-Ski3-Ski8 complex (section 4.2), the role of the Ski3 TPR scaffold (section 4.3) and the structure and function of the two Ski8 subunits and the implications for the role of Ski8 in meiotic recombination (section 4.4). A final section discusses the two regulatory mechanisms of the SKI complex in context of the exosome (section 4.5).

### 4.1 Ski2 contains a conserved DExH box core and a variable insertion domain

The helicase region of Ski2 was defined by limited proteolysis to encompass residues 296 - 1287 (Ski2 $\Delta$ N) and was crystallized in complex with adenosine 5'-( $\beta,\gamma$ -imido)triphosphate (AMPPNP). The helicase core consists of a ring-like arrangement of the two RecA domains, the ratchet and winged helix (WH) domains (Fig. 4.1). It is well conserved in sequence and highly similar in structure to other DExH box helicases like Mtr4 and Hel308 which have been structurally characterized in complex with RNA substrates (Büttner et al., 2007; Weir et al., 2010). This suggests that in Ski2 RNA is bound along a similar path through the helicase core. Consistently, Ski2 also contains a conserved  $\beta$ -hairpin at the presumable

RNA entry site that has been shown to melt double stranded DNA in the structure of archaeal Hel308 (Büttner et al., 2007). AMPPNP is bound through the canonical SF2 motifs in a conformation that is very similar to the Mtr4-ADP-RNA structure (Weir et al., 2010). Thus, the overall architecture of the Ski2 helicase core is well conserved with other enzymes of the DExH box family.

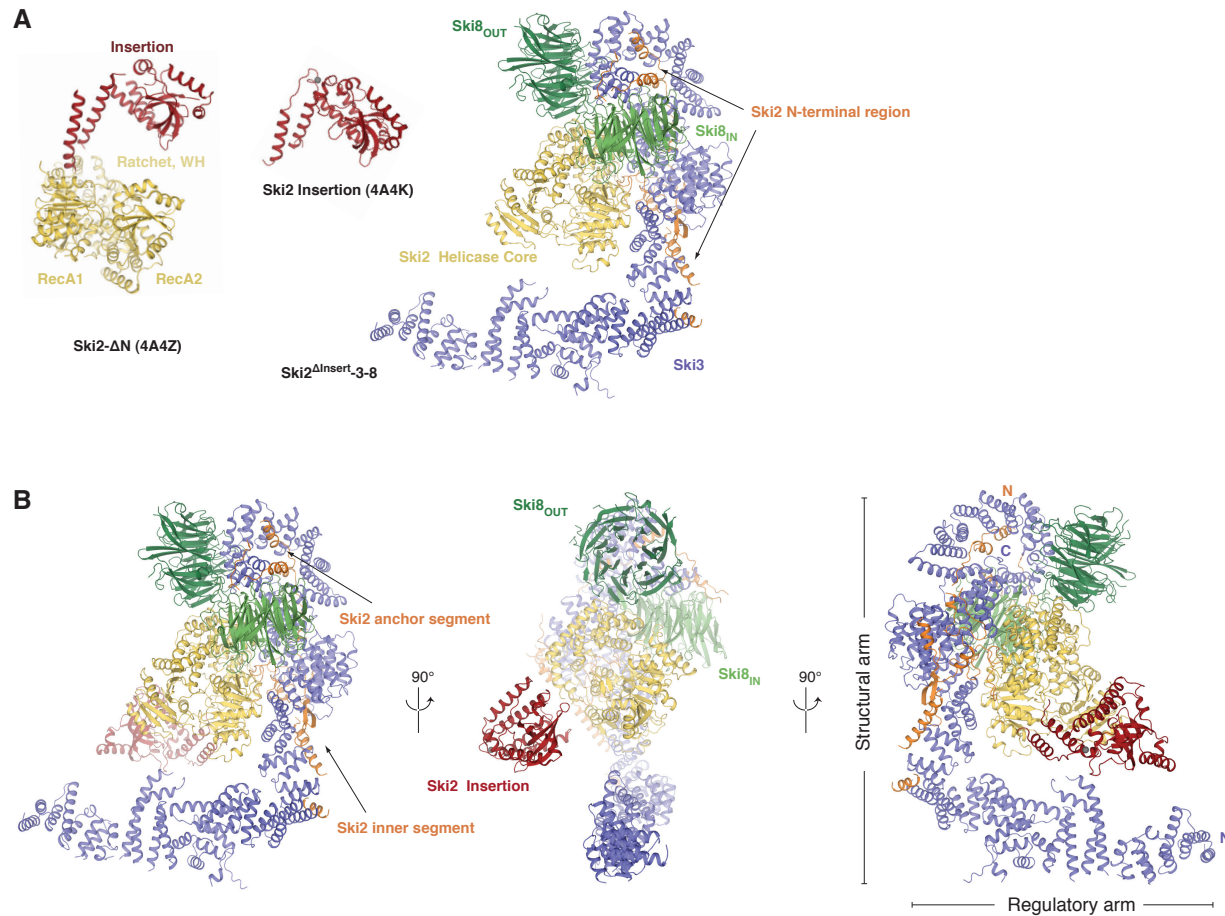


**Figure 4.1** | Structural description of the *S. cerevisiae* Ski2-Ski3-Ski8 complex. (A) Individual crystal structures of Ski2 $\Delta$ N, Ski2 insertion domain and Ski2 $\Delta$ insert-Ski3-Ski8. The two Ski8 subunits in the complex are denoted Ski8<sub>IN</sub> and Ski8<sub>OUT</sub> according to their central or peripheral position, respectively. Ski2 is colored in orange (N-terminal region), yellow (helicase core) or red (insertion domain); Ski3 is in blue, Ski8<sub>IN</sub> in light green and Ski8<sub>OUT</sub> in dark green. PDB codes are indicated in brackets where available. (B) A structural model for the full-length Ski2-Ski3-Ski8 complex is created by superposition of the Ski2 insertion domain to the Ski2 $\Delta$ N structure, which in turn was aligned to the Ski2 helicase core of the Ski2 $\Delta$ insert-Ski3-Ski8 structure.

From the globular helicase core of Ski2 the so-termed insertion domain emerges (residues 835 - 1085). It consists of a globular  $\beta$ -barrel that is connected to the helicase core through a flexible  $\alpha$ -helical stalk. A comparison with the Mtr4 insertion domain (also termed KOW domain) shows that both domains share a similar architecture (consisting of a helical stalk and a  $\beta$ -barrel). While the presence of the Ski2 insertion domain and the position where it emerges from the enzyme core (within the WH domain above the RNA entry site) is conserved with Mtr4, the domain itself is not conserved in sequence even among Ski2 proteins from other yeast species.

On the functional level, both domains differ, too. The Mtr4 KOW domain has been shown to bind structured RNAs *in vitro* (Weir et al., 2010) and has been linked to rRNA maturation *in vivo* (Jackson et al., 2010; Klauer and van Hoof, 2013). In contrast, electrophoretic mobility shift assays (EMSAs) indicate that the Ski2 insertion domain binds RNA unspecifically, consistent with the presence of a positively charged surface patch. The promiscuous RNA-binding properties and the location above the RNA entry site in the helicase core suggest that the Ski2 insertion domain plays a general role in substrate loading.

## 4.2 The structure of the SKI complex: a framework for Ski2 to function in concert with the exosome

The fact that the Ski2 insertion domain protrudes from the globular helicase core without being required for formation of the Ski2-Ski3-Ski8 complex (Fig. 3.1.4) suggested its removal for purposes of structure determination. The resulting Ski2 <sup>$\Delta$ insert</sup>-Ski3-Ski8 complex could be readily crystallized and the structure was solved by a single wavelength anomalous diffraction (SAD) experiment.

The crystal structure of the Ski2 <sup>$\Delta$ insert</sup>-Ski3-Ski8 complex revealed the architecture of the yeast SKI complex (Fig. 4.1). Ski3 consists of 33 TPR motifs that form a long superhelical solenoid with an N-terminal and a C-terminal arm. The C-terminal arm binds both Ski8 subunits as well as the N-terminal and the helicase region of Ski2. The two Ski8 subunits (Ski8<sub>IN</sub>, central position. Ski8<sub>OUT</sub>, peripheral position. See also Fig. 4.1) bind back to the helicase core. The helicase is thus centrally located within complex, reflecting the presumably pivotal role of its activity for function of the SKI complex. In the Ski2 <sup>$\Delta$ insert</sup>-Ski3-Ski8 complex structure (representing the apo state), the Ski2 DExH core has a conformation that is nearly identical to Ski2 $\Delta$ N bound to AMPPNP (Fig. 3.2.4). It

is possible that the other subunits induce this conformation in the helicase core, but more experimental data (e.g. in the form of RNA- or nucleotide-bound structures) is needed to clarify whether Ski3 and Ski8 actively trigger any conformational changes in the Ski2 helicase core.

Nevertheless, formation of the Ski2-Ski3-Ski8 complex leads to a series of structural rearrangements in Ski2. First, the Ski2 insertion domain is positioned at the entry site of the RNA to the helicase core. The insertion domain is not present in the Ski2<sup>Δinsert</sup>-Ski3-Ski8 structure, but modeling it in this position (Fig. 4.1) does not produce any steric clashes, which makes it reasonable to assume a similar orientation as in the Ski2<sup>ΔN</sup> structure. Second, the RG-loop segment of the Ski2 N-terminal region is placed by Ski3 such that its conserved Arg-Gly dipeptide flanks the canonical RNA-interacting SF2 motifs towards the 3' end of the RNA (see Fig. 3.2.4). This extends the *bona fide* RNA-binding path through the helicase core. Third, portions of Ski8<sub>IN</sub> and Ski3 are arranged around the presumable exit site of the RNA 3' end from the helicase core. Even though the electrostatic potential and the conservation of involved surface patches do not show any striking features, a cleft is created through which the RNA can leave the complex.

All three structural features cluster along the RNA-binding path of Ski2 and thus highlight the importance of RNA-routing through the SKI complex. They point towards a functional interplay with the exosome where a helicase would need to accept substrates or control their access (via the insertion domain), unwind secondary structure elements and transfer the substrate to the exosome (via the extension of the RNA-binding path by the RG-loop and the formation of an RNA exit cleft). In agreement with such a model, the Ski2-Ski3-Ski8 complex displays RNA-dependent ATPase activity and unwinds RNA duplexes with 3' overhang. The resulting single stranded RNA substrates could then be readily degraded by the exosome (Bonneau et al., 2009).

It thus appears that formation of the Ski2-Ski3-Ski8 complex sets a structural framework that primes the helicase core of Ski2 for assisting the exosome in substrate degradation. Consistent with this model, direct substrate channeling between both complex is observed and will be discussed in section 4.5.

### 4.3 The Ski3 TPR scaffold organizes the SKI complex

Mapping of domain interactions within the Ski2-Ski3-Ski8 complex in yeast *in vivo* suggested that Ski3 is involved in all subunit interactions (Wang et al., 2005). The crystal

structure of the Ski2<sup>Δinsert</sup>-Ski3-Ski8 complex rationalizes this observation by revealing how the TPR solenoid of Ski3 acts as scaffold for the entire complex.

Containing 33 TPRs, Ski3 can be divided in an N-terminal arm and a C-terminal arm. The C-terminal arm binds the remaining subunits and thus organizes the architecture of the complex (Fig. 4.1). It extensively interacts with a series of motifs in the Ski2 N-terminus that but also binds to the helicase core of Ski2 (the RecA1 and ratchet domains). Interestingly, the interfaces with the helicase core are conserved in higher eukaryotes, suggesting a similar complex topology. The Ski3 C-terminal arm also binds both Ski8 subunits (see section 4.4).

### **Size, versatility and flexibility predestine TPR proteins as molecular scaffolds**

TPR proteins and particularly their complexes with peptides have been well characterized in terms of structure and biochemistry (D'Andrea and Regan, 2003; Zeytuni and Zarivach, 2012). Their ability to engage in protein-protein interactions has earned them a reputation as scaffold subunits in protein complexes, but structural characterization of such entire assemblies remains scarce. The unusually large TPR array of Ski3 illustrates several properties of TPR proteins that allow them to efficiently organize large complexes.

First, if a protein acts as central hub within a complex, i.e. it interacts with all or most of the other subunits, a large surface must be dedicated to forming interfaces with those proteins. Structures of TPR proteins with up to 14 consecutive repeats have been reported, for instance those of O-linked glycosyl transferase (Jinek et al., 2004) or the anaphase promoting complex subunit Cdc16 (Zhang et al., 2010). The finding that the Ski3 C-terminus contains 23 consecutive canonical repeats (Fig. 3.2.2) illustrates that TPR scaffolds can be considerably longer than assumed. It can be anticipated that uncharacterized TPR-containing proteins may form even longer solenoids. The size creates sufficient surface area that can be dedicated to interactions with partner proteins. Probably more important than the mere molecular size is the surface-to-residue ratio. In TPR proteins, the superhelical stacking leads to an extended solenoid shape of the molecule. Compared to a globular protein of similar size, such a fold results in a considerably higher ratio of surface area to residues. Thus, the combination of molecular size and its efficient transformation into binding surfaces enables TPR proteins to form highly optimized protein interaction platforms.

Second, TPR proteins are versatile binders. Typically, a ligand binds as an extended polypeptide to the concave surface of the TPR superhelix, even though the convex surface

regions have also been described as interfaces (D'Andrea and Regan, 2003; Zeytuni and Zarivach, 2012). The Ski2<sup>Δinsert</sup>-Ski3-Ski8 structure shows how in a single TPR protein many different surface types can be used as a binding site. For instance, the Ski2 outer segment binds to the convex surface of Ski3 (Fig. 4.2B). Similarly, loops that connect two consecutive repeats or two helices within a repeat serve as binding sites (e.g. RG-loop domain binding to TPRs 17 - 18 and TPRs 21 - 22, Fig. 4.2C). Yet another binding mode is encountered at the Ski3 C-terminus where the capping helix engages the Ski2 anchor segment, creating a pseudo-TPR motif (Fig. 4.2D). A comparable diversity is found in the conformation of the bound ligands. They bind as an extended peptide (e.g. Ski2 inner segment), an  $\alpha$ -helix (e.g. Ski2 anchor segment), a  $\beta$ -hairpin (Ski2 inner segment) or a folded protein (e.g. Ski8<sub>OUT/IN</sub>) (compare Figs. 4.2A-C).

Third, variations in the superhelical twist and pitch allow TPR proteins to fine-tune the orientation of their binding sites. For instance, the axes of the two C-terminal superhelical turns of Ski3 (TPRs 26 - 32 and 27 - 33) are oriented in a nearly perpendicular fashion on to the other (Fig. 4.1). This allows the Ski8 subunits to bind back on the Ski2 core that is located closer to the Ski3 N-terminus (TPRs 17 - 24). Such an arrangement would be sterically impossible in the case of a strictly linear solenoid.

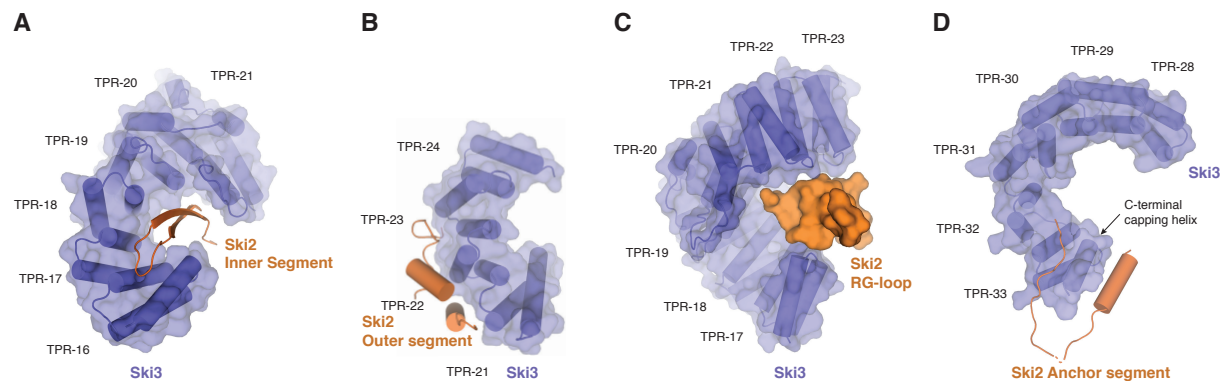


**Figure 4.2** | Variability in ligand conformation and binding surface types in the Ski3 TPR scaffold. (A) A part of the Ski2 inner segment (residues 101 - 122) binds as a long  $\beta$ -hairpin to the concave side of the Ski3 TPR solenoid. (B) A stretch of the Ski2 outer segment (residues 178 - 220) binds in  $\alpha$ -helical conformation to the convex side of Ski3. (C) The Ski2 RG-loop segment (residues 127 - 165) interacts with the inter- and intra-TPR loops of Ski3. (D) The Ski2 anchor segment (residues 1 - 39) creates a pseudo-TPR repeat by stacking against the C-terminal capping helix of Ski3. Ski2 segments are colored in orange, Ski3 in blue and TPRs are numbered as established in Fig. 3.2.2.

These properties appear to be intrinsic to TPR proteins, but there may be a mutual dependency between scaffold and binding target. For instance, the Ski2 N-terminal segment threads through the C-terminal arm of Ski3, thereby stabilizing it (Fig. 3.2.3). This may help to properly orient the remaining binding sites (e.g. of the Ski8 subunits).

### **In Ski3, conservation of the TPR fold correlates with binding site functionality**

TPRs are ancient motifs that most likely have been present in the last common ancestor since they are found in bacteria, archaea and eukaryotes. However, conservation of the motif is poor in terms of sequence identity. Rather, classes of amino acids (small vs. large) are conserved on a given position, in-line with the “hole-and-knobs” model for interaction between the helices (Hirano et al., 1990). In contrast, the entire fold is well conserved, and TPR blocks in unrelated proteins from distinct species are structurally very similar, often with a root mean square deviation (r.m.s.d.) below 1.5 Å. Variations are usually only found in the loops that connect the helices of a given motif or two entire motifs.

The structural information on Ski3 now offers the opportunity to analyze how the TPR fold and presence of binding sites correlate within a single polypeptide. In Ski3, the C-terminal arm forms the binding platform for Ski2 and both Ski8 subunits (Fig. 4.1) and thus has been under evolutionary pressure to maintain its binding interfaces (see also Fig. 3.2.S3). The C-terminal arm is built from canonical TPRs that are structurally very similar to other *bona fide* TPR proteins, e.g. O-linked glycosyl-transferase (Jinek et al., 2004) (Fig. 3.2.S2). The N-terminal arm also contains a block of three canonical TPR motifs that according to surface conservation presumably form a functional site (Fig. 3.2.S2). Only the linker region between the two arms contains non-canonical TPRs that deviate considerably from the typical fold in terms of geometry and length of the individual helices. It thus appears that functionality as a binding interface correlates with conservation of the TPR fold. Only in the linker region, which was not subjected to evolutionary pressure to maintain interactions with partner proteins, atypical TPR motifs could evolve.

## **4.4 Ski8 is a versatile adapter protein with multiple roles**

The Ski2-Ski3-Ski8 complex contains two Ski8 subunits (Ski8<sub>IN</sub> and Ski8<sub>OUT</sub>, see Fig. 4.1), in line with previous mass-spectrometric data (Synowsky and Heck, 2008). Both Ski8

polypeptides adopt a highly similar fold that is nearly invariant to the structure of Ski8 in isolation (Cheng et al., 2004; Madrona and Wilson, 2004). The only exception is an acidic loop (residues 335 - 356) that supports binding to Ski3 in two different conformations (Fig. 3.2.5). Both Ski8 subunits have a main interface to the Ski3 scaffold but also bind back to the Ski2 helicase core. In both main interfaces, Ski3 binds the  $\beta$ -propeller through a Q-R-x-x-F/Y motif that inserts into the hydrophobic top surface of Ski8 (Fig. 3.2.5), rationalizing why a mutation at the top surface of Ski8 abrogates binding to Ski3 *in vivo* (Cheng et al., 2004).

### **Ski8<sub>IN</sub> and Ski8<sub>OUT</sub> have distinct roles in stability and function of the Ski2-Ski3-Ski8 complex**

Both Q-R-x-x-F/Y motifs are well conserved in structure. However, the motif that interacts with the Ski8<sub>IN</sub> subunit is only moderately conserved in sequence (and less well than for instance most interface residues of Ski3 to the Ski2 helicase core) (Fig. 3.2.5). The motif that binds to Ski8<sub>OUT</sub> is even less well conserved (Fig. 3.2.5), suggesting that the Ski8<sub>OUT</sub> subunit may have been acquired during a later stage of evolution, possibly to fine-tune complex functionality. Consistent with this idea is the finding that Ski8<sub>IN</sub> is an integral structural component of the Ski2-Ski3-Ski8 complex. It buries a larger surface area than Ski8<sub>OUT</sub> (1000 Å<sup>2</sup> compared to 400 Å<sup>2</sup>), and a Ski2-Ski3-Ski8<sub>OUT</sub> complex with 1:1:1 stoichiometry (mutation of the Ski8<sub>IN</sub>-binding motif in Ski3) is not soluble.

Ski8<sub>OUT</sub>, on the other hand, can be removed without compromising the stability of the complex. Such a Ski2-Ski3-Ski8<sub>IN</sub> complex shows weaker RNA-binding by the helicase core in the presence adenosine diphosphate (ADP)-beryllium fluoride (Fig. 3.2.5) as compared to the wild-type. Thus, RNA-binding not only depends on the nucleotide state but also on the presence of Ski8<sub>OUT</sub>. It is possible that Ski8<sub>OUT</sub> achieves this effect by stabilizing a certain conformation of the helicase core that has high affinity for RNA. The crystal structure of the complex shows that both Ski8 subunits are anchored in the Ski3 scaffold but bind back to the helicase core. This suggests that they act as a structural buffer system that relays conformational restraints to the helicase in order to modify its function.

### **Mutually exclusive binding to Ski3 or Spo11 separates the two roles of Ski8 in mRNA decay and meiotic recombination**

Ski8 is unique among all exosome and SKI complex subunits in that it has a second role in initiation of DSBs during meiotic recombination. The catalytic activity for DSB-formation

resides in the topoisomerase-like protein Spo11 (Keeney et al., 1997) that needs to associate with Ski8 to perform its function (Tesse et al., 2003; Arora et al., 2004). In the Ski2-Ski3-Ski8 complex, both Ski8 subunits are recruited to Ski3 through the structurally well conserved Q-R-x-x-F/Y motif. Such a motif (Q-R-E-I-F, residues 376 - 380) is also present in the C-terminus of *S. cerevisiae* Spo11. Pull-down experiments indicate that this motif is indeed responsible *in vitro* for the association of Spo11 with Ski8 (Fig. 3.2.5). These results agree with *in vivo* experiments that annotated the C-terminal region of Spo11 as the binding interface to Ski8 in general (Nag et al., 2006), and a set of residues (Q376, R377/E378) in particular (Arora et al., 2004). The analogy to the Ski3-Ski8 interaction also suggests that the top surface of Ski8 forms the interface to Spo11. Consistently, mutations at the Ski8 top surface abrogate binding to Spo11 *in vivo* (Cheng et al., 2004).

Both Ski3 and Spo11 use a similar motif to bind to the same interface on Ski8, making the formation of either complex (Ski2-Ski3-Ski8 or Spo11-Ski8) mutually exclusive of the other. Mutually exclusive binding, in turn, explains how Ski8 can separate its two distinct roles in mRNA degradation and meiotic recombination.

### Towards a structural description of the Spo11-Ski8 complex

Spo11 is homologous to archaeal topo VI-A. The crystal structure of *M. jannaschii* topo VI-A (Nichols et al., 1999) reveals an N-terminal 5Y-CAP domain and a C-terminal toprim domain. The 5Y-CAP domain is found in other topoisomerases and bears a conserved tyrosine residue that is believed to perform the transesterification reaction with the phosphodiester backbone of the DNA substrate. The homology with the archaeal topo VI-A allows one to create a structural model of Spo11 using the program PHYRE (Kelley and Sternberg, 2009).

The model (Fig. 4.3A) lacks 37 residues at the N-terminus (which are not conserved) but contains a 5Y-CAP (residues 38 - 170) and a toprim domain (residues 171-398). Both domains are connected by a linker and are arranged in a similar fashion as in the *M. jannaschii* topo VI-A structure (Fig. 4.3A). Importantly, the Q-R-x-x-F motif of Spo11 (residues 376 - 380) is located on a helix in the toprim domain and is accessible to solvent. The motif is structurally well conserved with the motifs found in Ski3 (Fig. 3.2.5). Using the Ski3-Ski8 interaction as a template, Ski8 can be modeled to the Spo11 Q-R-x-x-F motif. In the resulting dimer, no clashes are produced at the interface when using the conformation of the acidic loop that is found in Ski8<sub>OUT</sub>. Thus, the model appears to be structurally sound and agrees with biochemical and *in vivo* experiments that mapped the

interface between both proteins (this study and Cheng et al., 2004; Arora et al., 2004; Nag et al., 2006).

In the crystals of the *M. jannaschii* topo VI-A, a two-fold non-crystallographic symmetry axis is present. Homodimerization occurs at a primary interface between the toprim domains of both protomers. A secondary interface is formed by the 5Y-CAP domain of one protomer binding back *in trans* to the toprim domain of the other protomer (Nichols et al., 1999). Experiments in yeast cells indicated that dimerization of Spo11 occurs *in vivo* concomitantly with the formation of DSBs (Sasanuma et al., 2007). Using the *M. jannaschii* topo VI-A dimer as a template, a dimer of the Spo11-Ski8 complex was constructed (Fig. 4.3B).

The resulting tetramer (dimer of a dimer) produces only minor steric clashes in the region of the primary interface at the toprim domain. A continuous, positively charged cleft is formed by the toprim and 5Y-CAP domains (Fig. 4.3C), creating the putative DNA-binding site. Both Ski8 subunits flank the binding cleft but do not contribute to the basic surface. Obeying the two-fold symmetry restraints, a DNA duplex of 25 nt length can be placed in the DNA-binding groove manually. The shortest distance between a phosphodiester bond and the putative active-center residue Tyr-135 of Spo11 is about 12 Å. The active site is completed by a magnesium ion that is coordinated by a set of conserved acidic residues (Fig. 4.3C).

### Possible roles for Ski8 in the Spo11-Ski8 complex

Due to the lack of experimental data, the structural model of the Spo11-Ski8 complex has to be interpreted cautiously. Nevertheless, it helps to discuss two possible roles of Ski8 in the Spo11-Ski8 complex.

In the Spo11-Ski8 model, the active site appears in a state that is not competent for catalysis (the reactive Tyr-135 is placed about 12 Å away from the DNA backbone). It appears unlikely that Ski8 directly contacts or rearranges the DNA since it does not contribute to the positively charged binding groove (Fig. 4.3C). However, binding of Ski8 may lead to a conformational change in Spo11 that renders the active site competent for cleavage. Upon binding, Ski8 is positioned close to the putative active site of Spo11, which is formed *in trans* by association of the 5Y-CAP and the toprim domains. Particularly one loop of Ski8 (residues 278 - 286) is close enough to interact with the active site (Fig. 4.3B). In the Ski2-Ski3-Ski8 complex, this loop binds back to the Ski2 helicase core in Ski8<sub>IN</sub> but remains unstructured in Ski8<sub>OUT</sub>. It can be speculated that Ski8 induces a local

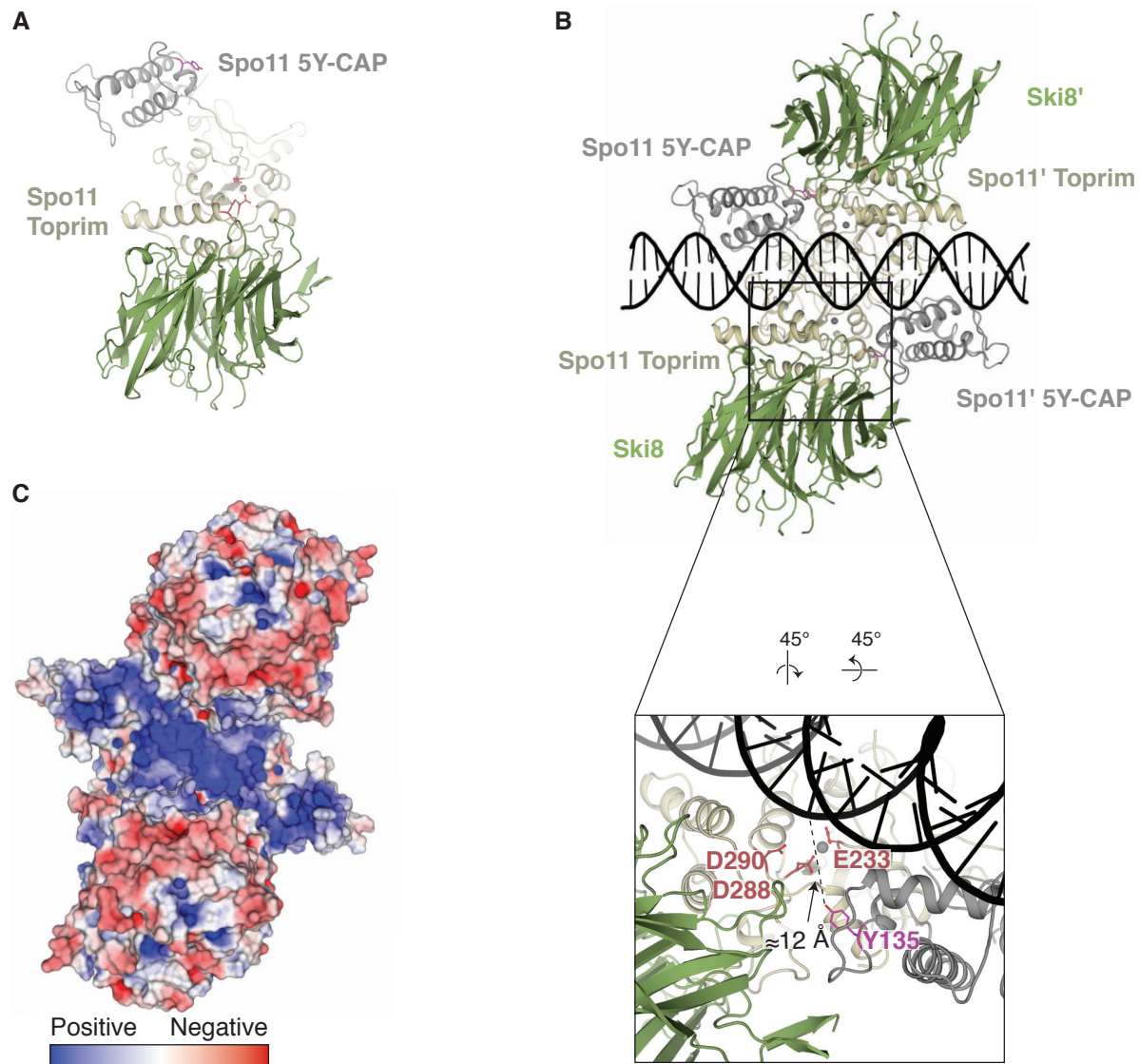


**Figure 4.3** | Towards a structural model for the Spo11-Ski8 subcomplex. (A) A PHYRE model of *S. cerevisiae* Spo11 $\Delta$ N (residues 38 - 398) bound to Ski8. The Spo11 5Y-CAP domain is colored in gray, the Spo11 toprim domain in beige and Ski8 in green. Three conserved acidic residues that form a putative magnesium binding site (shown as gray sphere) are colored in red, and the putative active site residue Y-135 is colored in magenta. (B) Model of the tetrameric Spo11-Ski8 assembly bound to a 25 nt DNA duplex (in black). Generation of the tetramer was guided by the dimer axis observed in crystals of *M. jannaschii* topo VI-A (Nichols et al., 1999). The DNA duplex was placed manually using symmetry constraints (e.g. equidistance of equivalent atoms to the active sites). A zoom-in view shows that Ski8 binds close to the active site. (C) Electrostatic surface potential of the tetrameric Spo11-Ski8 complex.

rearrangement of the active site of Spo11 to render it competent for catalysis. Clearly, this hypothesis needs to be validated by more reliable structural information and a thorough biochemical characterization.

A second possible function of Ski8 is related to its role in the Ski2-Ski3-Ski8 complex. Ski8 may act as an adapter protein that recruits other subunits of the DSB-initiation complex, e.g. Rec102 and Rec104 (Kee et al., 2004). Consistent with this idea, the interfaces through which Ski8 binds Ski2 and Ski3 are oriented into solution in the Spo11-Ski8 complex and remain available for other binding partners. The position of Ski8 flanking the DNA binding groove creates a deep pocket for the substrate, suggesting that other subunits may bridge both Ski8 copies to fully enclose the nucleic acid.

## 4.5 The SKI complex regulates exosome function

The observation that Ski2, Ski3, Ski7 and Ski8 are required for all known functions of the cytoplasmic exosome (Anderson and Parker, 1998; Araki et al., 2001) led to the proposal that the Ski2-Ski3-Ski8 complex, together with Ski7, is a general activator of the exosome. The presence of the RNA helicase Ski2 within the complex suggested that activation might occur through remodeling of RNPs or by unwinding RNA secondary structures and thus presenting a more favorable substrate to the exosome. In the nucleus, the TRAMP complex is a general cofactor of the exosome. It contains an RNA helicase (Mtr4), the activity of which has been shown to be required *in vivo* for degradation of certain substrates like *tRNA<sub>i</sub><sup>Met</sup>* (Wang et al., 2008). In the case of Ski2, no experimental evidence links its helicase activity to exosome nuclease activity. Still, the presence of two (highly related) RNA helicases in the two general exosome cofactors suggests that unwinding or translocation activity may be a general mechanism of activation of the exosome.

### **The Ski2-Ski3-Ski8 complex remains constitutively associated to the exosome**

Recruitment of the Ski2-Ski3-Ski8 complex to the exosome is best understood in budding yeast, where the eRF3-homolog Ski7 has been shown to interact *in vivo* with both the Ski2-Ski3-Ski8 complex and the exosome (Araki et al., 2001; Wang et al., 2005). The N-terminal domain of *S. cerevisiae* Ski7 contains two separate regions that bind to the Ski2-Ski3-Ski8 complex (residues 1 - 96) or to the exosome (residues 97 - 264) (Fig. 2.5, Araki et al., 2001).

Pull-down experiments with purified recombinant proteins confirm these interactions

(Fig. 3.2.S6) and also show that both complexes can simultaneously bind to Ski7, a prerequisite for any functional interplay. Moreover, Ski2 and Ski8 require Ski3 to interact with Ski7, and the N-terminal region of Ski3 is dispensable for binding to Ski7 (Fig. 3.2.S6). These results suggest that the C-terminus of Ski3 not only serves as scaffold for the Ski2-Ski3-Ski8 complex but also as interaction platform for Ski7. In these *in vitro* experiments, the SKI-exosome complex appeared to be stable at physiological salt concentrations, suggesting that the exosome remains constitutively associated with Ski7 and with the Ski2-Ski3-Ski8 complex rather than being recruited at a given time or for a particular incoming substrate.

### **Direct substrate channeling occurs between the Ski2-Ski3-Ski8 complex and the exosome**

As pointed out in section 4.2, the clustering of structural features along the RNA-binding path of Ski2 together with its unwinding activity suggests that the helicase may resolve secondary structures and transfer the substrate to the exosome. The channeling of RNA through the Ski2-Ski3-Ski8 complex cannot directly be observed in the crystal structure (which corresponds to the apo state) but other structural data support this model. Crystal structures of the two closest relatives of Ski2 (yeast Mtr4 and archaeal Hel308) bound to nucleic acid have been solved (Weir et al., 2010; Büttner et al., 2007). They show that the nucleic acid is contacted by the canonical SF2 motifs and funnelled through a channel formed by the ring-like assembly of RecA1, RecA2 and helical domains. Given the high similarity of Ski2 and Mtr4 (or Hel308) in terms of structure and sequence, it seems reasonable to assume that in Ski2 the RNA substrate takes a similar path.

Intriguingly, the physical interaction between the exosome and the Ski2-Ski3-Ski8 complex changes the RNA-binding properties of both complexes. In a Ski7-dependent fashion, a joint RNA binding channel of 41 - 43 nt length is created (Fig. 3.2.6). This joint channel appears as an extension of the 31 - 33 nt RNA-binding path in the central cavity of the exosome that has been characterized by structural (Malet et al., 2010), biochemical (Bonneau et al., 2009) and *in vivo* experiments (Wasmuth and Lima, 2012). The extension of 9 - 10 nt depends on all four Ski proteins and corresponds to the length of an RNA-binding path in Ski2-Ski3-Ski8 in presence of an ATP-analog (Fig. 2.2.1).

It has to be noted that the joint 41 - 43 nt RNA channel of the SKI-exosome complex is not the only possible mode of RNA-binding. In fact, the 31 - 33 nt exosome path is still dominant in RNase protection experiments, suggesting that alternative RNA paths exist

that may bypass the Ski2-Ski3-Ski8 complex when bound to the exosome. Furthermore, the role of these pathways *in vivo* remains to be clarified.

The extension of the exosome's RNA channel also points towards the S1/KH ring as the interaction site with Ski7. Since the Rrp44<sup>D171N, D551N</sup> double mutant used in the RNase protection experiments buries the 3' end of the RNA (Lorentzen et al., 2008), any additional factors must bind the nucleic acid at the 5' end that emerges from the S1/KH ring of the central channel, consistent with electron microscopy data using 5' -labeled RNA (Malet et al., 2010). In line with these observations, *in vivo* experiments identified the C-terminus of the S1/K1 ring member Csl4 as a crucial component for the functions of the cytoplasmic exosome. (Schaeffer et al., 2009; van Hoof et al., 2000b).

Together, these results suggest a model according to which Ski7 binds to the S1/KH ring of the exosome (Fig. 3.4A). It then recruits the Ski2-Ski3-Ski8 complex most likely through Ski3. In this way, the RNA 3' exit site from the helicase complex is positioned very close to the RNA entry site on the S1/KH ring. A joint substrate channel is formed that connects the helicase activity of Ski2 to the nuclease activities of Rrp44. Thus, secondary structures in RNA substrates could be effectively unwound by Ski2-Ski3-Ski8 and the single stranded substrate could be funnelled through the joint substrate channel to reach the Rrp44 active sites for degradation. Even though direct evidence (e.g. in form of structural data) is still missing, these results represent the first indications of how the Ski2-Ski3-Ski8 complex activates the exosome.

### **The Ski2 insertion domain and the Ski3 N-terminal arm cooperate to regulate access of RNA to Ski2**

Inspection of the structural model for the full-length Ski2-Ski3-Ski8 complex reveals two domains that protrude from the core complex that is arranged around the C-terminal arm of Ski3 (Fig. 4.1): the Ski2 insertion domain and the N-terminal arm of Ski3. Both domains are flexible (Fig. 3.1.S1 and Fig. 3.2.S2) and dispensable for complex formation or binding to Ski7 (Fig. 3.1.4 and Fig. 3.2.S6).

The Ski2 insertion domain is structurally and topologically related to the Mtr4 KOW domain (Weir et al., 2010; Jackson et al., 2010) and binds RNA apparently unspecifically (Fig. 3.1.3). Its location above the entry site of the RNA into the helicase core suggests a role for substrate loading. Indeed, removal of the Ski2 insertion domain promotes the formation of the 41 - 43 nt RNA channel as judged by RNase protection assays (Fig. 3.2.6). Similarly, its removal enhances unwinding activity of Ski2-Ski3-Ski8 and stimulates

ATPase activity of the complex approximately 10-fold (Fig. 3.2.S6). In contrast, deletion of the insertion domain does not affect ATPase activity of Ski2 in isolation, suggesting that complex formation contributes an element that is required for the inhibitory effect of this domain.

Consistent with this hypothesis, removal of the N-terminal arm of Ski3 (residues 1 - 487) prompts a similar activation of helicase and ATPase activities of the Ski2-Ski3-Ski8 complex (Fig. 3.2.S6). The flexibility of both domains as observed in the crystal structures and in normal mode analyses suggests that both domains can potentially come into contact. However, the Ski3 N-terminal arm (containing the conserved surface patch on TPRs 1 and 2) does not interact with the Ski2 insertion domain in size-exclusion chromatography experiments (not shown), but transient interactions cannot be excluded.

Both inhibitory domains do not act redundantly since removal of any one is sufficient to prompt the inhibitory effect. Additionally, the effects of removal of each domain are similar in magnitude. Together, this suggests that both domains act cooperatively to exert their function. Considering the flexibility, the location at the RNA entry site and particularly the effect on formation of a joint substrate channel, the Ski2 insertion domain can be

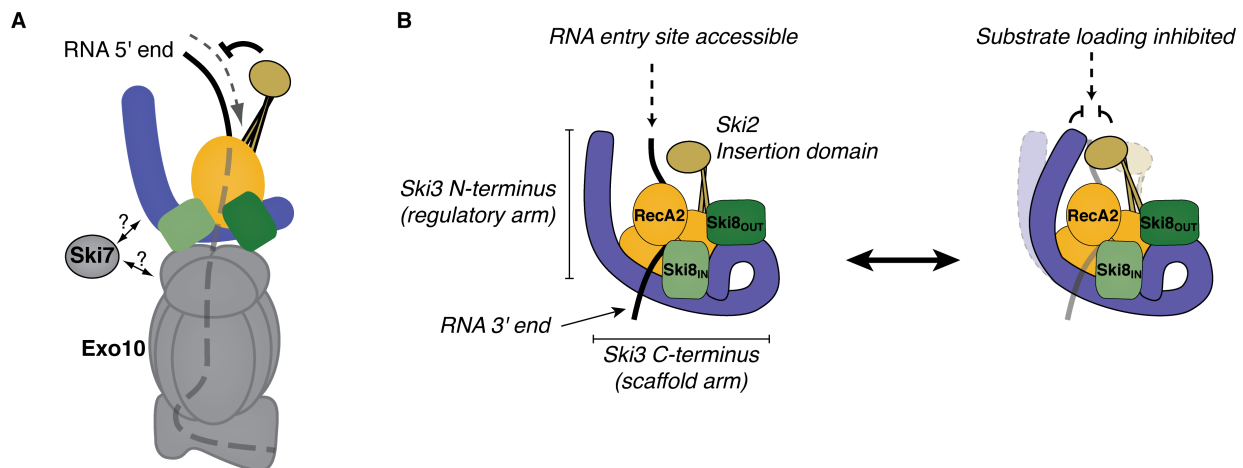


**Figure 4.4** | A model for activation of the cytoplasmic exosome by the Ski2-Ski3-Ski8 complex. (A) A model of how Ski7 bridges the Ski2-Ski3-Ski8 and Exo10 complexes, leading to a joint RNA channel between both assemblies. This connects the helicase and the nuclease activities of Ski2-Ski3-Ski8 and of the exosome, respectively. It remains unclear where Ski7 binds on both complexes (indicated by the question marks). (B) The Ski2 insertion domain and the Ski3 N-terminus cooperate to inhibit the ATPase and helicase activity of the Ski2-Ski3-Ski8 complex, most likely by regulating substrate access into the helicase core of Ski2.

speculated to block substrate access to the helicase core when the Ski3 N-terminal arm is present, effectively shutting down the helicase. Given the fact that helicase activity is linked to nuclease activity by the joint substrate channel, this would also provide a means of down-regulating exosome activity. Conversely, activation of the Ski2-Ski3-Ski8 complex might then require the Ski3 N-terminal arm to be recruited away from the insertion domain, possibly by binding events that target the conserved surface patch on TPRs 1 and 2 (Fig. 3.2.S2).

## 4.6 Major conclusions

All three subunits of the SKI complex are required for exosome-mediated mRNA degradation in the cytoplasm. The results of this PhD thesis offer a first view to understand the role of the individual subunits in the complex, thus rationalizing why each protein is essential for the entire biological process.

Ski2 contains in addition to its canonical DExH box core a variable insertion domain that appears to regulate substrate access to the helicase. Ski3 forms a large TPR array that is formed by two arms. The N-terminal regulatory arm cooperates with the Ski2 insertion domain to control substrate loading. The C-terminal arm acts as scaffold for the other subunits and may provide the interface to Ski7.

The finding that the Ski2-Ski3-Ski8 complex contains an internal regulatory mechanism is intriguing because it lends a broader perspective to the notion of the SKI complex as a general cofactor of the cytoplasmic exosome. First, its ATP-dependent remodeling capabilities along with the described direct substrate channeling mechanism may activate the exosome to degrade structured substrates. Second, the identified internal inhibitory mechanism in the Ski2-Ski3-Ski8 complex may also inhibit exosome activity indirectly by refusing substrate transfer. Both kinds of regulation (positive and negative) would provide tools that - together with a yet to be identified sensory system - could control the exosome's substrate specificity.

## 5 Outlook

The structure of the Ski2-Ski3-Ski8 complex and its functional characterization are a first step to understand the mechanisms by which the cytoplasmic exosome is regulated. The next step will include a structural characterization of the exosome bound to Ski7 and the Ski2-Ski3-Ski8 complex. This will help to understand the details of how Ski7 recruits the helicase complex to the nuclease complex. In particular it will shed more light on the function of the Ski7 N-terminus as an adapter between both complexes. More structural data, possibly including cryo-electron microscopy studies, will also help to analyze the RNA-channelling between both complexes on the molecular level.

On the functional level, the joint substrate channel needs to be characterized in more detail by different techniques, e.g. electron microscopy or a combination of chemical cross-linking and mass-spectrometry. The role of alternative entry paths for RNA into the exosome remains to be examined. While the current data support the presence of an internal inhibitory mechanism of Ski2-Ski3-Ski8 complex that controls substrate loading, the details of the process have to be elucidated. Particularly interesting is also the question of how this inhibition is released once the helicase complex binds to the exosome. Related to this problem may be the question of how upstream factors of quality control pathways interact with the Ski2-Ski3-Ski8 complex. Finally, it needs to be confirmed that degradation of certain substrates by the exosome is directly promoted by means of the helicase activity of Ski2.

The long-term goal on the functional level is to understand how the substrate specificity of the exosome is regulated, and the above-mentioned questions can contribute substantially to clarify this question. However, a comprehensive understanding of all other exosome cofactors (e.g. the TRAMP complex), specifically in terms of their activities and interactions with the exosome, will be indispensable to tackle this problem.

Another somewhat unrelated aspect is the function of Ski7 and the Ski2-Ski3-Ski8 complex in the context of the ribosome, e.g. during no-go decay. Crystallographic and electron

microscopy analysis of ribosome particles bound to translational factors are technically well established. They offer the possibility to investigate how Ski7 positions the Ski2-Ski3-Ski8 complex on the ribosome and to understand how stalling mRNAs are relayed to the degradation system. Of specific interest is the role of the Ski7 GTPase domain: does it act like a true eRF3-homolog and are other translational factors (like eRF1-homologs) required for its interaction with the ribosome? Since Ski7 is not present in other eukaryotic *geni* than *Saccharomyces*, it will be intriguing to find out how the Ski2-Ski3-Ski8 complex interacts with the exosome and the ribosome in higher eukaryotes.

# A Appendix

ID	number	name	species	protein	start	end	size	tag	vector	resistance	sequencing_status	date	lab_book	comment	primer_f	primer_rev
0	c001	sCSK2	s. cerevisiae	SK2	1	1287	146	his	prastbac_hia	amp	S132L_N884S	09.02.08	1.12		1	2
1	c002	sCSK2	s. cerevisiae	SK2	1	1287	146	his	prastbac_1	amp	S132L_N884S	11.02.08	1.22	insert lost	1	2
2	c003	sCSK3	s. cerevisiae	SK3	1	1432	164	his	prastbac_hia	amp	OK	21.02.08	-	cloned by jet		
3	c004	sCSK8	s. cerevisiae	SK8	1	397	44	his	pel_mon	amp	OK	21.02.08	-	cloned by fabiana		
4	c005	sCSK6	s. cerevisiae	SK6	1	397	44	his	prastbac_hia	amp	OK	22.02.08	1.36		5	6
5	c006	sCSK2	s. cerevisiae	SK2	1	1287	146	his	prastbac_hia	amp	N884S	27.02.08	1.41	qc on c001		
6	c007	sCSK2	s. cerevisiae	SK2	1	1287	146	his	prastbac_hia	amp	OK	17.03.08	1.42	qc on c006		
7	c008	sCSK3	s. cerevisiae	SK3	1	1432	164		prastbac_1	amp	OK	17.03.08	1.44	qc on c003		4
8	c009	sCSK8	s. cerevisiae	SK8	1	397	44		prastbac_1	amp	OK	17.03.08	1.44	qc on c004		5
9	c010	hsSK2	h. sapiens	SK2	1	1246	138	gst	pcmv_tap	amp	n.a.			cloned by D. Lindner		6
10	c011	hsSK3	h. sapiens	SK3	1	1564	175	gst	pcmv_tap	amp	n.a.			cloned by D. Lindner		
11	c012	hsSK8	h. sapiens	SK8	1	305	34	gst	pgex_cs	amp	OK			cloned by D. Lindner		
12	c013	sCSK7cnp	s. cerevisiae	SK7	1	747	85	cnp	pecktl_cnp	kan	n.a.	10.05.08	1.72	gDNA cloned		47
13	c014	sPSK8	s. pombe	SK8	1	302	33		puc_18	amp	n.a.	10.05.08	1.82	CDNA cloned		55
14	c015	hsSK8	h. sapiens	SK8	1	305	34		puc_18	amp	OK	10.05.08	1.72, 1.84, 1.101	CDNA cloned		53
15	c016	sCSK2	s. cerevisiae	SK2	1	1287	146	his	prastbac_1	amp	OK	05.05.08	1.80	pcr on c7		47
16	c017	sCSK7 1-26scdp	s. cerevisiae	SK7	1	265		his_cnp	pecktl_cnp	kan	n.a.	13.05.08	1.102	pcr on c13		87
17	c018	sCSK7 116-26scdp	s. cerevisiae	SK7	116	265		his_cnp	pecktl_cnp	kan	n.a.	13.05.08	1.102	pcr on c13		85
18	c019	sCSK7 116-747cnp	s. cerevisiae	SK7	116	747		his_cnp	pecktl_cnp	kan	n.a.	13.05.08	1.102	pcr on c13		85
19	c020	sCSK7sumo	s. cerevisiae	SK7	1	747		his_sumo	pecktl_sumo	kan	OK	14.05.08	1.116	pcr on c13		88
20	c021	sCSK7 116-Csumo	s. cerevisiae	SK7	116	747		his_sumo	pecktl_sumo	kan	n.a.	14.05.08	1.116	pcr on c13		89
21	c022	sCSK7 1-26sumo	s. cerevisiae	SK7	1	265		his_sumo	pecktl_sumo	kan	n.a.	14.05.08	1.116	pcr on c13		88
22	c023	sCSK7 116-26sumo	s. cerevisiae	SK7	116	265		his_sumo	pecktl_sumo	kan	n.a.	14.05.08	1.116	pcr on c13		89
23	c024	hsSK2	h. sapiens	SK2	1	1246			pcsc_b	amp	Q1133stop, R1133X	01.06.08	1.106	CDNA cloned		50
24	c025	hsSK3	h. sapiens	SK3	1	1564			pcsc_b	amp	OK	01.06.08	1.106	CDNA cloned		52
25	c026	sCSK2 D444N	s. cerevisiae	SK2	1	1287	146	his	prastbac_1	amp	OK (D444N)	30.07.08	1.133	qc on c16, D444N mutant		98
26	c027	sCSK2 E445Q	s. cerevisiae	SK2	1	1287	146	his	prastbac_hia	amp	OK (E445Q)	30.07.08	1.133	qc on c7, E445Q		99
27	c028	sCSK2 D444N	s. cerevisiae	SK2	1	1287	146	his	prastbac_hia	amp	OK (D444N)	10.09.08	1.132	qc on c7, D444N		101
28	c029	sCSK2 E445Q	s. cerevisiae	SK2	1	1287	146	his	prastbac_1	amp	OK (E445Q)	10.09.08	1.132	qc on c16, E445Q		99
29	c030	sCSK3 1-52gst	s. cerevisiae	SK3	1	522	88	gst	pecktl_gst	kan	n.a.	17.10.08	2.8	pcr on c3		100
30	c031	sCSK7gst	s. cerevisiae	SK7	1	747	113	gst	pecktl_gst	kan	n.a.	17.10.08	2.8	pcr on c20a		103
31	c032	sCSK7 116-747gst	s. cerevisiae	SK7	116	747		gst	pecktl_gst	kan	n.a.	17.10.08	2.8	pcr on c20a		85

Table A.1 | Constructs generated during my PhD work (continued on pages 89-93).

ID	number	name	species	protein	start	end	size	tag	vector	resistance	sequencing_status	date	lab_book	comment	primer_f	primer_rev
32	c033	scsSk7_1-265gst	s. cerevisiae	SK7	1	265		gst	pedkh1_gst	kan	n.a.	17.10.08	2.8	pcr on c20a	47	87
33	c034	scsSk7_116-265gst	s. cerevisiae	SK7	116	265		gst	pedkh1_gst	kan	n.a.	17.10.08	2.8	pcr on c20a	85	87
34	c035	scdRp44cnp	s. cerevisiae	np44	1	1001		cnp	pedkh1_cnp	kan	n.a.	04.03.09	-	Jerome	107	108
35	c036	scsSk8_3c	s. cerevisiae	SK8	1	397		his	pedk3c_his	kan	ok	02.03.09	2.46	pcr on c005	121	122
36	c037	scsSk2_3c	s. cerevisiae	SK2	1	1287		his	pedk3c_his	kan	ok	07.04.09	2.46		117	118
37	c038	scsSk3_3c	s. cerevisiae	SK3	1	1432		his	pedk3c_his	kan	ok	07.04.09	2.46		133	138
38	c039	scsSk2AN_sumo	s. cerevisiae	SK2	296	1287		his_sumo	pedkh1_sumo	kan	ok	16.04.09	2.52		133	137
44	c040	scsSk2_NReca_sumo	s. cerevisiae	SK2	296	515		his_sumo	pedkh1_sumo	kan	ok	16.04.09	2.52		134	138
45	c041	scsSk2_CRecaC_sumo	s. cerevisiae	SK2	607	1287		his_sumo	pedkh1_sumo	kan	ok	16.04.09	2.52		139	141
46	c042	scsSk7_3c_gst	s. cerevisiae	SK7	1	747		gst	pedk3c_gst	kan	ok	16.04.09	2.52		139	140
47	c043	scsSk7AC_gst	s. cerevisiae	SK7	1	515		gst	pedk3c_gst	kan	ok	16.04.09	2.52		128	130
48	c044	scsSk2_CRecaC_gst	s. cerevisiae	SK2	607	1287		gst	pedk3c_gst	kan	ok	16.04.09	2.52		128	129
49	c045	scsSk2_CRecaC_his	s. cerevisiae	SK2	607	1287		his	pedk3c_his	kan	ok	16.04.09	2.52		127	128
50	c046	scsSk2_NReca_gst	s. cerevisiae	SK2	296	515		gst	pedk3c_gst	kan	ok	16.04.09	2.52		127	128
51	c047	scsSk2AN_gst	s. cerevisiae	SK2	296	1287		gst	pedk3c_gst	kan	ok	16.04.09	2.52		123	124
52	c048	scsSk2AN_his	s. cerevisiae	SK2	296	1287		his	pedk3c_his	kan	ok	16.04.09	2.52		142	144
53	c049	scsSk2AC_his	s. cerevisiae	SK2	1	136		his	pedk3c_his	kan	ok	16.04.09	2.52		147	148
54	c050	scsSk2	s. cerevisiae	3	1	1287		his	prastbac_1	amp	ok	23.04.09	2.57	pcr on c37	142	144
55	c051	scsSk3	s. cerevisiae	SK3	1	1432		his	prastbac_1	amp	ok	23.04.09	2.57	pcr on c38	142	144
56	c052	scsSk8	s. cerevisiae	SK8	1	397		his	prastbac_1	amp	ok	23.04.09	2.57	pcr on c36	142	144
57	c053	scsSk2AC	s. cerevisiae	SK2	1	136		his	prastbac_1	amp	ok	23.04.09	2.57	pcr on c59	142	144
58	c054	scsSk2AN	s. cerevisiae	SK2	296	1287		his	prastbac_1	amp	ok	23.04.09	2.57	pcr c48	142	144
59	c055	scsSk2CRecaC	s. cerevisiae	SK2	607	1287		his	prastbac_1	amp	ok	23.04.09	2.57	pcr on c45	142	144
60	c056	scsSk2ANAC_his	s. cerevisiae	SK2	17	136		his	pedk3c_his	kan	ok	24.04.09			125	124
61	c057	scsSk2NReca_his	s. cerevisiae	SK2	296	515		his	pedk3c_his	kan	ok	24.04.09			127	129
62	c058	hSK2	h. sapiens	SK2	1	1246		his	psc_b	amp	ok (Q1133)	28.05.09	2.71	qc on c24, R151X left	94	95
63	c059	SPSK2	s. pombe	SK2	1	1213		his	pedk3c_his	kan	ok	28.05.09	2.83	gDNA cloned	149	150
64	c060	SPSK3	s. pombe	SK3	1	1389		his	pedk3c_his	kan	ok	28.05.09	2.83	gDNA cloned	151	152
66	c061	SPSK7	s. pombe	SK7	1	695		his	pedk3c_his	kan	ok	28.05.09	2.83	CDNA cloned	155	156
68	c062	SPSK8	s. pombe	SK8	1	302		his	pedk3c_his	kan	ok	28.05.09	2.83	CDNA cloned	153	154
67	c063	hSK2	h. sapiens	SK2	1	1246		his	psc_b	amp	F10E2L, rest ok (Q19477)	04.06.09		qc on c58	96	97
68	c064	pFLASpel	s. cerevisiae	SK2	17	136		his	pFL	amp	ok	09.06.09	2.102	ASpel downstream of polh	163	164
69	c065	scsSk2ANAC_his	s. cerevisiae	SK2	17	136		his	prastbac_1	amp	ok	09.06.09	2.61	pcr on c56	142	143

ID	number	name	species	protein	start	end	size	bg	vector	resistance	sequencing_status	date	lab_book	comment	primer_f	primer_rev
70	c066	sCSK12Reca_his	s. cerevisiae	sk12	296	515		his	pfastbac_1	amp	ok	09.06.09	2.61	pcr on c57	142	145
71	c067	spSK12_his	s. pombe	sk12	1	1213		his	pfastbac_1	amp	ok	17.06.09	2.92	pcr on c59	188	172
72	c068	spSK12	s. pombe	sk12	1	1213		his	pfastbac_1	amp	ok	17.06.09	2.92	pcr on c59	171	172
73	c069	spSK17_his	s. pombe	sk17	1	695		his	pfastbac_1	amp	ok	17.06.09	2.92	pcr on c61	188	174
74	c070	spSK17	s. pombe	sk17	1	695		his	pfastbac_1	amp	ok	17.06.09	2.92	pcr on c61	173	174
75	c071	spSK18_his	s. pombe	sk18	1	302		his	pfastbac_1	amp	ok	17.06.09	2.92	pcr on c062	188	176
76	c072	spSK18	s. pombe	sk18	1	302		his	pfastbac_1	amp	ok	17.06.09	2.92	pcr on c062	175	176
77	c073	LLC_sumo	lambda	llc	1	221		his_sumo	peckhi_sumo	kan	ok	19.06.09	2.141	pcr on c062	189	190
78	c074	spSK3	s. pombe	sk13	1	1389		his	pfastbac_1	amp	ok	01.07.09	2.94	clones from dba	189	170
79	c075	sCSK8	s. cerevisiae	sk18	1	397		his	pFL	amp	ok	03.07.09	2.112	pcr on 3c::SK18 in MCS1	196	195
80	c076	spSK13_his	s. pombe	sk13	1	1389		his	pfastbac_1	amp	ok	29.07.09	2.96	pcr on c60	202	169
81	c077	sCSK13_mbd_his	s. cerevisiae	sk13	1	1432		his	pFLdspe	amp	ok	14.08.09	2.116	sk13 in MCS2; MCS1 empty; pcr on c038	205	206
82	c078	sCSK13his:sCSK18pFL	s. cerevisiae	sk13, sk18	1			his	pFLdspe	amp	ok	27.08.09	2.118	sk13 in MCS2; sk18 in MCS1	196	195
83	c079	sCSK12pFL	s. cerevisiae	sk12	1	1287		his	pFLdspe	amp	ok	27.08.09	2.123	sk12 in MCS2; MCS1 empty	197	198
84	c080	sCSK1238pFL	s. cerevisiae	sk12, sk13, sk18	1			his	pFLdspe	amp		13.10.09	2.132	c78 ligated into c79		
85	c081	sCSK12AC:pFL	s. cerevisiae	sk12	1	136		his	pFLdspe	amp		20.10.09	2.145	sk12-1-136 in MCS1	214	214
86	c082	sCSK12ANAsialk_his	s. cerevisiae	sk12	296	1287	84	his	peck3c_his	kan	A1255D; rest OK	04.03.10	2.164	ANAsialk::296-834-GSRG-1086-1287	227	228
88	c083	sCSK12ANAsialk_gst	s. cerevisiae	sk12	296	1287	84	gst	peck3c_gst	kan		04.03.10	2.164	ANAsialk::296-834-GSRG-1086-1287	227	228
89	c084	sCSK12Asialk_his	s. cerevisiae	sk12	1	1287	117	his	peck3c_his	kan	V1147L; S1fragment not seq	04.03.10	2.164	Asialk::1-834-GSRG-1086-1287	227	228
90	c085	sCSK12Asialk_gst	s. cerevisiae	sk12	1	1287	117	gst	peck3c_gst	kan		04.03.10	2.164	Asialk::1-834-GSRG-1086-1287	227	228
91	c086	sCSK12_S4H8_his	s. cerevisiae	sk12	835	1085	29	his	peck3c_his	kan	ok	05.03.10		cloned by P&T	231	236
92	c087	sCSK12_S4H8_gst	s. cerevisiae	sk12	835	1085		gst	peck3c_gst	kan	ok	05.03.10		cloned by P&T	231	236
93	c088	sCSK12_S2H8_his	s. cerevisiae	sk12	867	1048		his	peck3c_his	kan	ok	05.03.10		cloned by P&T	232	235
94	c089	sCSK12_S2H8_gst	s. cerevisiae	sk12	867	1048		gst	peck3c_gst	kan	ok	05.03.10		cloned by P&T	232	235
95	c090	sCSK12_S8_his	s. cerevisiae	sk12	893	1018		his	peck3c_his	kan	ok	05.03.10		cloned by P&R	233	234
96	c091	sCSK12_S8_gst	s. cerevisiae	sk12	893	1018		gst	peck3c_gst	kan	ok	05.03.10		cloned by P&R	233	234
97	c092	spSK12As_fl	s. pombe	sk12	1	1213	108	his	peck3c_his	kan	ok	09.04.10	2.170	Asialk; V758GSRG1014	241	242
98	c093	sCSK12_ANAs	s. cerevisiae	sk12	296	1287	84	his	peck3c_his	kan	A1255E backmut., rest?	07.04.10	2.172	qc on c82; Asialk	243	244
99	c094	sCSK12_As_fl	s. cerevisiae	sk12	1	1287	117	his	peck3c_his	kan	V1147 backmut., rest?	07.04.10	2.172	qc on c84; Asialk	245	246

ID	number	name	species	protein	start	end	size	tag	vector	resistance	sequencing_status	date	lab_book	comment	primer_f	primer_rev
100	c095	spsSK12_Ds_fl	s. pombe	SK12	1	1213	108	his	pFastbac_1	amp	ok	13.04.10	2.176	pcr on c092	142	172
101	c096	sccSK12_Ds_fl	s. cerevisiae	SK12	1	1287	117	his	pFastbac_1	amp	F330V	27.04.10	2.182	pcr on c094	142	144
102	c097	sccSK12_DeltaS	s. cerevisiae	SK12	296	1287	84	his	pFastbac_1	amp	ok	27.04.10	2.182	pcr on c093	142	144
103	c098	sccSK12_Ds_fl	s. cerevisiae	SK12	1	1287	117		pFL	amp	F330V, 834/c frameshift	27.04.10	2.182	pcr on c094	197	198
104	c099	sccSK12_Ds_fl	s. cerevisiae	SK12	1	1287	117	his	pFastBac1	amp	ok	25.05.10	2.185	qc on c96	254	255
105	c100	sccSK12_arch01	s. cerevisiae	SK12	891	985	10	his	peck3c_his	kan		07.06.10	2.191		259	260
106	c101	sccSK12_arch02	s. cerevisiae	SK12	891	989	10	his	peck3c_his	kan		07.06.10	2.191		259	261
107	c102	sccSK12_arch03	s. cerevisiae	SK12	891	1078	21	his	peck3c_his	kan		07.06.10	2.191		259	262
108	c103	sccSK12_arch04	s. cerevisiae	SK12	891	1078	21	his_sumo	peckh_sumo	kan		07.06.10	2.191		263	266
109	c104	sccSK12_arch12	s. cerevisiae	SK12	851	1073	26	his	peck3c_his	kan	ok	13.07.10	3.2	pcr on c047	268	273
110	c105	sccSK12_arch13	s. cerevisiae	SK12	859	1066	24	his	peck3c_his	kan	ok	13.07.10	3.2	pcr on c047	269	272
111	c106	sccSK12_arch11	s. cerevisiae	SK12	841	1082	28	his	peck3c_his	kan	50k	22.07.10	3.3	pcr on c047	267	274
112	c107	sccSK12_arch11	s. cerevisiae	SK12	862	1063	23	his	peck3c_his	kan	ok	22.07.10	3.3	pcr on c047	270	271
113	c108	sccSK12_SM_1	s. cerevisiae	SK12	865	1050	22	his	peck3c_his	kan	ok	10.09.10		cloned by P&T	275	278
114	c109	sccSK12_SM_2	s. cerevisiae	SK12	870	1045	21	his	peck3c_his	kan	ok	10.09.10		cloned by P&T	276	277
115	c110	spsSK12_SM_3	s. pombe	SK12	789	976	22	his	peck3c_his	kan	ok	01.10.10		cloned by P&T	279	280
116	c111	sccSK18_3AN_his	s. cerevisiae	SK13, SK18				his	pFLdsp	amp	ok	14.01.11	3.22	MCS1 sk8 ok, MCS2 SK13DN601 ok		
117	c112	sccSK18_SK13A328_his	s. cerevisiae	SK13, SK18				his	pFLdsp	amp	ok	18.01.11	3.24	MCS2 1.-328-GSG-408-c-ok, MCS1 1.-397ok		
118	c113	sccSK18_SK13A338_his	s. cerevisiae	SK13, SK18				his	pFLdsp	amp	ok	03.02.11	3.27	MCS 2 1.-338-GSGS-404-C, MCS1 SK18 fl		
119	c114	sccSK12_LSM_897D- 903A	s. cerevisiae	SK12	835	1085	30	his	peck3c_his	kan	ok	02.02.11	3.29	H897D, R903A	291	292
120	c115	sccSK17_N40_sumo	s. cerevisiae	SK17	1	40	15	his_sumo	peckh_sumo	kan	ok	24.02.11	3.37		295	296
121	c116	sccSK17_N62_sumo	s. cerevisiae	SK17	1	62	18	his_sumo	peckh_sumo	kan	ok	24.02.11	3.37		295	297
122	c117	sccSK17_N75_sumo	s. cerevisiae	SK17	1	75	19	his_sumo	peckh_sumo	kan	ok	24.02.11	3.37		295	298
123	c118	sccSK17_N87_sumo	s. cerevisiae	SK17	1	87	21	his_sumo	peckh_sumo	kan	ok	24.02.11	3.37		295	299
124	c119	sccSK13_522A_Dloop3 38	s. cerevisiae	SK13	1	523	53	his_sumo	peckh_sumo	kan	ok	07.04.11	3.38	w/ Chem His tag!! PCR on c113	102	103
125	c120	sccSK13A522Dloop338	s. cerevisiae	SK13	1	523	50	his_sumo	peckh_sumo	kan	ok	15.04.11	3.40	stop after 522 w/ qc on c119		
126	c121	sccSK12_835- 1085_R903E	s. cerevisiae	SK12	835	1085	29	his	peck3c_his	kan	ok to 1037, rest not yet seq	18.05.11	3.42	PCR on c86	308	309
127	c122	sccSK12_835- 1085_T920A	s. cerevisiae	SK12	835	1085	29	his	peck3c_his	kan	ok to 1018, rest no yet	25.05.11	3.43	PCR on c86	306	307
128	c123	sccSK12_835- 1085_H897D	s. cerevisiae	SK12	835	1085	29	his	peck3c_his	kan	ok to 1042, rest not seq	14.07.11	3.44	PCR on c86	303	302

ID	number	name	species	protein	start	end	size	tag	vector	resistance	sequencing_status	date	lab_book	comment	primer_f	primer_rev
129	c124	scSKiA160his:scSKi8 :pFL	s. cerevisiae	skI3, skI8	161	1432	148	his	pFLdspe	amp	ok	08.09.11	3.57	from c78		
130	c125	scSKiA279his:scSKi8 :pFL	s. cerevisiae	skI3, skI8	280	1432	129	his	pFLdspe	amp	ok	08.09.11	3.57	from c78		
131	c126	scSKiA487his:scSKi8 :pFL	s. cerevisiae	skI3, skI8	488	1432	109	his	pFLdspe	amp	ok	08.09.11	3.58	from c78		
132	c127	scSKiA521his:scSKi8 :pFL	s. cerevisiae	skI3, skI8	522	1432	106	his	pFLdspe	amp	ok	08.09.11	3.59	from c78		
133	c128	scSKiA555his:scSKi8 :pFL	s. cerevisiae	skI3, skI8	556	1432	102	his	pFLdspe	amp	ok	08.09.11	3.61	from c78		
134	c129	scSKi2R149D:3his:8 Loopin	s. cerevisiae	skI2, skI3, skI8				his	pFLdspe	amp	ok (N-termini, backbone not seq'd)	23.02.12	3.71	quickchanged c80	320	321
135	c130	scSKi238_ZRRK- LoopOut	s. cerevisiae	skI2, skI3, skI8				his	pFLdspe	amp	(ok) not seq'd: 8-1- 80.2.1-28.1091- 1193.3.1-20	23.02.12	3.71	quickchanged c80	325	326
136	c131	scSKi238_8_301- Loopin	s. cerevisiae	skI2, skI3, skI8				his	pFLdspe	amp	(ok) not seq'd: 8-1- 81.2.1-22.3.1- 28.1363-c	23.02.12	3.71	quickchanged c80	327	328
137	c132	scSKi238_A8in	s. cerevisiae	skI2, skI3, skI8				his	pFLdspe	amp	(ok) not seq'd: 2-1- 23.3.1-22.8.1-81	23.02.12	3.71	quickchanged c80	331	332
138	c133	scSKi238_ZRRK	s. cerevisiae	skI2, skI3, skI8				his	pFLdspe	amp		01.03.12	3.76	quickch'g c129	323	324
139	c134	scSKi238_ZCHOb	s. cerevisiae	skI2, skI3, skI8				his	pFLdspe	amp		01.03.12	3.76	quickch'g c80	319	320
140	c135	scSKi238_3Q1046R_ P1050R	s. cerevisiae	skI2, skI3, skI8				his	pFLdspe	amp		01.03.12	3.76	quickch'g c80	337	338
141	c136	scSKi238_3RecA1	s. cerevisiae	skI2, skI3, skI8				his	pFLdspe	amp		23.03.12	3.78	quickch'g c135	339	340
142	c137	scSKi238_A8out	s. cerevisiae	skI2, skI3, skI8				his	pFLdspe	amp		24.04.12	3.93	quickch'g c80	352	353
143	c138	scSpp11_ΔN	s. cerevisiae	spo11	170	398	26	his_ZTA	p-EC-K-HT- ZTA	kan	ok	01.03.12		cloned by p&T		
145	c139	scSKi8_Δ GST	s. cerevisiae	skI8	1	397	44	his GST	p-EC-K-3C- GST	kan	ok	16.05.12		clones by p&T		
146	c140	scSpp11_ΔN_ΔQRF	s. cerevisiae	spo11	170	398	26	his_ZTA	p-EC-A-GST ZTA	kan	ok	28.05.12	3.100	Q376A_R377D_F380D_QC on c138	354	355
147	c141	scSKi8 GST	s. cerevisiae	skI8	1	397	44	his GST	p-EC-A-GST	amp	ok	30.05.12	3.100		105	106
148	c142	scSpp11_Δ Y135F	s. cerevisiae	spo11	1	398	44	his GST	p-EC-K-3C- GST	kan	ok	05.11.12		Y135F, cloned by p&T		
149	c143	scSpp11ΔC	s. cerevisiae	spo11	1	170	19	his TRX	p-EC-K-TEV- TRX	kan	ok	05.11.12		cloned by p&T		
150	c144	scSpp11ΔNΔC	s. cerevisiae	spo11	38	170	15	his TRX	p-EC-K-TEV- TRX	kan	ok	05.11.12		cloned by p&T		

<i>ID</i>	<i>number</i>	<i>name</i>	<i>species</i>	<i>protein</i>	<i>start</i>	<i>end</i>	<i>size</i>	<i>tag</i>	<i>vector</i>	<i>resistance</i>	<i>sequencing_status</i>	<i>date</i>	<i>lab_book</i>	<i>comment</i>	<i>primer_f</i>	<i>primer_rev</i>
151	c145	sSpor11ΔC_Y135F	s. cerevisiae	spo11	1	170	19	hisTRX	p-ECK-TEV-TRX	kan	ok	05.11.12		Y135F, cloned by p&T		
152	c146	sSpor11ΔNΔC_Y135F	s. cerevisiae	spo11	38	170	15	hisTRX	p-ECK-TEV-TRX	kan	ok	05.11.12		Y135F, cloned by p&T		

#	Name	For/Rev	Insert	Restriction	Vector	Tag	Sequence
1	ySkI2_pfbacta_f	f	ySkI2p fl	Sall	FastBac HT	6xHis	ATATGTCACAGATGTCGAGGGATTGAGTACG
2	ySkI2_pfbacta_r	r	ySkI2p fl	XbaI	FastBac HT	6xHis	GGCGCTAGACTATAAATAACAACCTGCGGGG
3	003ySkI3fl_pfbhta_f	f	ySkI3p fl	BamHI	FastBac HT	6xHis	GCAGGATCGGATGCGGATATTAACACAGC
4	004ySkI3fl_pfbhta_r	r	ySkI3p fl	XhoI	FastBac HT	6xHis	GAGCTCGAGTTAGAACAACCTCGTTAGCGCC
5	005ySkI8_fl_pfbHTA_f	f	ySkI8p fl	Sall	FastBac HT	6xHis	GCTGTGACGACATGCCAAAGTGTTTATTGC
6	006ySkI8_fl_pfbHTA_r	r	ySkI8p fl	XhoI	FastBac HT	6xHis	GCTGTGAGTTATTTACCGCCAGTCTCTCAAAC
7	007ySkI8_fl_pGexP1_f	f	ySkI8p fl	Sall	pGexP1	GST	ACTGTGACCGATGTCCTAAAGTGTTTATTGC
8	008ySkI8_fl_pGexP1_r	r	ySkI8p fl	NcoI	pGexP1	GST	ATAGGGCCGCTTTTACCGCCAGC
9	009_pfbGST_f	f	GST_precision	BamHI	pFastBacI	GST	ATCGATCCATGTCCTTACTAGGTATTGGG
10	010_pfbGST_r	r	GST_precision	EcoRI	pFastBacI	GST	ATAGAATTCACGGGGCCCTGGAAACAG
11	011_pBac_f	f	-	-	astBac 1/ H	-	CCGGAAATTAATGATCATGG
12	012_pBac_r	r	-	-	astBac 1/ H	-	CAAGTTAAACAACAACATTC
13	013_pBac_6his	f	-	-	FastBac HT	-	CATCACCATCACCATCACG
14	014_M13-f	f	-	-	H10 Bacmri	-	GTTTTCCAGTCACGAC
15	015_M13-r	r	-	-	H10 Bacmri	-	CAAGAAAGCAGCTATGAC
16	016_ySkI8fl_pfbac-f	f	ySkI8p fl	NcoI	astBac 1/ H	6xHis	GAGCCATGGCCATGTCCTAAAGTGTTTATTGCC
17	017_ySkI8fl_pfbac-r	r	ySkI8p fl	HindIII	astBac 1/ H	6xHis	GCCAGCTTTTATTACCGCCAGCTCTCTAAACCC
18	018_ySkI8fl_pfbac-f	f	ySkI8p fl	Sall	astBac 1/ H	6xHis	CCGGTCGACGAATGTCCTAAAGTGTTTATTGCC
19	019_ySkI2_S132-f	f	ySkI2	-	-	-	GGAAATTGCAAAATGCCAATGCATCAAACTCACTGTGCGATTACGAGAAGTCAACC
20	020_ySkI2_S132-r	r	ySkI2	-	-	-	GGTTGATCTTCTCGTAATCGACAGTGAATTTGATGCGATGGCATTTCGCAACTTC
21	021_ySkI2_N884-f	f	ySkI2	-	-	-	GCTGGCATAAAGGAGCCACAGCAACCTAATGCAAGAAATGGTTAAATCGCC
22	022_ySkI2_N884-r	r	ySkI2	-	-	-	GGCGATTAAACATTCTTGCATAGGTGACTGTTGCCTCCTTATATGCCAGC
23	023_ySkI3_+889	f	ySkI3p	-	-	-	CTGGACAACATGGATGCCCC
24	024_ySkI3+180	f	ySkI3p	-	-	-	CCATAAGTCGGATTGCACC
25	025_pfastBac_-190	f	-	-	astBac 1/ H	-	GGTTGGCTACGTATACCTCG
26	026_hsSKI2+145	f	hsSKI2	-	-	-	CCTTGTGCCCAGATGTGC
27	027_hsSKI2+649	f	hsSKI2	-	-	-	CCTGTGATTTGGGTGGG
28	028_hsSKI2+1155	f	hsSKI2	-	-	-	GGATGTACAGCTGCATCCG
29	029_hsSKI2+1683	f	hsSKI2	-	-	-	CCGCACACGTCGCCAGTTGC
30	030_hsSKI2+2132	f	hsSKI2	-	-	-	CCACAGGCACCGTTATCC
31	031_hsSKI2+2622	f	hsSKI2	-	-	-	GGTCTTGTGTATAAGCCC
32	032_hsSKI2+3135	f	hsSKI2	-	-	-	GGATCAGTCATGCTGCTGC
33	033_hsSKI3+5	f	hsSKI3	-	-	-	CCAGCAGGAGCTGAAGACTGC
34	034_hsSKI3+498	f	hsSKI3	-	-	-	CCTGGCTGAAAGTACAGAG
35	035_hsSKI3+986	f	hsSKI3	-	-	-	GCAGTCAAGCTCGAAGACTG
36	036_hsSKI3+1537	f	hsSKI3	-	-	-	GCTCGTGGATGTTATAGG
37	037_hsSKI3+2024	f	hsSKI3	-	-	-	GCCATCTATGATGGCAAAAGC
38	038_hsSKI3+2521	f	hsSKI3	-	-	-	GGAAATTTAGCCCTTGTCTCAGC
39	039_hsSKI3+2991	f	hsSKI3	-	-	-	GGAAAGCAGCAATGCATACC
40	040_hsSKI3+3482	f	hsSKI3	-	-	-	GGTCCCTTGTATCATGCG
41	041_hsSKI3+3963	f	hsSKI3	-	-	-	CCAGTCCCTTGAAGTGGG
42	042_hsSKI3+4421	f	hsSKI3	-	-	-	CCTTGAAGCTTGTCTTTGTCC
43	043_hsSKI8+129	f	hsSKI8	-	-	-	GGTGAAGGCTGGAAGTGG
44	044_hsSKI8+538	f	hsSKI8	-	-	-	GGAAAACTCTGCATACCTGG
45	045_scSKI7_pFast-f	f	scSKI7	NcoI	astBac 1/ H	6xHis	CGATACCATGGGATGCTGTTATTAGAGCAATTAGC
46	046_scSKI7_pFast-r	r	scSKI7	HindIII	astBac 1/ H	6xHis	CGTACTGAAGCTTTACTGGCATGCAATCTGCCC
47	047_scSKI7_pLIC-f	f	scSKI7	-	pLIC (TEV)	-	CCAGGAGCAGCCCTCGTATGCTTATTAGAGCAATTAGC
48	048_scSKI7_pLIC-r	r	scSKI7	-	pLIC (TEV)	-	GCAAGCAGCCGCTCGTATTTACTGGCATGCAATCTGCCC
49	049_hsSKI2_pFast-f	f	hsSKI2	EcoRI	pFast	6xHis	CGCATGAATTCATGATGGAGACAGCGCATTTGTC
50	050_hsSKI2_pFast-r	r	hsSKI2	HindIII	pFast	6xHis	CCTATGAAGCTTCACTGGGTGTAGAGGCTGG
51	051_hsSKI3_pFast-f	f	hsSKI3	BamHI	pFast	6xHis	GCATAGGATCCAATGCCAGCAAGGAAGTGAAGACTGC
52	052_hsSKI3_pFast-r	r	hsSKI3	XbaI	pFast	6xHis	GGTATCTAGATTTATGAGGCAACATCTGTATCAGTTCC
53	053_hsSKI8_pFast-f	f	hsSKI8	NcoI	pFast	6xHis	GCATACATGGGTAGACCAACAGTACGGTATTCTC
54	054_hsSKI8_pFast-r	r	hsSKI8	EcoRI	pFast	6xHis	GCTGGCAATTTCTAAATGGCAATCATAGATGAAATTC
55	055_spSKI8_pFast-f	f	spSKI8	BamHI	pFast	6xHis	GCATAGGATCCGATGAGGAAGAGTATCTCGTTAGCC
56	056_spSKI8_pFast-r	r	spSKI8	EcoRI	pFast	6xHis	GGATGAATCTTATTCTGTAGCAGCAGCTCATACC
57	057_spSKI2_pFast-f	f	spSKI2	NcoI	pFast	6xHis	GCATACCATGGGATGCTTCTAAACTTGTAGATGCAATCAACG
58	058_spSKI2_pFast-r	r	spSKI2	XbaI	pFast	6xHis	GCTGTCTAGATTCACATACAGTGAAGGGC
59	059_spSKI3_pFast-f	f	spSKI3	BamHI	pFast	6xHis	TTATAGATCCGATGGCAAAACAGCCCTCAAAGC
60	060_spSKI3_pFast-r	r	spSKI3	XhoI	pFast	6xHis	CGTATCTGAGCTGCAAGCATCTGAAACTAGTGC
61	061_spSKI8+222	f	spSKI8	-	-	-	CGTITTTGGCGATTGG
62	062_spSKI8+721	f	spSKI8	-	-	-	GGTGATTTGTGCTTCCGCC
63	063_spSKI3+6	f	spSKI3	-	-	-	AAAACAGCCCTCAAAGC
64	064_spSKI3+496	f	spSKI3	-	-	-	GAAAGCATGGATCGTTGC
65	065_spSKI3+980	f	spSKI3	-	-	-	ACAATAGCGCTGAACTAGC
66	066_spSKI3+1465	f	spSKI3	-	-	-	CTACTTTAGACGACCCAGC
67	067_spSKI3+1947	f	spSKI3	-	-	-	CAATTTGGATCATCACTCC
68	068_spSKI3+2424	f	spSKI3	-	-	-	CGCATGTTTATCACTCTGCC
69	069_spSKI3+2897	f	spSKI3	-	-	-	TGTGGGCAAAATATGGTGC
70	070_spSKI3+3389	f	spSKI3	-	-	-	TCGGCAGGTTATATTGGC
71	071_spSKI3+3831	f	spSKI3	-	-	-	CCTCAACAAAGTTCAGATTATGG
72	072_spSKI2+18	f	spSKI2	-	-	-	AGATGCAATCAACGAAGTAGC
73	073_spSKI2+525	f	spSKI2	-	-	-	TTCCATGACAGCGACATCC
74	074_spSKI2+1051	f	spSKI2	-	-	-	GGAAATTTAAGCTGGTATGTC
75	075_spSKI2+1543	f	spSKI2	-	-	-	GGCGTTCAAACGAATATGATGC
76	076_spSKI2+1948	f	spSKI2	-	-	-	GCAATGGGTGAATATGCCC
77	077_spSKI2+2432	f	spSKI2	-	-	-	TCGAGCAATAACTACTGC
78	078_spSKI2+2924	f	spSKI2	-	-	-	CCGGAAATCCAATATCTGC
79	079_spSKI2+3413	f	spSKI2	-	-	-	TGGAGGTTTGTCTACGAGTGG
80	080_scSKI7+3	f	scSKI7	-	-	-	GTCGTTATTAGAGCAATTAGC
81	081_scSKI7+494	f	scSKI7	-	-	-	CATCAATCCCTTATGTCG
82	082_scSKI7+952	f	scSKI7	-	-	-	AAGTCACTTAGACAATACC
83	083_scSKI7+1397	f	scSKI7	-	-	-	GTTCCGGTTTATTAGGTTGC
84	084_scSKI7+1860	f	scSKI7	-	-	-	GCAATTTCACTTCTGAAGGG
85	085_scSKI7_116C_pLIC	f	scSKI7	-	pLIC (TEV)	LIC	CCAGGGAGCAGCCTCGGATGATAAATCAACTTGAAGAGTCATGG
86	086_scSKI7_266C_pLIC	f	scSKI7	-	pLIC (TEV)	LIC	CCAGGGAGCAGCCTCGTGAATTTGACATGTTTGTCTCGG
87	087_scSKI7_N265_pLIC	f	scSKI7	-	pLIC (TEV)	LIC	GCAAGGACACCGCCTCGTTAAGGATGGTGGCAATGATG
88	088_scSKI7_pLICsumo	f	scSKI7	-	ΔLIC (Sumo)	LIC	ACCAGGAACAACCGGGCCGCTCGATGCTGTTATTAGAGCAATTAGC
89	089_scSKI7_116C_pLICsumo	f	scSKI7	-	ΔLIC (Sumo)	LIC	ACCAGGAACAACCGGGCCGCTCGGATAAATCAACTTGAAGAGTCATGG
90	090_spSKI3_pLIC_cry-f	f	spSKI3	BamHI	pLIC (TEV)	-	CCAGGGAGCAGCCTCGGATCCGATGGCAAAACAGCCCTCAAAGC
91	091_spSKI3_pLIC_cry-r	r	spSKI3	XhoI	pLIC (TEV)	-	GCAAGCAGCCGCTCGTTACTGAGCTACGAAGCATCACTGAAACTAGTGC
92	092_spSKI2_pLIC_cry-f	f	spSKI2	NcoI	pLIC (TEV)	-	CCAGGGAGCAGCCTCGGATGGGATGCTCTTAAACTTGTAGATGCAATCAACG
93	093_spSKI2_pLIC_cry-r	r	spSKI2	XbaI	pLIC (TEV)	-	GCAAGCAGCCGCTCGTTACTGATGTTACATATACAGTGAAGGGC
94	094_hsSKI2_Q1133-f	f	hsSKI2	-	-	-	GCTCCAAACACCCCTCAAGCAGCAATAGAACGTTGC
95	095_hsSKI2_Q1133-r	r	hsSKI2	-	-	-	CACACGTTCTATCCCTGCTTGAAGGTGTTTGGAGC
96	096_hsSKI2_R151-f	f	hsSKI2	-	-	-	CCTTATGGGAAATCCAACCTCGTATCCCTCTGGCCAGG
97	097_hsSKI2_R151-r	r	hsSKI2	-	-	-	CCTGGCCAGAAAGGATCCGATGGATTTCGCCATAAGG
98	098_scSKI2_D444N_f	f	scSKI2	-	-	-	GATGTAGAGTTTGTCTTTTCAATGAAGTCACTACGTTAATGATCAAGACCGTGG
99	099_scSKI2_D444N_r	r	scSKI2	-	-	-	CCACGGTCTGTATCAATGATGTAAGTCACTTCAATGAAATGACAAACTCTACATC
100	100_scSKI2_E445_Q_f	f	scSKI2	-	-	-	GATGTAGAGTTTGTCTTTTGGATGAAGTCACTACGTTAATGATCAAGACCGTGG
101	101_scSKI2_E445_Q_r	r	scSKI2	-	-	-	CCACGGTCTGTATCAATGATGTAAGTCACTTCAATGAAATGACAAACTCTACATC
102	102_scSKI3_N522_f	f	scSKI3	-	SUMO LIC	SUMOHis	ACCAGGAACAACCGGGCCGCTCGATGCTGGATATTAACACAGC
103	103_scSKI3_N522_r	r	scSKI3	-	UMO/TEV LIC	SUMOHis	GCAAGCAGCCGCTCGTTATTTTCTTCAATAAAATACCTTTGCC
104	104_scSKI3_N522_pLIC-f	f	scSKI3	-	TEV LIC	TEV cassette	CCAGGGAGCAGCCTCGATGTCGGATATTAACACAGC
105	105_scSKI8_pLIC-f	f	scSKI8	-	pLIC TEV	TEV cassette	CCAGGGAGCAGCCTCGATGTCCTAAAGTGTTTATTGCC
106	106_scSKI8_pLIC-r	r	scSKI8	-	pLIC TEV	TEV cassette	GCAAGCAGCCGCTCGTATTACCGCCAGCTCTCTAAACC
107	107_scSKI8_3C_1f	f	scSKI8	-	pLIC 3C	3C cassette	CCAGGGCCGACTGATGTCCTAAAGTGTTTATTGC
108	108_scSKI8_3C_397r	r	scSKI8	-	pLIC 3C	3C cassette	CCAGGGCCGACTGCTTATTAGCCAGCTTCTCTAAACC
109	109_scSKI3_1_f	f	scSKI3	EcoRI	FastBac Du	-	GGCGAATTCATGCGGATATTAACACAGC

Table A.2 | PCR primers generated during my PhD work (continued on pages 95-97).





327	327_ski8_302GRRS303_f	f		GAGTCTATCGTTTAAATGATTCTGGACGACGTTCCGGGTGAACAATTATGCAGTGCCGG
328	328_ski8_302GRRS303_r	r		CGGGCACTGCATAATGTTTCCACCGAACGTCGTCCAGAATCATAAACGATAGACTC
329	329_dSki8out_f	f		CGATACCGGTAAACAAGTATGGCGACAGTCCGGACTTTTTCCCTAATAACCTCAAGG
330	330_dSki8_out_r	r		CCTTGAGGTTATAGGGAAAAGTCCGCACTGTCTGCCATACCTTGTITACCGGTATCG
331	331_dSki8_in_f	f		GAGAGTAAGAATTTGAGAAGCATAGCAGCGGTATGGATTTTGGCCCTTGGAACTTACTGC
332	332_dSki8_in_r	r		GCAGTAACGTTCCAAAGGGCACAATCCATACCGTCTGCTATGCTCTCAAAATCTTACTCTC
333	333_ski3_751D757D_f	f		GCATACCACGGGTGTGGTATATAGAAGCATCTATCCAGCGTTTTTGACAAGGC
334	334_ski3_751D757D_r	r		GCCTTGCAAAACGTCGATAGATGCTTCTATATACCACACCGCGTGGTATGC
335	335_ski3_751D757D730D_f	f		GAGTGGTTTCAATCTGCTTTAGATGTTGATCCAAATGATGTAGATCATGG
336	336_ski3_751D757D730D_r	r		CCATGACTTACATCATTITGGATCAACATCTAAAGCAGATTGAAACCACTC
337	337_ski3_1046A1050R_f	f		GGTCTTGAATAAATTAGCAAGCCTTGGCCGACAAGATTGGTCACTTGG
338	338_ski3_1046A1050R_r	r		CCAAGTGACGAATCTTGTCCGGCAAGGCTTGTAAATTTATTCAGAACC
339	339_ski3_1046A1050R1078A_f	f		GGAAAGTCTAAACTTTTTGCAGCCTCCTCATATATCTAATGGAAGG
340	340_ski3_1046A1050R1078A_r	r		CCTTCCATTAGATAATGAAGGAGGCTGCAAAAAGTTAGAACTTCC
341	css17A10			TTTTTTTTTAAGUGAUGGUGUGGGG
342	342_Css17			AAGUGAUGGUGUGGGG
343	343_ski2_325r	r		CCTGAATTTTACCTCTAACCC
344	344_ski3_240r	r		CCTTCCACGCTAAAAGG
345	345_ski8_390r	r		GGCACCCCATTTTATGCC
346	346_scSki3_1f	f	SUMO LIC	ACCAGGAACAACCGGGCCGCTCGATGTCGGATATTAACAGCTATTGAAGG
347	347_scSki3_160rv	r	SUMO LIC	GCAAAAGCACCGGCTCGTTAACCAATAGTTTCCGCCATTAGCG
348	348_scSki3_nat_1f	f	LIC CBP Ndel	CAGACATATGTCGGATATTAACAGCTATTGAAGGAAGCC
349	349_scSki3_nat_160rv	r	LIC CBP XhoI	ATATCTCGAGTGGGCCCTGGAAACAGACTTCCAGGCTCCCAATAGTTTCCGCCATTAGC
350	350_dSki8_out_f	f		CGATACCGGTAAACAAGTATGGGCTGATAGTCCGGACTTTTTCCCTAATAACCTCAAGGTTTGGG
351	351_dSki8_out_r	r		CCCAACCTTGAGGTTATAGGGAAAAGTCCGCACTATCAGCCATCTTGTACCGGTATCG
352	352_dSki8_out_short_f	f		GGTAACAAGTATGGGCTGATAGTCCGGACTTTTTCCCTAATAACC
353	353_dSki8_out_short_r	r		GGTTATTAGGAAAAAGTCCGCACTATCAGCCATCTTGTTTACC
354	354_ySpo11_ORF_f	f		CGTCATCATAGAATGTCGGACGAAATGATTTCCAAAAGAAAGC
355	355_ySpo11_ORF_r	r		GCCTTTGTTGGAAATCAATTTGGTCCGCACTTGTATGAGC
356	356_scSpo11_Y135F_f	f		CAGTGAGAGATATCTTCTTCCCAACGTGGAATGTTTCAAGAC
357	357_scSpo11_Y135F_r	r		GTCTTTGAAACAATTCACGTTGGAGAAGAATATCTCTCACTG
358	358_scSpo11_1F	f	TEV-LIC	CCAGGGAGCAGCCTCGATGGCTTTGGAGGATTGCG
359	359_scSpo11_38F	f	TEV-LIC	CCAGGGAGCAGCCTCGATGACTCCCTGTTCAAAGCGAGATG
360	360_scSpo11_170Rv	r	TEV-LIC	GCAAAAGCACCGGCTCGTTATGGTATAATGTTAAGGATTTCTGGAG



# Bibliography

- Allmang, C., Kufel, J., Chanfreau, G., Mitchell, P., Petfalski, E., and Tollervey, D. (1999). Functions of the exosome in rRNA, snoRNA and snRNA synthesis. *EMBO J*, 18(19):5399–410.
- Anderson, J. S. and Parker, R. P. (1998). The 3' to 5' degradation of yeast mRNAs is a general mechanism for mRNA turnover that requires the SKI2 DEVH box protein and 3' to 5' exonucleases of the exosome complex. *EMBO J*, 17(5):1497–506.
- Araki, Y., Takahashi, S., Kobayashi, T., Kajihio, H., Hoshino, S., and Katada, T. (2001). Ski7p G protein interacts with the exosome and the Ski complex for 3'-to-5' mRNA decay in yeast. *EMBO J*, 20(17):4684–93.
- Arigo, J. T., Eyler, D. E., Carroll, K. L., and Corden, J. L. (2006). Termination of cryptic unstable transcripts is directed by yeast RNA-binding proteins Nrd1 and Nab3. *Mol Cell*, 23(6):841–851.
- Arora, C., Kee, K., Maleki, S., and Keeney, S. (2004). Antiviral protein Ski8 is a direct partner of Spo11 in meiotic DNA break formation, independent of its cytoplasmic role in RNA metabolism. *Mol Cell*, 13(4):549–59.
- Atkinson, G. C., Baldauf, S. L., and Hauryliuk, V. (2008). Evolution of nonstop, no-go and nonsense-mediated mRNA decay and their termination factor-derived components. *BMC Evol Biol*, 8:290.
- Badis, G., Saveanu, C., Fromont-Racine, M., and Jacquier, A. (2004). Targeted mRNA degradation by deadenylation-independent decapping. *Mol Cell*, 15(1):5–15.
- Becker, T., Armache, J.-P., Jarasch, A., Anger, A. M., Villa, E., Sieber, H., Motaal, B. A., Mielke, T., Berninghausen, O., and Beckmann, R. (2011). Structure of the no-go mRNA

- decay complex Dom34-Hbs1 bound to a stalled 80S ribosome. *Nat Struct Mol Biol*, 18(6):715–720.
- Beelman, C. A., Stevens, A., Caponigro, G., LaGrandeur, T. E., Hatfield, L., Fortner, D. M., and Parker, R. (1996). An essential component of the decapping enzyme required for normal rates of mRNA turnover. *Nature*, 382(6592):642–646.
- Benard, L., Carroll, K., Valle, R. C., Masison, D. C., and Wickner, R. B. (1999). The Ski7 antiviral protein is an EF1-alpha homolog that blocks expression of non-poly(A) mRNA in *Saccharomyces cerevisiae*. *J Virol*, 73(4):2893–2900.
- Benard, L., Carroll, K., Valle, R. C., and Wickner, R. B. (1998). Ski6p is a homolog of RNA-processing enzymes that affects translation of non-poly(A) mRNAs and 60S ribosomal subunit biogenesis. *Mol Cell Biol*, 18(5):2688–2696.
- Bergerat, A., de Massy, B., Gadelle, D., Varoutas, P. C., Nicolas, A., and Forterre, P. (1997). An atypical topoisomerase II from Archaea with implications for meiotic recombination. *Nature*, 386(6623):414–7.
- Bernstein, J., Patterson, D. N., Wilson, G. M., and Toth, E. A. (2008). Characterization of the essential activities of *saccharomyces cerevisiae* mtr4p, a 3'-5' helicase partner of the nuclear exosome. *J Biol Chem*, 283(8):4930–4942.
- Bernstein, J. A., Khodursky, A. B., Lin, P.-H., Lin-Chao, S., and Cohen, S. N. (2002). Global analysis of mRNA decay and abundance in *Escherichia coli* at single-gene resolution using two-color fluorescent DNA microarrays. *Proc Natl Acad Sci U S A*, 99(15):9697–9702.
- Bernstein, J. A., Lin, P.-H., Cohen, S. N., and Lin-Chao, S. (2004). Global analysis of *Escherichia coli* RNA degradosome function using DNA microarrays. *Proc Natl Acad Sci U S A*, 101(9):2758–2763.
- Bonneau, F., Basquin, J., Ebert, J., Lorentzen, E., and Conti, E. (2009). The yeast exosome functions as a macromolecular cage to channel RNA substrates for degradation. *Cell*, 139(3):547–59.
- Bousquet-Antonelli, C., Presutti, C., and Tollervey, D. (2000). Identification of a regulated pathway for nuclear pre-mRNA turnover. *Cell*, 102(6):765–75.

- Brown, C. E. and Sachs, A. B. (1998). Poly(A) tail length control in *Saccharomyces cerevisiae* occurs by message-specific deadenylation. *Mol Cell Biol*, 18(11):6548–6559.
- Brown, J. T., Bai, X., and Johnson, A. W. (2000). The yeast antiviral proteins Ski2p, Ski3p, and Ski8p exist as a complex in vivo. *RNA*, 6(3):449–57.
- Büttner, K., Nehring, S., and Hopfner, K. P. (2007). Structural basis for DNA duplex separation by a superfamily-2 helicase. *Nat Struct Mol Biol*, 14(7):647–52.
- Büttner, K., Wenig, K., and Hopfner, K. P. (2005). Structural framework for the mechanism of archaeal exosomes in RNA processing. *Mol Cell*, 20(3):461–71.
- Callahan, K. P. and Butler, J. S. (2008). Evidence for core exosome independent function of the nuclear exoribonuclease Rrp6p. *Nucleic Acids Res*, 36(21):6645–6655.
- Carpousis, A. J. (2007). The RNA degradosome of *Escherichia coli*: an mRNA-degrading machine assembled on RNase E. *Annu Rev Microbiol*, 61:71–87.
- Carroll, K. L., Ghirlando, R., Ames, J. M., and Corden, J. L. (2007). Interaction of yeast RNA-binding proteins Nrd1 and Nab3 with RNA polymerase II terminator elements. *RNA*, 13(3):361–373.
- Chang, Y.-F., Imam, J. S., and Wilkinson, M. F. (2007). The nonsense-mediated decay RNA surveillance pathway. *Annu Rev Biochem*, 76:51–74.
- Chen, C. K.-M., Chan, N.-L., and Wang, A. H.-J. (2011). The many blades of the  $\beta$ -propeller proteins: conserved but versatile. *Trends Biochem Sci*, 36(10):553–561.
- Chen, C. Y., Gherzi, R., Ong, S. E., Chan, E. L., Rajmakers, R., Pruijn, G. J., Stoecklin, G., Moroni, C., Mann, M., and Karin, M. (2001). AU binding proteins recruit the exosome to degrade ARE-containing mRNAs. *Cell*, 107(4):451–464.
- Chen, L., Muhrad, D., Hauryliuk, V., Cheng, Z., Lim, M. K., Shyp, V., Parker, R., and Song, H. (2010). Structure of the Dom34-Hbs1 complex and implications for no-go decay. *Nat Struct Mol Biol*, 17(10):1233–1240.
- Cheng, Z., Liu, Y., Wang, C., Parker, R., and Song, H. (2004). Crystal structure of Ski8p, a WD-repeat protein with dual roles in mRNA metabolism and meiotic recombination. *Protein Sci*, 13(10):2673–84.

- Cole, F., Keeney, S., and Jasin, M. (2010). Evolutionary conservation of meiotic DSB proteins: more than just Spo11. *Genes Dev*, 24(12):1201–1207.
- Conti, E. and Izaurralde, E. (2005). Nonsense-mediated mRNA decay: molecular insights and mechanistic variations across species. *Curr Opin Cell Biol*, 17(3):316–325.
- Costello, J. L., Stead, J. A., Feigenbutz, M., Jones, R. M., and Mitchell, P. (2011). The C-terminal region of the exosome-associated protein Rrp47 is specifically required for box C/D small nucleolar RNA 3'-maturation. *J Biol Chem*, 286(6):4535–4543.
- D'Andrea, L. D. and Regan, L. (2003). TPR proteins: the versatile helix. *Trends in biochemical sciences*, 28(12):655–62.
- Dangel, A. W., Shen, L., Mendoza, A. R., Wu, L. C., and Yu, C. Y. (1995). Human helicase gene SKI2W in the HLA class III region exhibits striking structural similarities to the yeast antiviral gene SKI2 and to the human gene KIAA0052: emergence of a new gene family. *Nucleic Acids Res*, 23(12):2120–2126.
- Das, A. K., Cohen, P. W., and Barford, D. (1998). The structure of the tetratricopeptide repeats of protein phosphatase 5: implications for TPR-mediated protein-protein interactions. *The EMBO journal*, 17(5):1192–9.
- Daugeron, M. C., Mauxion, F., and Sraphin, B. (2001). The yeast POP2 gene encodes a nuclease involved in mRNA deadenylation. *Nucleic Acids Res*, 29(12):2448–2455.
- Davis, C. A. and Ares, M. (2006). Accumulation of unstable promoter-associated transcripts upon loss of the nuclear exosome subunit Rrp6p in *Saccharomyces cerevisiae*. *Proc Natl Acad Sci U S A*, 103(9):3262–3267.
- Dez, C., Houseley, J., and Tollervey, D. (2006). Surveillance of nuclear-restricted pre-ribosomes within a subnucleolar region of *Saccharomyces cerevisiae*. *EMBO J*, 25(7):1534–1546.
- Doma, M. K. and Parker, R. (2006). Endonucleolytic cleavage of eukaryotic mRNAs with stalls in translation elongation. *Nature*, 440(7083):561–564.
- Dunkley, T. and Parker, R. (1999). The DCP2 protein is required for mRNA decapping in *Saccharomyces cerevisiae* and contains a functional MutT motif. *EMBO J*, 18(19):5411–5422.

- Dziembowski, A., Lorentzen, E., Conti, E., and Seraphin, B. (2007). A single subunit, Dis3, is essentially responsible for yeast exosome core activity. *Nat Struct Mol Biol*, 14(1):15–22.
- Egecioglu, D. E., Henras, A. K., and Chanfreau, G. F. (2006). Contributions of Trf4p- and Trf5p-dependent polyadenylation to the processing and degradative functions of the yeast nuclear exosome. *RNA*, 12(1):26–32.
- Evguenieva-Hackenberg, E., Walter, P., Hochleitner, E., Lottspeich, F., and Klug, G. (2003). An exosome-like complex in *Sulfolobus solfataricus*. *EMBO Rep*, 4(9):889–893.
- Fairman-Williams, M. E., Guenther, U.-P., and Jankowsky, E. (2010). SF1 and SF2 helicases: family matters. *Curr Opin Struct Biol*, 20(3):313–324.
- Franks, T. M. and Lykke-Andersen, J. (2008). The control of mRNA decapping and P-body formation. *Mol Cell*, 32(5):605–615.
- Frischmeyer, P. A., van Hoof, A., O’Donnell, K., Guerrierio, A. L., Parker, R., and Dietz, H. C. (2002). An mRNA surveillance mechanism that eliminates transcripts lacking termination codons. *Science*, 295(5563):2258–2261.
- Garneau, N. L., Wilusz, J., and Wilusz, C. J. (2007). The highways and byways of mRNA decay. *Nature reviews. Molecular cell biology*, 8(2):113–26.
- Giaever, G., Chu, A. M., Ni, L., Connelly, C., Riles, L., Vronneau, S., Dow, S., Lucau-Danila, A., Anderson, K., Andr, B., Arkin, A. P., Astromoff, A., El-Bakkoury, M., Bangham, R., Benito, R., Brachat, S., Campanaro, S., Curtiss, M., Davis, K., Deutschbauer, A., Entian, K.-D., Flaherty, P., Foury, F., Garfinkel, D. J., Gerstein, M., Gotte, D., Gldener, U., Hegemann, J. H., Hempel, S., Herman, Z., Jaramillo, D. F., Kelly, D. E., Kelly, S. L., Ktter, P., LaBonte, D., Lamb, D. C., Lan, N., Liang, H., Liao, H., Liu, L., Luo, C., Lussier, M., Mao, R., Menard, P., Ooi, S. L., Revuelta, J. L., Roberts, C. J., Rose, M., Ross-Macdonald, P., Scherens, B., Schimmack, G., Shafer, B., Shoemaker, D. D., Sookhai-Mahadeo, S., Storms, R. K., Strathern, J. N., Valle, G., Voet, M., Volkcaert, G., yun Wang, C., Ward, T. R., Wilhelmy, J., Winzeler, E. A., Yang, Y., Yen, G., Youngman, E., Yu, K., Bussey, H., Boeke, J. D., Snyder, M., Philippsen, P., Davis, R. W., and Johnston, M. (2002). Functional profiling of the *Saccharomyces cerevisiae* genome. *Nature*, 418(6896):387–391.

- Hamill, S., Wolin, S. L., and Reinisch, K. M. (2010). Structure and function of the polymerase core of TRAMP, a RNA surveillance complex. *Proc Natl Acad Sci U S A*, 107(34):15045–15050.
- Hartung, S., Niederberger, T., Hartung, M., Tresch, A., and Hopfner, K.-P. (2010). Quantitative analysis of processive RNA degradation by the archaeal RNA exosome. *Nucleic Acids Res*, 38(15):5166–5176.
- He, F., Li, X., Spatrick, P., Casillo, R., Dong, S., and Jacobson, A. (2003). Genome-wide analysis of mRNAs regulated by the nonsense-mediated and 5' to 3' mRNA decay pathways in yeast. *Mol Cell*, 12(6):1439–1452.
- He, Y., Andersen, G. R., and Nielsen, K. H. (2010). Structural basis for the function of DEAH helicases. *EMBO Rep*, 11(3):180–6.
- Hilleren, P., McCarthy, T., Rosbash, M., Parker, R., and Jensen, T. H. (2001). Quality control of mRNA 3'-end processing is linked to the nuclear exosome. *Nature*, 413(6855):538–42.
- Hirano, T., Kinoshita, N., Morikawa, K., and Yanagida, M. (1990). Snap helix with knob and hole: essential repeats in *S. pombe* nuclear protein nuc2<sup>+</sup>. *Cell*, 60(2):319–28.
- Houalla, R., Devaux, F., Fatica, A., Kufel, J., Barrass, D., Torchet, C., and Tollervey, D. (2006). Microarray detection of novel nuclear RNA substrates for the exosome. *Yeast*, 23(6):439–54.
- Houseley, J. and Tollervey, D. (2009). The many pathways of RNA degradation. *Cell*, 136(4):763–76.
- Hsu, C. L. and Stevens, A. (1993). Yeast cells lacking 5'-3' exoribonuclease 1 contain mRNA species that are poly(A) deficient and partially lack the 5' cap structure. *Mol Cell Biol*, 13(8):4826–4835.
- Izaurrealde, E., Lewis, J., McGuigan, C., Jankowska, M., Darzynkiewicz, E., and Mattaj, I. W. (1994). A nuclear cap binding protein complex involved in pre-mRNA splicing. *Cell*, 78(4):657–668.
- Jackson, R. N., Klauer, A. A., Hintze, B. J., Robinson, H., van Hoof, A., and Johnson, S. J. (2010). The crystal structure of Mtr4 reveals a novel arch domain required for rRNA processing. *EMBO J*, 29(13):2205–16.

- Jankowsky, E. and Fairman, M. E. (2007). RNA helicases - one fold for many functions. *Curr Opin Struct Biol*, 17(3):316–324.
- Jinek, M., Rehwinkel, J., Lazarus, B. D., Izaurralde, E., Hanover, J. A., and Conti, E. (2004). The superhelical TPR-repeat domain of O-linked GlcNAc transferase exhibits structural similarities to importin alpha. *Nat Struct Mol Biol*, 11(10):1001–1007.
- Johnson, A. W. and Kolodner, R. D. (1995). Synthetic lethality of SEP1 (XRN1), SKI2 and SEP1 (XRN1) SKI3 mutants of *Saccharomyces cerevisiae* is independent of killer virus and suggests a general role for these genes in translation control. *Mol Cell Biol*, 15(5):2719–27.
- Kadaba, S., Wang, X., and Anderson, J. T. (2006). Nuclear RNA surveillance in *Saccharomyces cerevisiae*: Trf4p-dependent polyadenylation of nascent hypomethylated tRNA and an aberrant form of 5S rRNA. *RNA*, 12(3):508–521.
- Kee, K., Protacio, R. U., Arora, C., and Keeney, S. (2004). Spatial organization and dynamics of the association of Rec102 and Rec104 with meiotic chromosomes. *EMBO J*, 23(8):1815–1824.
- Keeney, S., Giroux, C. N., and Kleckner, N. (1997). Meiosis-specific DNA double-strand breaks are catalyzed by Spo11, a member of a widely conserved protein family. *Cell*, 88(3):375–84.
- Keller, W. and Minvielle-Sebastia, L. (1997). A comparison of mammalian and yeast pre-mRNA 3'-end processing. *Curr Opin Cell Biol*, 9(3):329–336.
- Kelley, L. A. and Sternberg, M. J. (2009). Protein structure prediction on the Web: a case study using the Phyre server. *Nature protocols*, 4(3):363–71.
- Kessler, S. H. and Sachs, A. B. (1998). RNA recognition motif 2 of yeast Pab1p is required for its functional interaction with eukaryotic translation initiation factor 4G. *Mol Cell Biol*, 18(1):51–57.
- Khemicci, V. and Carpousis, A. J. (2004). The RNA degradosome and poly(A) polymerase of *Escherichia coli* are required in vivo for the degradation of small mRNA decay intermediates containing REP-stabilizers. *Mol Microbiol*, 51(3):777–790.

- Khemici, V., Poljak, L., Toesca, I., and Carpousis, A. J. (2005). Evidence in vivo that the DEAD-box RNA helicase RhlB facilitates the degradation of ribosome-free mRNA by RNase E. *Proc Natl Acad Sci U S A*, 102(19):6913–6918.
- Kim, M., Vasiljeva, L., Rando, O. J., Zhelkovsky, A., Moore, C., and Buratowski, S. (2006). Distinct pathways for snoRNA and mRNA termination. *Mol Cell*, 24(5):723–734.
- Klauer, A. A. and van Hoof, A. (2013). Genetic interactions suggest multiple distinct roles of the arch and core helicase domains of Mtr4 in Rrp6 and exosome function. *Nucleic Acids Res*, 41(1):533–541.
- Krogan, N. J., Cagney, G., Yu, H., Zhong, G., Guo, X., Ignatchenko, A., Li, J., Pu, S., Datta, N., Tikuisis, A. P., Punna, T., Peregrn-Alvarez, J. M., Shales, M., Zhang, X., Davey, M., Robinson, M. D., Paccanaro, A., Bray, J. E., Sheung, A., Beattie, B., Richards, D. P., Canadien, V., Lalev, A., Mena, F., Wong, P., Starostine, A., Canete, M. M., Vlasblom, J., Wu, S., Orsi, C., Collins, S. R., Chandran, S., Haw, R., Rilstone, J. J., Gandi, K., Thompson, N. J., Musso, G., Onge, P. S., Ghanny, S., Lam, M. H. Y., Butland, G., Altaf-Ul, A. M., Kanaya, S., Shilatifard, A., O’Shea, E., Weissman, J. S., Ingles, C. J., Hughes, T. R., Parkinson, J., Gerstein, M., Wodak, S. J., Emili, A., and Greenblatt, J. F. (2006). Global landscape of protein complexes in the yeast *Saccharomyces cerevisiae*. *Nature*, 440(7084):637–643.
- Kshirsagar, M. and Parker, R. (2004). Identification of Edc3p as an enhancer of mRNA decapping in *Saccharomyces cerevisiae*. *Genetics*, 166(2):729–739.
- Kühn, U. and Wahle, E. (2004). Structure and function of poly(A) binding proteins. *Biochim Biophys Acta*, 1678(2-3):67–84.
- LaCava, J., Houseley, J., Saveanu, C., Petfalski, E., Thompson, E., Jacquier, A., and Tollervey, D. (2005). RNA degradation by the exosome is promoted by a nuclear polyadenylation complex. *Cell*, 121(5):713–24.
- Lapouge, K., Smith, S. J., Walker, P. A., Gamblin, S. J., Smerdon, S. J., and Rittinger, K. (2000). Structure of the TPR domain of p67phox in complex with Rac-GTP. *Mol Cell*, 6(4):899–907.
- Larimer, F. W. and Stevens, A. (1990). Disruption of the gene XRN1, coding for a 5’-3’ exoribonuclease, restricts yeast cell growth. *Gene*, 95(1):85–90.

- Lebreton, A., Tomecki, R., Dziembowski, A., and Seraphin, B. (2008). Endonucleolytic RNA cleavage by a eukaryotic exosome. *Nature*, 456(7224):993–6.
- Lee, H. H., Kim, Y.-S., Kim, K. H., Heo, I., Kim, S. K., Kim, O., Kim, H. K., Yoon, J. Y., Kim, H. S., Kim, D. J., Lee, S. J., Yoon, H. J., Kim, S. J., Lee, B. G., Song, H. K., Kim, V. N., Park, C.-M., and Suh, S. W. (2007). Structural and functional insights into Dom34, a key component of no-go mRNA decay. *Mol Cell*, 27(6):938–950.
- Lee, S. G., Lee, I., Park, S. H., Kang, C., and Song, K. (1995). Identification and characterization of a human cDNA homologous to yeast SKI2. *Genomics*, 25(3):660–666.
- Liu, H., Rodgers, N. D., Jiao, X., and Kiledjian, M. (2002). The scavenger mRNA decapping enzyme DcpS is a member of the HIT family of pyrophosphatases. *EMBO J*, 21(17):4699–4708.
- Liu, Q., Greimann, J. C., and Lima, C. D. (2006). Reconstitution, activities, and structure of the eukaryotic RNA exosome. *Cell*, 127(6):1223–37.
- Lohman, T. M., Tomko, E. J., and Wu, C. G. (2008). Non-hexameric DNA helicases and translocases: mechanisms and regulation. *Nat Rev Mol Cell Biol*, 9(5):391–401.
- Lorentzen, E., Basquin, J., Tomecki, R., Dziembowski, A., and Conti, E. (2008). Structure of the active subunit of the yeast exosome core, Rrp44: diverse modes of substrate recruitment in the RNase II nuclease family. *Mol Cell*, 29(6):717–28.
- Lorentzen, E. and Conti, E. (2005). Structural basis of 3' end RNA recognition and exoribonucleolytic cleavage by an exosome RNase PH core. *Mol Cell*, 20(3):473–81.
- Lorentzen, E., Dziembowski, A., Lindner, D., Seraphin, B., and Conti, E. (2007). RNA channelling by the archaeal exosome. *EMBO Rep*, 8(5):470–6.
- Lorentzen, E., Walter, P., Fribourg, S., Evguenieva-Hackenberg, E., Klug, G., and Conti, E. (2005). The archaeal exosome core is a hexameric ring structure with three catalytic subunits. *Nat Struct Mol Biol*, 12(7):575–81.
- Lykke-Andersen, S., Brodersen, D. E., and Jensen, T. H. (2009). Origins and activities of the eukaryotic exosome. *J Cell Sci*, 122(Pt 10):1487–94.
- Madrona, A. Y. and Wilson, D. K. (2004). The structure of Ski8p, a protein regulating mRNA degradation: Implications for WD protein structure. *Protein Sci*, 13(6):1557–65.

- Malet, H., Topf, M., Clare, D. K., Ebert, J., Bonneau, F., Basquin, J., Drazkowska, K., Tomecki, R., Dziembowski, A., Conti, E., Saibil, H. R., and Lorentzen, E. (2010). RNA channelling by the eukaryotic exosome. *EMBO Rep*, 11(12):936–942.
- Manley, J. L. and Takagaki, Y. (1996). The end of the message - another link between yeast and mammals. *Science*, 274(5292):1481–1482.
- Matsumoto, Y., Sarkar, G., Sommer, S. S., and Wickner, R. B. (1993). A yeast antiviral protein, Ski8, shares a repeated amino acid sequence pattern with beta-subunits of G proteins and several other proteins. *Yeast*, 9(1):43–51.
- Midtgaard, S. F., Assenholt, J., Jonstrup, A. T., Van, L. B., Jensen, T. H., and Brodersen, D. E. (2006). Structure of the nuclear exosome component Rrp6p reveals an interplay between the active site and the HRDC domain. *Proc Natl Acad Sci U S A*, 103(32):11898–11903.
- Milligan, L., Decourty, L., Saveanu, C., Rappsilber, J., Ceulemans, H., Jacquier, A., and Tollervey, D. (2008). A yeast exosome cofactor, Mpp6, functions in RNA surveillance and in the degradation of noncoding RNA transcripts. *Mol Cell Biol*, 28(17):5446–5457.
- Mitchell, P., Petfalski, E., Houalla, R., Podtelejnikov, A., Mann, M., and Tollervey, D. (2003). Rrp47p is an exosome-associated protein required for the 3' processing of stable RNAs. *Mol Cell Biol*, 23(19):6982–6992.
- Mitchell, P., Petfalski, E., Shevchenko, A., Mann, M., and Tollervey, D. (1997). The exosome: a conserved eukaryotic RNA processing complex containing multiple 3'-5' exoribonucleases. *Cell*, 91(4):457–66.
- Mitchell, P. and Tollervey, D. (2003). An NMD pathway in yeast involving accelerated deadenylation and exosome-mediated 3'-5' degradation. *Mol Cell*, 11(5):1405–13.
- Mühlrad, D., Decker, C. J., and Parker, R. (1994). Deadenylation of the unstable mRNA encoded by the yeast MFA2 gene leads to decapping followed by 5'-3' digestion of the transcript. *Genes Dev*, 8(7):855–866.
- Mühlrad, D., Decker, C. J., and Parker, R. (1995). Turnover mechanisms of the stable yeast PGK1 mRNA. *Mol Cell Biol*, 15(4):2145–2156.

- Nag, D. K., Pata, J. D., Sironi, M., Flood, D. R., and Hart, A. M. (2006). Both conserved and non-conserved regions of Spo11 are essential for meiotic recombination initiation in yeast. *Molecular genetics and genomics : MGG*, 276(4):313–21.
- Navarro, M. V. A. S., Oliveira, C. C., Zanchin, N. I. T., and Guimares, B. G. (2008). Insights into the mechanism of progressive RNA degradation by the archaeal exosome. *J Biol Chem*, 283(20):14120–14131.
- Nichols, M. D., DeAngelis, K., Keck, J. L., and Berger, J. M. (1999). Structure and function of an archaeal topoisomerase VI subunit with homology to the meiotic recombination factor Spo11. *EMBO J*, 18(21):6177–88.
- Orban, T. I. and Izaurralde, E. (2005). Decay of mRNAs targeted by RISC requires XRN1, the Ski complex, and the exosome. *RNA*, 11(4):459–69.
- Paczkowski, J. E., Richardson, B. C., Strassner, A. M., and Fromme, J. C. (2012). The exomer cargo adaptor structure reveals a novel GTPase-binding domain. *EMBO J*, 31(21):4191–4203.
- Parker, R. (2012). RNA degradation in *Saccharomyces cerevisiae*. *Genetics*, 191(3):671–702.
- Phillips, S. and Butler, J. S. (2003). Contribution of domain structure to the RNA 3' end processing and degradation functions of the nuclear exosome subunit Rrp6p. *RNA*, 9(9):1098–1107.
- Py, B., Higgins, C. F., Krisch, H. M., and Carpousis, A. J. (1996). A DEAD-box RNA helicase in the *Escherichia coli* RNA degradosome. *Nature*, 381(6578):169–172.
- Pyle, A. M. (2008). Translocation and unwinding mechanisms of RNA and DNA helicases. *Annu Rev Biophys*, 37:317–36.
- Rhee, S. K., Icho, T., and Wickner, R. B. (1989). Structure and nuclear localization signal of the Ski3 antiviral protein of *Saccharomyces cerevisiae*. *Yeast*, 5(3):149–158.
- Richter, J. D. and Sonenberg, N. (2005). Regulation of cap-dependent translation by eIF4E inhibitory proteins. *Nature*, 433(7025):477–480.
- Ridley, S. P., Sommer, S. S., and Wickner, R. B. (1984). Superkiller mutations in *Saccharomyces cerevisiae* suppress exclusion of M2 double-stranded RNA by L-A-HN and confer cold sensitivity in the presence of M and L-A-HN. *Mol Cell Biol*, 4(4):761–70.

- Roppelt, V., Klug, G., and Evguenieva-Hackenberg, E. (2010). The evolutionarily conserved subunits Rrp4 and Csl4 confer different substrate specificities to the archaeal exosome. *FEBS Lett*, 584(13):2931–2936.
- Sasanuma, H., Murakami, H., Fukuda, T., Shibata, T., Nicolas, A., and Ohta, K. (2007). Meiotic association between Spo11 regulated by Rec102, Rec104 and Rec114. *Nucleic acids research*, 35(4):1119–33.
- Schaeffer, D., Tsanova, B., Barbas, A., Reis, F. P., Dastidar, E. G., Sanchez-Rotunno, M., Arraiano, C. M., and van Hoof, A. (2009). The exosome contains domains with specific endoribonuclease, exoribonuclease and cytoplasmic mRNA decay activities. *Nat Struct Mol Biol*, 16(1):56–62.
- Schneider, C., Leung, E., Brown, J., and Tollervey, D. (2009). The N-terminal PIN domain of the exosome subunit Rrp44 harbors endonuclease activity and tethers Rrp44 to the yeast core exosome. *Nucleic Acids Res*, 37(4):1127–40.
- Seago, J. E., Chernukhin, I. V., and Newbury, S. F. (2001). The Drosophila gene twister, an orthologue of the yeast helicase SKI2, is differentially expressed during development. *Mech Dev*, 106(1-2):137–141.
- Sikorski, R. S., Boguski, M. S., Goebel, M., and Hieter, P. (1990). A repeating amino acid motif in CDC23 defines a family of proteins and a new relationship among genes required for mitosis and RNA synthesis. *Cell*, 60(2):307–17.
- Simon, E., Camier, S., and Sraphin, B. (2006). New insights into the control of mRNA decapping. *Trends Biochem Sci*, 31(5):241–243.
- Singleton, M. R., Dillingham, M. S., and Wigley, D. B. (2007). Structure and mechanism of helicases and nucleic acid translocases. *Annu Rev Biochem*, 76:23–50.
- Stead, J. A., Costello, J. L., Livingstone, M. J., and Mitchell, P. (2007). The PMC2NT domain of the catalytic exosome subunit Rrp6p provides the interface for binding with its cofactor Rrp47p, a nucleic acid-binding protein. *Nucleic Acids Res*, 35(16):5556–5567.
- Symmons, M. F., Jones, G. H., and Luisi, B. F. (2000). A duplicated fold is the structural basis for polynucleotide phosphorylase catalytic activity, processivity, and regulation. *Structure*, 8(11):1215–1226.

- Synowsky, S. A. and Heck, A. J. (2008). The yeast Ski complex is a hetero-tetramer. *Protein science : a publication of the Protein Society*, 17(1):119–25.
- Takahashi, S., Araki, Y., Sakuno, T., and Katada, T. (2003). Interaction between Ski7p and Upf1p is required for nonsense-mediated 3'-to-5' mRNA decay in yeast. *EMBO J*, 22(15):3951–9.
- Tarun, S. Z. and Sachs, A. B. (1995). A common function for mRNA 5' and 3' ends in translation initiation in yeast. *Genes Dev*, 9(23):2997–3007.
- Tarun, S. Z. and Sachs, A. B. (1996). Association of the yeast poly(A) tail binding protein with translation initiation factor eIF-4G. *EMBO J*, 15(24):7168–7177.
- Tarun, S. Z., Wells, S. E., Deardorff, J. A., and Sachs, A. B. (1997). Translation initiation factor eIF4G mediates in vitro poly(A) tail-dependent translation. *Proc Natl Acad Sci U S A*, 94(17):9046–9051.
- Tesse, S., Storlazzi, A., Kleckner, N., Gargano, S., and Zickler, D. (2003). Localization and roles of Ski8p protein in *Sordaria* meiosis and delineation of three mechanistically distinct steps of meiotic homolog juxtaposition. *Proceedings of the National Academy of Sciences of the United States of America*, 100(22):12865–70.
- Thiebaut, M., Kisseleva-Romanova, E., Rougemaille, M., Boulay, J., and Libri, D. (2006). Transcription termination and nuclear degradation of cryptic unstable transcripts: a role for the Nrd1-Nab3 pathway in genome surveillance. *Mol Cell*, 23(6):853–864.
- Toh, E. A., Guerry, P., and Wickner, R. B. (1978). Chromosomal superkiller mutants of *Saccharomyces cerevisiae*. *Journal of bacteriology*, 136(3):1002–7.
- Tomson, B. N. and Arndt, K. M. (2012). The many roles of the conserved eukaryotic Paf1 complex in regulating transcription, histone modifications, and disease states. *Biochim Biophys Acta*.
- Torchet, C., Bousquet-Antonelli, C., Milligan, L., Thompson, E., Kufel, J., and Tollervey, D. (2002). Processing of 3'-extended read-through transcripts by the exosome can generate functional mRNAs. *Mol Cell*, 9(6):1285–1296.
- Tucker, M., Valencia-Sanchez, M. A., Staples, R. R., Chen, J., Denis, C. L., and Parker, R. (2001). The transcription factor associated Ccr4 and Caf1 proteins are components of the

- major cytoplasmic mRNA deadenylase in *Saccharomyces cerevisiae*. *Cell*, 104(3):377–386.
- van Hoof, A., Frischmeyer, P. A., Dietz, H. C., and Parker, R. (2002). Exosome-mediated recognition and degradation of mRNAs lacking a termination codon. *Science*, 295(5563):2262–4.
- van Hoof, A., Lennertz, P., and Parker, R. (2000a). Yeast exosome mutants accumulate 3'-extended polyadenylated forms of U4 small nuclear RNA and small nucleolar RNAs. *Mol Cell Biol*, 20(2):441–52.
- van Hoof, A., Staples, R. R., Baker, R. E., and Parker, R. (2000b). Function of the Ski4p (Csl4p) and Ski7p proteins in 3'-to-5' degradation of mRNA. *Mol Cell Biol*, 20(21):8230–43.
- Vanacova, S., Wolf, J., Martin, G., Blank, D., Dettwiler, S., Friedlein, A., Langen, H., Keith, G., and Keller, W. (2005). A new yeast poly(A) polymerase complex involved in RNA quality control. *PLoS Biol*, 3(6):e189.
- Vasiljeva, L., Kim, M., Mutschler, H., Buratowski, S., and Meinhart, A. (2008). The Nrd1-Nab3-Sen1 termination complex interacts with the Ser5-phosphorylated RNA polymerase II C-terminal domain. *Nat Struct Mol Biol*, 15(8):795–804.
- Walbott, H., Mouffok, S., Capeyrou, R., Lebaron, S., Humbert, O., van Tilbeurgh, H., Henry, Y., and Leulliot, N. (2010). Prp43p contains a processive helicase structural architecture with a specific regulatory domain. *EMBO J*, 29(13):2194–204.
- Wang, L., Lewis, M. S., and Johnson, A. W. (2005). Domain interactions within the Ski2/3/8 complex and between the Ski complex and Ski7p. *RNA*, 11(8):1291–302.
- Wang, X., Jia, H., Jankowsky, E., and Anderson, J. T. (2008). Degradation of hypomodified tRNA(iMet) in vivo involves RNA-dependent ATPase activity of the DExH helicase Mtr4p. *RNA*, 14(1):107–116.
- Wasmuth, E. V. and Lima, C. D. (2012). Exo- and endoribonucleolytic activities of yeast cytoplasmic and nuclear RNA exosomes are dependent on the noncatalytic core and central channel. *Molecular cell*.

- Weir, J. R., Bonneau, F., Hentschel, J., and Conti, E. (2010). Structural analysis reveals the characteristic features of Mtr4, a DExH helicase involved in nuclear RNA processing and surveillance. *Proc Natl Acad Sci U S A*, 107(27):12139–44.
- Wells, S. E., Hillner, P. E., Vale, R. D., and Sachs, A. B. (1998). Circularization of mRNA by eukaryotic translation initiation factors. *Mol Cell*, 2(1):135–140.
- Widner, W. R. and Wickner, R. B. (1993). Evidence that the SKI antiviral system of *Saccharomyces cerevisiae* acts by blocking expression of viral mRNA. *Mol Cell Biol*, 13(7):4331–4341.
- Wiederhold, K. and Passmore, L. A. (2010). Cytoplasmic deadenylation: regulation of mRNA fate. *Biochem Soc Trans*, 38(6):1531–1536.
- Wyers, F., Rougemaille, M., Badis, G., Rousselle, J. C., Dufour, M. E., Boulay, J., Regnault, B., Devaux, F., Namane, A., Seraphin, B., Libri, D., and Jacquier, A. (2005). Cryptic Pol II transcripts are degraded by a nuclear quality control pathway involving a new poly(A) polymerase. *Cell*, 121(5):725–37.
- Zeytuni, N. and Zarivach, R. (2012). Structural and functional discussion of the tetratripeptide repeat, a protein interaction module. *Structure*, 20(3):397–405.
- Zhang, Z., Kulkarni, K., Hanrahan, S. J., Thompson, A. J., and Barford, D. (2010). The APC/C subunit Cdc16/Cut9 is a contiguous tetratricopeptide repeat superhelix with a homo-dimer interface similar to Cdc27. *EMBO J*, 29(21):3733–3744.
- Zhu, B., Mandal, S. S., Pham, A.-D., Zheng, Y., Erdjument-Bromage, H., Batra, S. K., Tempst, P., and Reinberg, D. (2005). The human PAF complex coordinates transcription with events downstream of RNA synthesis. *Genes Dev*, 19(14):1668–1673.
- Zuo, Y. and Deutscher, M. P. (2001). Exoribonuclease superfamilies: structural analysis and phylogenetic distribution. *Nucleic Acids Res*, 29(5):1017–1026.



# Acknowledgements

I would like to thank my family in the first place: thank you **Mom & Dad**, and thank you, **Tobi**, for all the different kinds of support you gave me during the years that have passed!

Thanks to **my friends!** For not giving up on me when I was working weekends and late hours in the lab.

**Elena**, I won't go back to the proteolysis, but: thanks for the trust you put in me and for supporting me during my thesis.

**My dear colleagues:** I am grateful for you making this lab a place that I (nearly) always looked forward to coming to. I am much obliged to **Michaela** for all the energy you invested in the project, particularly for getting all those expressions going. **Rajan**, you soon filled up the empty spot in our bay and I couldn't imagine a better bay mate. While others joined, you left, **Holger**, but not before having introduced me to the lab. It was good fun with you on the slopes (and in the lab, too). We didn't catch that train, **Ben**, but I am glad that you did jump on the MPI express along with your thoughtfulness and empathy. Dear **Sutapa**, you joined the same time I did, and I hope you'll take the next step not much later than me. And don't you forget that Yosemite trip that is still pending! **Uma & Prakash**, without you the lab isn't the same anymore, so see you in Edinburgh. I am thankful for all the help and discussion on the project, **Fabien**. Still, what I enjoyed most were our rock trips to the mountains. Thanks for your patience, **Christian**, and for not freaking out on all the questions I threw at you. I enjoyed the conversations about all things different from science. **Ingmar**, thanks for the music and the movies, but most of all thanks for your honesty and open-minded critical thinking. **Eva**, keep on rocking in the Ski world! (You know which one I'm talking about). **Ajla**, thanks for sharing all those nicely quiet lunch breaks in the sun and for communicating your culinary coordinates of the city. **Sebastian**, thanks for being modest and well-balanced (and for equilibrating in the cold-room in the few exceptions you were not). Please, survive the canteen - it would be

boring without you in the lab. **Jerome & Claire**, thanks for helping me with diffraction & fluorescence, and for your extra help especially at the beginning. **Atlanta**, thanks for teaching me to not get greedy for the tenths of Ångstroms. In the end, it all turned out to be fine. Dear **Gretel**, I very much enjoyed your quiet presence in the lab. I'll miss the Monday morning chats about the latest news and matches. **Peter**, Säulenheiliger, thanks for keeping those chaperones off my preps. And for staying for that extra beer. Thanks to **Petra** for keeping the bureaucracy monster chained. I much liked our chats in the kitchen and your distinct view of things. **Masami-san**, your steady supply with Japanese sweets, specialities and moist air made our bay a special place to work in. But most of all, your courage and curiosity was inspiring. **Katharina**, thanks for your quietness and music. Many thanks to **Judith** for teaching me how to purify proteins and for all the help in the beginning, as well as for keeping the lab running. **Varun & Humayun**, I am grateful for all the Thursday's lunches and for your special connections to the subcontinent's fine foods. **Esben, Christian & Naoko**, you brought fresh air to this department - thanks for discussions and frank opinions. When we hit the slopes next time, **Sagar**, I expect so see some turns! In the meantime thanks for filling the second floor and our lab with life. And that holds true for you, too, **Ira & Justine**. We named it, you fixed it - thanks **Walter**! Also many thanks to **Mark** for the Spo11 preps, to **Petra & Tatjana** for cloning and thanks to **Ariane** for expression tests. **Karina, Sabine & Laura**: I guess the pile of plates you set up for me is larger than any of you, so thanks a lot! Jörg, yet another one working on the special Ski project. I'd also like to thank **Marion, Christel & Sylvie** for keeping the kitchen clean.

I would like to acknowledge the **Boehringer Ingelheim Fonds** for supporting me with a Ph.D. fellowship. Particularly, I am very grateful to the people involved with this: **Dr. Claudia Walther, Sandra Schedler, Dr. Anja Hoffmann** and **Kirsten Achenbach**.